

CHARACTERIZATION OF PRECIOUS METAL MINERAL OCCURRENCES IN
THE NORTHMET DEPOSIT OF THE PARTRIDGE RIVER INTRUSION, DULUTH
COMPLEX, MINNESOTA, USA

A THESIS
SUBMITTED TO THE FACULTY OF THE GRADUATE SCHOOL
OF THE UNIVERSITY OF MINNESOTA
BY

Daniel O. Cervin

IN PARTIAL FULFILLMENT OF THE REQUIREMENTS
FOR THE DEGREE OF
MASTER OF SCIENCE

Advisors: James Miller, Penelope Morton, Richard Patelke

August, 2011

Acknowledgements

This project would not have been possible without the guidance of my advisors, Dr. James Miller, Dr. Penelope Morton, and Richard Patelke. Thank you for the numerous suggestions, edits, and encouragement which helped bring this project to completion. Thanks also to Drs. John Swenson and Carlos Carranza-Torres for serving on my committee. During work on this thesis, I was fortunate to receive financial support from the Society of Economic Geologists, UMD Department of Geological Sciences, and PolyMet Mining Company; it would have been difficult to earn my master's degree without this financial support.

I would also like to thank Bryan Bandli – UMD SEM Lab Manager – who taught me how to use the electron beam microscope and answered countless questions about microscopy and mineralogy. Thanks also to the faculty and other graduate students at the University of Minnesota Duluth, for your support during this work.

Special thanks are due to the geology department at Northland College – Tom Fitz and Bruce Goetz- for introducing me to geology and challenging me to pursue my masters. The classes and field trips were a great experience.

Finally, I would like to thank my family: first and foremost my wife Suzy for supporting me in my decisions, even when the sacrifices were large and the outcomes uncertain.

Abstract

The NorthMet deposit is a Cu-Ni-PGE magmatic sulfide ore body located along the northwestern margin of the Partridge River Intrusion (PRI), which is part of the 1.1 Ga Duluth Complex. PolyMet Mining Company is currently seeking a permit to develop an open pit mine at the site, which is about 7 miles south the town of Babbitt, MN. During pilot-plant test runs by PolyMet, approximately 75% of the total mass of precious metals (75% is the average recovery of Pd, Pt, and Au) known to exist from assay data were recovered; total sulfide recovery was 90%. In a sulfide flotation beneficiation process, it is assumed that precious metals are contained within sulfide minerals as small (micron-sized) platinum group minerals (PGM), as Au-Ag minerals, or in solid solution. The 75% recovery implies that some precious metal mineral (PMM) phases may not be hosted by sulfide minerals.

This study seeks to characterize the mineralogical and textural occurrences of PMM in the NorthMet ore feed and concentrates. This information is not only of importance to the beneficiation of NorthMet ores, but also to the understanding of the metallogensis of PGE-Au in magmatic sulfide deposits. The energy dispersive spectrometer-equipped scanning electron microscope at University Minnesota Duluth was used in backscatter electron composition mode (BEC) to conduct detailed compositional scanning of polished thin sections to locate PMM.

As the 75% precious metal recovery would predict, NorthMet PMM primarily occur in association with sulfide minerals. Of the 346 PMM investigated in this study, 267 (77%) were hosted by sulfide minerals (mostly chalcopyrite and pentlandite), either as

inclusions or at sulfide grain boundaries. The remaining 23% (79) of PMM were found in a variety of primary silicates, secondary silicates, and apatite. Forty-eight percent of sulfide-hosted PGM are located at sulfide grain boundaries, 52% occur as inclusions in sulfide.

1) The lower recovery rate of precious metals relative to base metals in NorthMet ores is largely due to the textural and mineralogical occurrence of Au-Ag minerals, of which 55% are hosted by silicates and apatite. Furthermore, most Au-Ag minerals do not appear to be strongly attached to and intergrown with sulfide host minerals either as inclusions or at grain boundaries and are likely lost to tailings prior to introduction to sulfide flotation systems.

2) Platinum group minerals have a strong sulfide association: at least 90% are hosted in sulfide minerals. PGM occur in secondary silicates (7%) and in association with apatite (3%) in contact with, or close to sulfides. PGM primarily occur at sulfide grain boundaries in sulfide halo textures, usually in plagioclase. PGM do not occur as inclusions in primary silicate minerals. Sulfide boundary PGM are often intimately intergrown with adjacent silicate minerals.

3) An orthomagmatic model is invoked to explain the genesis of NorthMet ores. The strong sulfide association of PGM, the indirect sulfide association of Au-Ag, the general paucity of hydrous, secondary minerals in PGM-bearing sulfide halo textures, and the mostly well-preserved primary igneous textures indicate that magmatic processes formed the NorthMet ore body.

Table of Contents

List of Tables	vi
List of Figures	vii
1. Introduction.....	1
1.1 Statement of the Problem.....	3
1.2 Overview of Magmatic Cu-Ni-PGE Sulfide Deposit Models	7
1.3 Fractional Crystallization of Sulfide Liquid and the Distribution of Platinum Group Minerals and Gold	13
1.4 Geologic Setting of the NorthMet Deposit	17
2. Methods.....	22
2.1 Sample selection	23
2.2 SEM Analyses and Imaging of PMM in Ore Samples	25
2.3 SEM Analyses and Imaging of PMM in Ore Concentrate Samples	28
2.4 Reflected and Transmitted Light Microscopy	28
3. Results.....	29
3.1 Gold and Silver Minerals	38
3.2 Platinum Group Minerals (PGM)	42
3.3 PGM in Sulfides.....	44
3.4 PGM in Secondary Silicates and Apatite.....	55
3.5 Apparent PGM in Primary Silicates	60
3.6 PolyMet's C5 Concentrate.....	67
3.7 Results Summary	75

Table of Contents - Continued

4. Discussion.....	78
4.1 Metallogensis of Au-Ag Minerals in NorthMet.....	78
4.2 Orthomagmatic Origin of PGM in NorthMet.....	80
4.3 Origin of PGM-enriched Sulfide Halos.....	83
4.4 Cause of Low Precious Metal Recoveries.....	88
5. Conclusion.....	91
Bibliography.....	94
Appendix A.....	98
Appendix B.....	147

List of Tables

Table 1: Sample Data: drill-hole number, depth, and assay	24
Table 2: Precious metal minerals with sulfide mineral associations	31
Table 3: Precious metal minerals without sulfide mineral associations	33
Table 4: Precious metal minerals in PolyMet's C5 concentrate	70

List of Figures

Figure 1: Northeastern Minnesota bedrock map.....	7
Figure 2: Cu-Ni-PGE magmatic sulfide model	18
Figure 3: Fractionating PGE+Au-rich sulfide droplet	21
Figure 4: Magmatic sulfide deposits of the Duluth Complex.....	25
Figure 5: Partridge River Intrusion igneous stratigraphy	26
Figure 6: Precious metal minerals (PMM) in sulfide histogram.....	38
Figure 7: PMM in silicates and apatite histogram	40
Figure 8: PMM in ore samples grain size distribution.....	41
Figure 9a: Gold in olivine fracture photomicrograph.....	42
Figure 9b: Electrum in orthopyroxene fracture photomicrograph	42
Figure 9c: Electrum at boundary between biotite and ilmenite photomicrograph.....	43
Figure 9d: Electrum in cubanite fracture photomicrograph	43
Figure 10: Electrum inclusion in chalcopyrite photomicrograph	46
Figure 11: Electrum in recess within plagioclase photomicrograph	47
Figure 12: Missing electrum grain location photomicrograph	47
Figure 13: Cu-Fe-S ternary diagram.....	52
Figure 14: Fe-Ni-S ternary diagram.....	53
Figure 15a: Fine-grained sulfides photomicrograph.....	56
Figure 15b: PGM inclusion in sulfide photomicrograph	56
Figure 16a-b: PGM in sulfide halo photomicrographs	57

List of Figures - Continued

Figure 16c: PGM inclusion in sulfide grain photomicrograph	58
Figure 17a: Fine-grained sulfide halo with PGM photomicrograph.....	58
Figure 17b: Sulfide boundary PGM photomicrograph	59
Figure 17c: Sulfide boundary PGM photomicrograph	59
Figure 18: Sulfide boundary PGM photomicrograph	60
Figure 19: Sperrylite in contact with apatite photomicrograph	64
Figure 20a: PGM-bearing sulfide halo photomicrograph.....	64
Figure 20b-c: PGM in secondary silicate photomicrograph	65
Figure 21a-b: Apparent PGM inclusion in plagioclase photomicrograph	69
Figure 21c-d: Apparent PGM inclusion in plagioclase photomicrograph	70
Figure 22a-b: Apparent PGM inclusion in clinopyroxene photomicrograph	71
Figure 23a-b: Apparent PGM inclusion in orthopyroxene photomicrograph.....	72
Figure 24: PMM in Concentrate C5 histogram.....	77
Figure 25: Types of PMM in Concentrate C5 histogram	78
Figure 26: PMM in Concentrate C5 grain size distribution histogram.....	78
Figure 27a-b: PGM in Concentrate C5 photomicrographs	79
Figure 27c-d: PGM in Concentrate C5 photomicrographs	80
Figure 28: PGM-bearing plagioclase anorthite number histogram.....	92

1. INTRODUCTION

The NorthMet deposit is one of about a dozen Cu-Ni-PGE magmatic sulfide ore bodies located along the northwestern edge of the Duluth Complex (DC) near Ely, Minnesota (Fig. 1). The Duluth Complex is composed of a series of multiply-emplaced intrusive igneous bodies that form the largest intrusive component of the 1.1 Ga Midcontinent Rift (Miller et al., 2002). The Duluth Complex is primarily composed of tholeiitic mafic layered intrusions along with some felsic and anorthositic bodies (Miller et al., 2002). In addition to its large size, the Duluth Complex is renowned for containing the world's largest known undeveloped deposits of copper, nickel, and precious metals (Eckstrand and Hulbert, 2007).

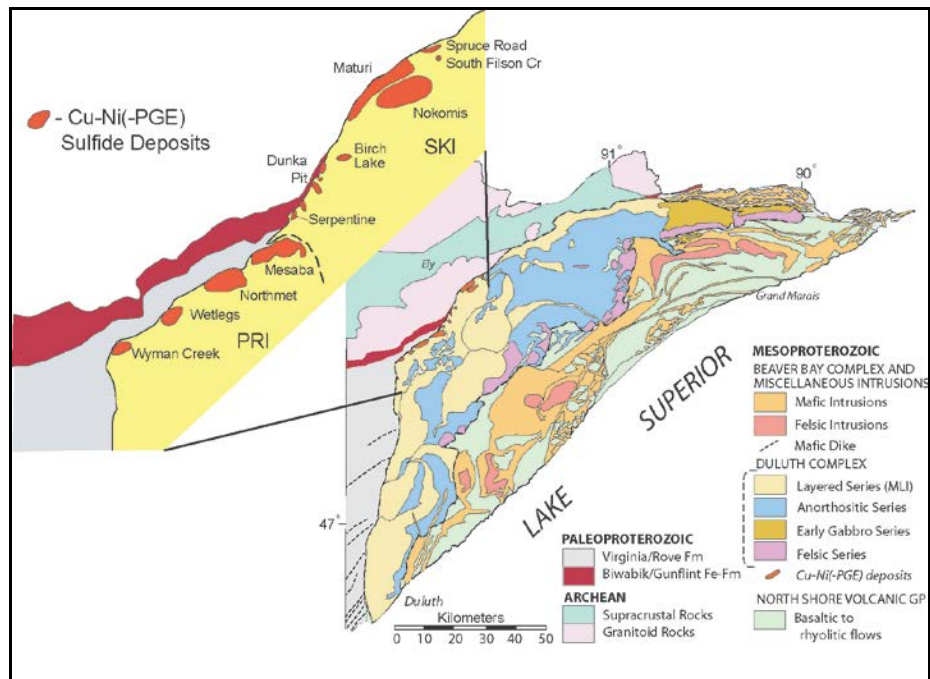


Figure 1: Geology of northeastern Minnesota highlighting the locations of the Cu-Ni (PGE) deposits occurring along the northwestern margin of the Partridge River intrusion (PRI) and the South Kawishiwi intrusion (SKI) (unpublished figure from Miller, 2010).

These multiple intrusions were emplaced into the lower section of the comagmatic North Shore Volcanic Group. Many of the intrusions are floored against Paleoproterozoic sedimentary rocks of the Animikie Group and locally against Archean granite of the Giant's Range Batholith.

Economic concentrations of copper, nickel, cobalt, and platinum group elements associated with sulfide mineralization are found at or near the base of two troctolitic intrusions forming the northwestern margin of the Duluth Complex: the South Kawishiwi and the Partridge River. Minnesota Department of Natural Resources (Listerud and Meineke, 1977) estimates that, collectively, these deposits contain about 4.4 billion tons of mineral resources grading at 0.66% copper and 0.20% nickel. The NorthMet deposit, which is currently being permitted for mining by PolyMet Mining, a Canadian junior company, is located in the Partridge River intrusion. This deposit was initially explored in the early 1970's by US Steel and was known as the Dunka Road deposit (Severson & Hauck, 1990). Metals of interest at NorthMet, in order of abundance, are copper, nickel, cobalt, palladium, platinum, and gold. Current estimates of inferred and indicated mineral resources in NorthMet (PolyMet, 2011) are 274.7 million short tons grading 0.28% copper, 0.08% nickel, and 0.01 opt of precious metals (palladium, platinum and gold). At these grades the deposit contains 769,000 tons of copper; 220,000 tons of nickel; 7,200 tons of cobalt, and 2,747,000 troy ounces of precious metals.

As of spring of 2011, PolyMet plans to employ froth flotation of sulfide concentrate followed by a hydrometallurgical (HydroMet) process utilizing a high pressure autoclave to concentrate and extract base and precious metals from crushed ore.

After initial crushing and fine-grinding, the sulfide minerals - which are presumed to host most of the base and precious metals - are separated from gangue by standard flotation processes and fed into the autoclave. In the froth flotation process metals that are bound to sulfur attach to a surfactant and float on the surface of the slurry, thereby allowing them to be selectively removed. Only metals that are bound to sulfide minerals are recovered. The HydroMet process combines water, oxygen, and surfactants with finely crushed ore inside a pressurized vessel to separate the base and precious metals from sulfur.

1.1 Statement of Problem

During pilot-plant test runs by PolyMet, approximately 75% of the total mass of precious metals (platinum, palladium, and gold) known to exist from assay data, were recovered; total sulfide recovery was 90% (Patelke, 2009, unpublished data). This suggests that non-sulfide phases may host some of the precious metals. According to Severson & Hauck's (2003) report on platinum group elements (PGE)¹ occurrences within the Duluth Complex deposits, the grain size of many platinum group minerals (PGM)² in the NorthMet ores is very small: 1-2 micrometers. In sulfide flotation it is assumed that precious metal minerals (PMM)³ containing PGE and Au-Ag are located within sulfide minerals as inclusions, exsolved phases, or in solid solution.

¹ Platinum Group Elements include platinum (Pt), palladium (Pd), osmium (Os), ruthenium (Ru), rhodium (Rh), and iridium (Ir).

² Platinum Group Minerals include all minerals containing PGE as significant components of the mineral (>25%).

³Precious Metal Minerals collectively refers to both PGM and Au-Ag minerals.

The difference between base metals and precious metals recovery has potentially important implications for the assumption that PMM predominately occur in sulfide minerals in Cu-Ni-PGE deposits associated with layered mafic intrusions (Naldrett, 2004). Because of the strongly chalcophile nature of PGE and Au-Ag, many metallogenic models of magmatic ore deposits (e.g., Naldrett, 2004; Mungall, 2005) conclude that PGE and Au-Ag are scavenged from silicate melts by immiscible sulfide liquid and then crystallize as PMM or PGE-enriched sulfide minerals. However, some authors have suggested that PGM crystallize directly from the silicate melt without pre-concentration by sulfide liquid and may then be collected by adherence to sulfide liquid droplets or chromite grains (e.g., Finnigan et al., 2008, Mungall, 2005). All PGM that crystallize in this manner may not be chemically collected by chromite or sulfide, implying the possible occurrence of PGM in late-forming gangue minerals as inclusions. Mungall (2005) observed that PGE can form alloys called micro-nuggets that appear to be in equilibrium with enclosing silicate melts or aqueous fluids.

Several studies have noted that the infiltration of chlorine-rich deuteric fluids may result in dissolution of sulfide and replacement by hydrothermal minerals, but does not appear to mobilize PGM (e.g. Li et al., 2004; Joslin, 2004; Andersen, 2006). Alternately, some authors suggest mobilization and concentration of PGE and Au-Ag by chlorine-rich late magmatic fluids (Foose and Weiblen, 1986; Boudreau & McCallum, 1992; Severson, 1994). These studies and preliminary characterization of PGM in Duluth Complex ores (Severson & Hauck, 2003) suggest that there may be primary and secondary processes which would explain the separation of PGM from sulfide minerals. This study

documents the physical association of PMM and sulfide minerals in NorthMet ores and provides additional empirical data that constrains proposed models of PMM metallogenesis.

Moreover, this research could have significant economic implications both for NorthMet and kindred Cu-Ni-PGE ore deposits occurring along the northwestern margin of the Duluth Complex. Although low-grade, the enormous copper-nickel-PGE sulfide deposits of the Duluth Complex constitute the world's largest copper resource, third largest Ni resource, and fourth largest PGE resource among magmatic sulfide deposits (Eckstrand & Hulbert, 2007). The NorthMet deposit (formerly Dunka Road; Geerts 1991, Theriault et al., 2000) contains 2.74million ounces of precious metals (PolyMet, 2011). At 75% recovery, about 625,000 ounces of precious metals could be lost to tailings over the life of the mine. A conservative estimate, using the current price for palladium (\$775 per ounce on 7/11/2011) to represent all precious metals in the deposit, equates to approximately ten million dollars a year (Patelke, 2010, unpublished data).

The greatest losses of PGE during metallurgical processing occur during the first steps of beneficiation: comminution and concentration (Merkle & McKenzie, 2002). One reason for this is the diversity of platinum group minerals, of which 109 are known to exist (Merkle & McKenzie, 2002; Cabri, 2002). The diversity of PGM is reflected in varying chemical properties and mineral associations, which may enhance or deteriorate amenability to sulfide froth flotation methods. Another factor affecting recovery rates is the generally small size (micron-scale) of PGM, which dictates the degree of milling necessary to liberate PGM from gangue. The balance between liberating fine-grained

PGM and over-milling is difficult to achieve. Over-milling produces PGM that do not float due to their exceedingly small size (Merkle & McKenzie, 2002).

The majority of PGM in magmatic sulfide deposits are presumed to be hosted by sulfide minerals. Previous work by Severson and Hauck (2003) concluded that PGM in Duluth Complex deposits occur in the following types of mineralogical and textural settings:

- Within interstitial sulfides that partially enclose olivine, which are both partially enclosed by late plagioclase.
- Within interstitial sulfides along plagioclase boundaries or surrounded by plagioclase laths. Usually the PGM are present as minute inclusions in sulfide halos within plagioclase that is adjacent to interstitial sulfide.
- Within orthopyroxene-sulfide symplectite grains.
- In plagioclase cleavage adjacent to interstitial sulfides.
- Within and on the rims of interstitial sulfides.
- Within oxides.
- Within orthopyroxene – sulfide symplectite.
- Within chlorite-filled veins and patches.
- Within chalcopyrite veins that connect earlier formed interstitial sulfides.
- Boundaries between oxides and silicates, or between sulfides and silicates.

Some of these occurrences suggest the possibility that PGMs may be mobilized or concentrated not only by magmatic processes, but by deuteritic fluids or postmagmatic hydrothermal activity. For example, some PGM were located in hydrous, secondary minerals.

The principal objective of this project is to characterize the mineralogical and textural occurrences of PGM and Au-Ag in the NorthMet ore feed and concentrates. The results of this study have the potential of not only enhancing our understanding of PGM metallogenesis in Duluth Complex Cu-Ni-PGE ores, but also may have the practical benefit of explaining the cause of the relatively lower beneficiation rates of PGE and Au-Ag from the PolyMet's NorthMet ore body.

1.2 Overview of Magmatic Cu-Ni-PGE Sulfide Deposit Models

Magmatic sulfide deposits form during emplacement and crystallization of mafic/ultramafic magmas through four principal steps (Naldrett, 2004; Arndt et al., 2005; Mungall, 2005).

1. Partial melting of the mantle generates a sulfur under-saturated and metal-enriched mafic or ultramafic magma. This melt separates from the residual solid mantle, followed by ascent of magma and subsequent emplacement in or on the earth's crust. During adiabatic ascent, sulfide solubility of the magma increases, which causes the magma to become progressively more sulfur-undersaturated.
2. This sulfur-undersaturated magma interacts with wall rocks in a conduit or magma chamber leading to assimilation of crustal rocks which may contain sulfur. Ultimately, this may lead to the magma becoming sulfur-saturated to over-saturated, followed by the segregation of an immiscible sulfide liquid.

3. The exsolved sulfide melt interacts with a relatively larger volume of metal-bearing silicate magma wherein chalcophile elements like Cu, Ni, Co, PGE, and Au-Ag are preferentially concentrated in the sulfide liquid.
4. This concentrated metal-rich sulfide melt then settles to the base of the magma body due to greater density than the silicate melt to form an ore deposit.

The most important factor in developing a magmatic sulfide deposit enriched in PGE is the concentration of PGE in the mantle source and the subsequent concentration of these elements in the magma generated by partial melting. The degree of partial melting of the mantle and mantle composition determine the PGE content of a melt (Naldrett, 2004). A mantle source rock that is rich in sulfides, oxides, or PGE alloys will tend to preferentially retain PGE at lower degrees of partial melting because sulfide is not completely melted and PGE are chalcophile elements, meaning that if sulfide remains in the mantle source, so do PGE (Mungall, 2005). Composition of the mantle depends on degree of previous melting and the degree of metasomatism typically resulting from introduction of volatiles by a descending oceanic slab.

In the most general sense, the concentration of PGE in a mantle melt fraction has a positive correlation to the degree of melting up to the point of sulfide depletion in the mantle. The maximum concentration of PGE is removed from the mantle at approximately 15% partial melting of the mantle. After 15% melting, PGE content of mantle melts decreases and nickel content increases due to melting of nickel-bearing olivine (Naldrett, 2004). It should be noted that although the mantle contains some sulfur, the concentration is low and it is estimated to be in the range of 125 - 600 ppm (Arndt et

al., 2005). This is an important detail regarding the sulfur content of mantle melts, and will be referred to later in this paper with reference to sulfur- under-saturation of basaltic melts.

The processes by which PGE concentration varies in mafic melts is not well-understood. Little is known about the distribution of these elements within the mantle. Abundance of PGE in basalts is low in economic terms, but high relative to most other igneous rocks. Average continental basaltic magmas contain 1-10 ppb Pt and Pd, though mid-ocean ridge basalts (MORB) are depleted in PGE containing < 1 ppb Pt and Pd, due to multiple, extended melting events (Naldrett, 2004). Relatively high PGE values of non-MORB melts indicates that these magmas are not sulfide-saturated as they leave the mantle and did not reach sulfide saturation during their ascent. Because the mantle is low in sulfur these melts are generally sulfur under-saturated prior to interaction with crustal rocks. Although PGE are both siderophile and chalcophile in the mantle, they are predominantly chalcophile in the upper mantle and crust (Arndt et al., 2005). Experiments looking at the effect of pressure on sulfide solubility in mafic magmas show that solubility increases with decreasing pressure (Mavrogenes and O'Neill, 1999). Thus, silicate magmas become more sulfur-undersaturated and have the capability to dissolve more sulfur at progressively shallower levels in the crust.

The principal path to sulfur-saturation in all economic magmatic sulfide deposits is through assimilation of crustal rocks in a magma chamber or magma conduit (Naldrett, 2004). As stated above, basaltic melts typically arrive at the near surface under-saturated in sulfur. Sulfur-saturation occurs due to incorporation of sulfur-rich crustal

rocks, but may also result due to the addition of SiO_2 or Al_2O_3 , a sharp reduction in temperature, or a depletion in FeO concentration, all of which decrease the solubility of sulfur in a silicate melt (Naldrett, 2004). At the point of sulfur-saturation, sulfur is liquated from the silicate melt forming an immiscible sulfide liquid. This liquid strongly attracts PGE and Au-Ag due to their chalcophile behavior, thereby scavenging chalcophile metals from the silicate melt. The model of magmatic sulfide deposits is based on this concept of immiscible sulfide liquid collecting base and precious metals from silicate magma that it is in contact with. The specific gravity of the sulfide melt is about 4 whereas that of the silicate melt is about 2.7-3 (Naldrett & Duke, 1980). This density difference causes the sulfide liquid to settle within the silicate magma, which results in chalcophile metals being scavenged from the magma column. In addition to collecting metals during gravitational settling, the sulfide melt may accumulate in a depression or area of lower flow in a conduit, after which subsequent pulses of PGE-bearing silicate magma pass over, thereby furthering the upgrading process.

Distribution (or partition) coefficients (D) are important parameters that predict the distribution of an element between two phases. $D^{\text{sul-sil}}(\text{X})$ is the distribution coefficient for element X between a silicate melt and an immiscible sulfide melt. This coefficient is the ratio of the metal in sulfide divided by the metal in the silicate at equilibrium. Elements with high $D^{\text{sul-sil}}$ values are termed chalcophile elements because they share with copper a strong tendency to be in sulfide liquid. Experimentally determined $D^{\text{sul-sil}}$ values for base metals commonly found in magmatic sulfide deposits are Ni ~ 275, Cu ~ 245, Co ~ 80, whereas $D^{\text{sul-sil}}$ for Pt and Pd are 10,000 and 15,000,

respectively (Naldrett, 2004 and references therein). These values imply that if a sulfide melt is in contact with a PGE-bearing silicate melt, that PGE are at least 10,000 times more likely to partition into a sulfide phase than a silicate phase.

For an economic magmatic sulfide deposit to form, the ratio of silicate melt to sulfide melt should be high; in other words, a relatively small volume of sulfide liquid should come in contact with a large volume of PGE-bearing silicate melt. This ratio is termed the R-factor (Campbell and Naldrett, 1979). Magmatic sulfide deposits with very high values of R show a strong concentration of PGE in the sulfide melt and a complimentary depletion of PGE in the silicate melt. Because Cu is less efficiently enriched in the sulfide than PGE, Cu/Pd and Cu/Pt ratios in the sulfide-scavenged silicate magma commonly show 2- to 3-orders of magnitude increases (Barnes and Maier, 2002; Barnes and Lightfoot, 2005).

Once PGE in a parental magma have been concentrated in an immiscible sulfide liquid that has segregated from the silicate melt, these newly formed metal-rich sulfide phases must collect and concentrate in order to form an ore deposit (Fig. 2). The optimal location for accumulating these phases is in a magma conduit through which a large volume of magma passes in open magmatic systems. For this to occur, magma must reach saturation at the same location in the conduit, causing sulfides to collect at the same point in the conduit. A second way that accumulation can occur in a conduit is for magma that contains immiscible sulfides in suspension to drop these phases due to a change in flow velocity in the conduit, preferentially depositing at a single site.

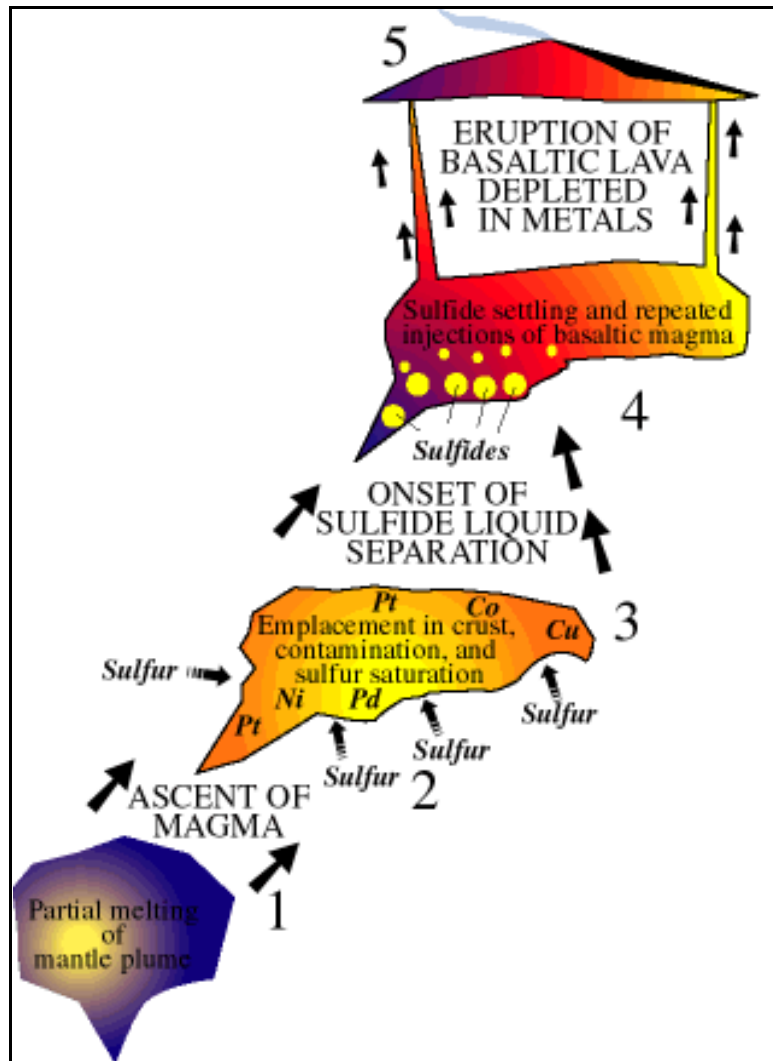


Figure 2: Cu-Ni-PGE magmatic sulfide model (http://pubs.usgs.gov/info/mwni_cu/ 2011).

1.3 Fractional Crystallization of Sulfide Liquid and the Distribution of Platinum Group Minerals and Gold

Previous studies have documented the chalcophile nature of PGE and Au-Ag and the textural occurrence of precious metals as spatially related to and hosted by sulfide minerals has been well-documented (Li et al., 1995; Naldrett, 2004; Mungall, 2005; Godel et al. 2010; Holwell and McDonald, 2010). Researchers have investigated and documented the fractional crystallization sequence of sulfide liquid in the Fe-Ni-Cu-S system with respect to partitioning of PGE + Au during the crystallization of mono-sulfide solid solution (mss) and subsequently intermediate-sulfide solid solution (iss). As a liquated sulfide liquid begins to crystallize, the first phase to enter the solid state is mss, which is an iron, nickel, and sulfur compound. The remaining sulfide liquid then becomes enriched in copper (considered incompatible in the Fe-Ni-Cu-S system), which upon further cooling crystallizes to iss. After additional cooling mss re-crystallizes to pyrrhotite (Fe_{1-x}S) and pentlandite ($(\text{Fe}, \text{Ni})_9\text{S}_8$); iss re-crystallizes to chalcopyrite (CuFeS_2).

Platinum, palladium, and gold are incompatible with mss and iss. However, iridium, osmium, ruthenium (IPGE), and rhodium are compatible with mss and occur in solid solution in the end products of mss crystallization: pyrrhotite and pentlandite (Peregoedova, 1998, Holwell and McDonald, 2010). Semi-metals have been shown to have a large influence on partitioning of Pt, Pd, and Au and tend to concentrate with Pt, Pd, and Au in Cu-rich sulfide liquid, which at a lower temperature will crystallize iss. As sulfide liquid crystallizes first into mss, Pt, Pd, and Au partition into the copper-enriched

residual melt. Upon further cooling, as iss begins to crystallize, Pt, Pd, and Au do not partition into iss and are concentrated in an immiscible semi-metal rich melt, as they are also incompatible with iss. Holwell and McDonald (2010) have demonstrated that PGE+Au in iss tend to form discrete PMM around the margins of sulfide droplets/ blebs and that when Cu-rich sulfide liquid begins to crystallize iss, Pt, Pd, and Au continue to behave incompatibly, crystallizing PGE semi-metal minerals during the final stages of crystallization of a PGE+Au-enriched Cu-sulfide droplet (Fig. 3).

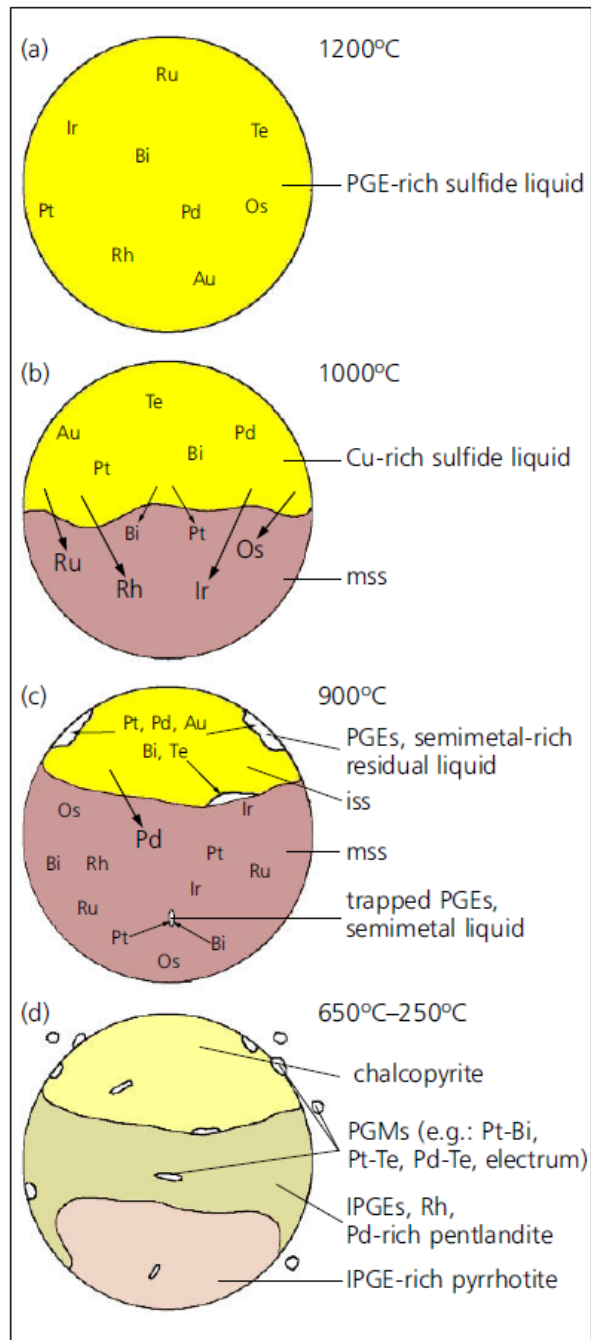


Figure 3: Fractionating PGE+Au-rich sulfide droplet, demonstrating how PGE+Au are concentrated at the boundary of crystallizing iss (IPGE = iridium, osmium, and ruthenium) (Holwell and McDonald, 2010).

The textural location of Pt, Pd, and Au in sulfide minerals is of critical importance to the understanding of PGE + Au ore-forming processes and beneficiation. PGM primarily occur in association with sulfide minerals and scavenging of PGE + Au from silicate magma by an immiscible sulfide liquid is believed to be the primary mechanism by which PGE are concentrated in magmatic sulfide deposits. Holwell and McDonald (2010) utilized laser ablation inductively coupled plasma mass spectrometry to identify PGMs + Au at sulfide grain boundaries in polished sections and noted that many PMM become isolated from sulfides as a result of replacement and alteration of sulfides by secondary silicate minerals. Hence, the occurrence of PMM at sulfide grain boundaries makes them more susceptible to alteration than if they were evenly distributed throughout the sulfide grain. Three-dimensional imaging studies on sulfide ores using high-resolution x-ray computed tomography adds further support to the conclusion that the majority of sulfide-hosted PMM are located at sulfide grain boundaries. Godel et al., (2010) determined that less than 0.7% of PMM were totally enclosed in sulfide. This result differs significantly from estimates made in previous 2-D studies conducted by Godel et al. (2010) of the same samples in which 33% of PMM were considered totally enclosed in sulfide.

Use of advanced analytical tools and techniques has firmly established that the majority of PMM are located at sulfide grain boundaries, which implies that Pd, Pt, and Au are incompatible with mss and iss and tend to be present as late-forming phases at the boundaries of sulfide grains. This provides support to the model of sulfide as a collector of PGE+Au but indicates that few PMM are totally enclosed in sulfide. The occurrence of

PMM at sulfide boundaries may be due to 1) late crystallization of PMM from the sulfide liquid, or 2) it could be due to nucleation of PMM at sulfide-silicate interface, or 3) it could imply that early crystallized PMM in the silicate magma are physically attracted to sulfide droplets. This has profound implications for PGE+Au beneficiation because PMM at sulfide boundaries are more susceptible to liberation from sulfide by deuteric fluids and subsequently becoming enclosed in secondary silicates: PMM in silicates are not recovered by sulfide flotation metallurgical processes. Additionally, PMM at grain boundaries are more likely to be mechanically separated from sulfides during comminution, i.e., they are broken off of the sulfide grains and are lost to tailings even before entering the first step in recovery: sulfide flotation.

1.4 Geologic Setting of the NorthMet Cu-Ni-PGE Magmatic Sulfide Deposit Partridge River Intrusion, Duluth Complex

Rocks of the Duluth Complex are varied and can be placed into four groups: 1. Early felsic series (~1108 Ma) consisting primarily of massive granophyre and occurring along the roof zone of the complex; 2. Early gabbroic series (~1108 Ma) of layered sequences of gabbroic cumulates; 3. Anorthositic series of plagioclase-rich gabbroic cumulates emplaced throughout the complex during main stage magmatism (~1099 Ma); 4. Layered series of stratiform troctolitic to ferro-gabbroic cumulates comprised of at least 11 variably differentiated mafic layered intrusions, occurring primarily along the base of the complex. These intrusions were emplaced during main stage magmatism, but likely after the anorthositic series (~1099) (Miller et al., 2002). In the vicinity of Babbitt,

Minnesota the layered series has been divided into three intrusive bodies: Partridge River intrusion (PRI), South Kawishiwi intrusion (SKI), and the Bald Eagle intrusion (Foose & Weiblen, 1986).

The NorthMet deposit is a low-grade Cu-Ni PGE ore body located within the PRI, which occurs along the northwestern margin of the Duluth Complex in northeastern Minnesota. NorthMet is one of approximately 12 large Cu-Ni-PGE sulfide deposits within the SKI and PRI (Figs. 1 and 4). From northeast to southwest and respective to the two main parts of the layered series in this vicinity, these are: SKI: Nickel Lake, Spruce Road, South Filson Creek, Nokomis, Maturi, Birch Lake, Dunka Pit, Serpentine; PRI: Mesaba, NorthMet, Wetlegs, and Wyman Creek (Miller and Severson, 2002).

At the NorthMet deposit, the footwall of the PRI is primarily in contact with black shales of Paleoproterozoic Virginia Formation and to a smaller extent Biwabik iron formation. Troctolitic and gabbroic rock of the PRI is approximately 1000 meters thick in areas that have been investigated in drill core and extends along strike for 24 kilometers in length (Miller and Severson, 2002). The top of the PRI contacts a number of rock types including anorthositic rocks, gabbroic rocks, mafic volcanic hornfels, and an unique cross-bedded sedimentary hornfels (Miller and Severson, 2002 and references therein). The lower part of the PRI profiled in drill core has been divided into seven major units (Fig. 5) with unit one being at the basal contact with Virginia formation shale (Miller and Severson, 2002). Rock types present in NorthMet are troctolite, leucotroctolite, troctolitic anorthosite, augite troctolite, and olivine gabbro, along with associated ultramafic subunits (melatroctolite to feldspathic dunite). Usually, the transition from

one unit to another is marked by a basal ultramafic unit composed of serpentinized olivine that appears as black, fine-grained, compact layers (Geerts, 1991; Miller and Severson, 2002). The ultramafic layer at the base of each unit is interpreted to result from settling out of cumulus, ferromagnesian minerals, with each unit representing different injections of magma into a magma chamber (Miller & Severson, 2002).

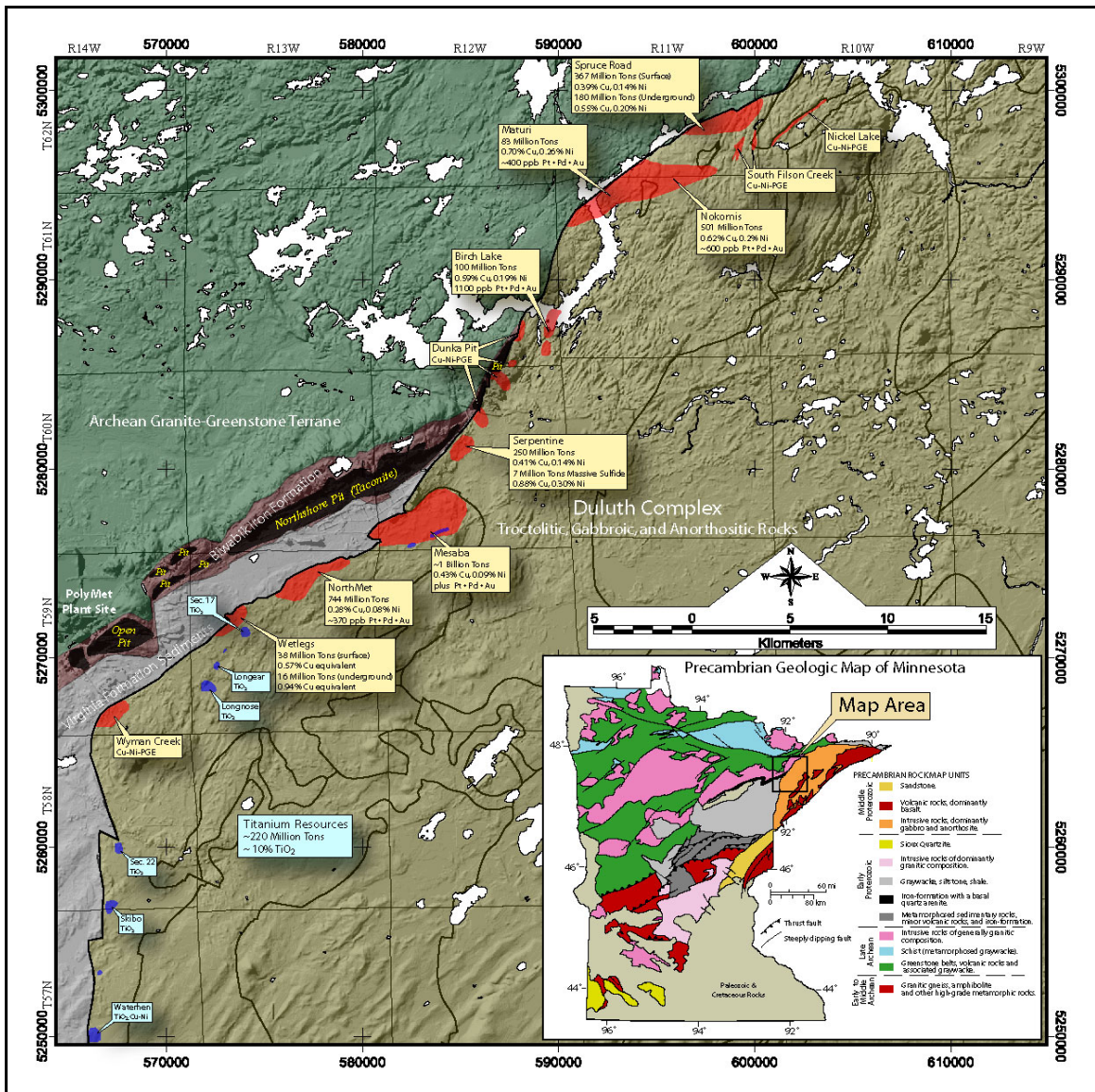


Figure 4: Cu-Ni-PGE deposits of the SKI and PRI (Dean Peterson, personal communication, 2011).

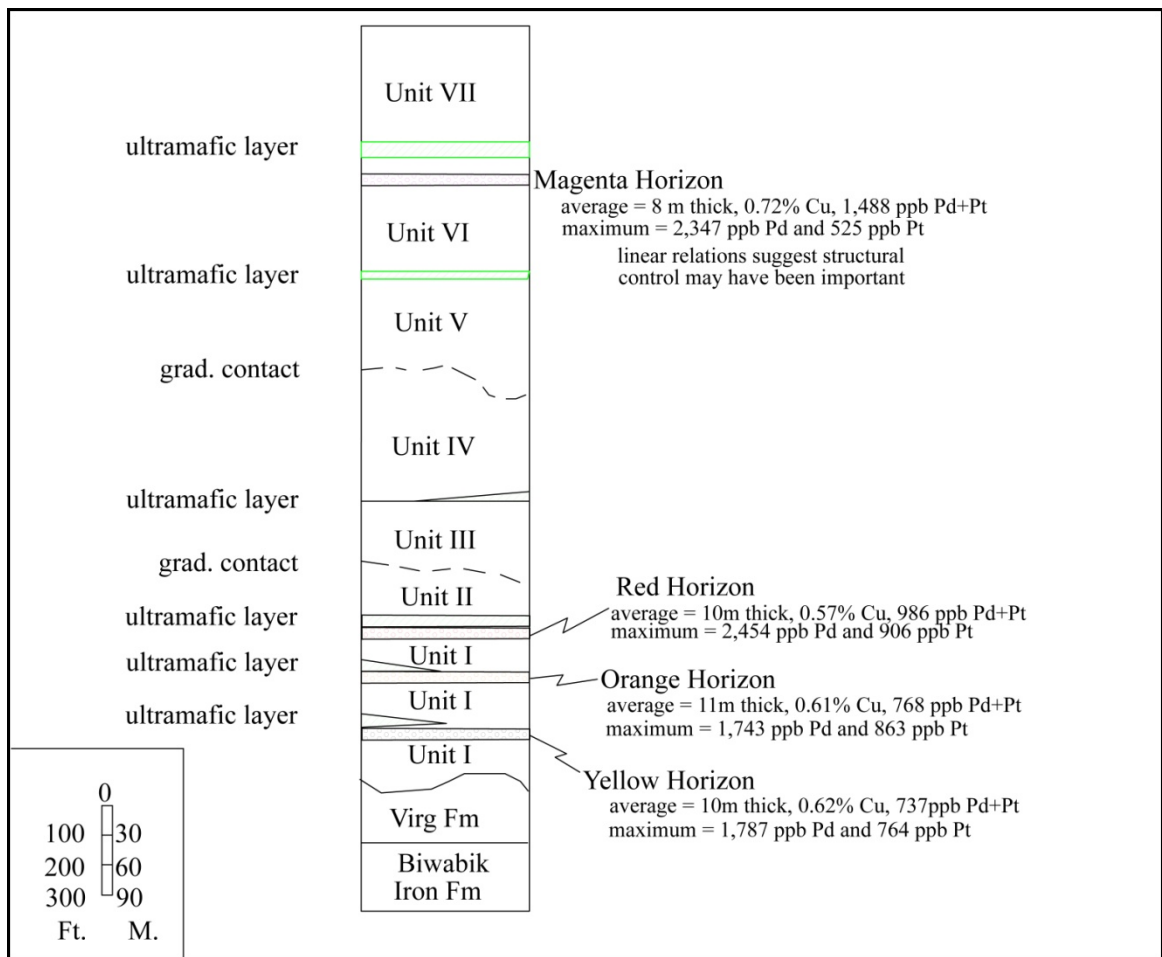


Figure 5: Igneous stratigraphy of the Partridge River intrusion in the vicinity of the NorthMet deposit (Severson and Hauck, 2003).

Unit I is the only unit that contains significant sulfide and precious metal mineralization; it is approximately 450 feet thick, ranging from 205 to 1,047 feet thick. Unit VI also has Cu-Ni-PGE mineralization, referred to as the Magenta zone; it is located near the top of Unit VI near the bottom of the ultramafic layer that defines the base of Unit VII (Geerts, 1991; Geerts 1994; Severson & Hauck, 2003). Units I and VI are principally composed of anorthositic troctolite and augite troctolite. PGE are present in Unit I with average values around 1 ppm Pd + Pt and are located at the base of ultramafic

layers; the average PGE value of Unit VI is 1.4 ppm (Geerts, 1994; Severson and Hauck, 1990, 2003).

Unit I contains abundant xenoliths of the underlying Virginia Formation, which are associated with an increase in sulfide mineralization, typically pyrrhotite (Ripley, 1981). The main sulfide minerals in Unit I are: chalcopyrite, pyrrhotite, cubanite, and pentlandite (Geerts, 1991; Geerts, 1994). About 75% of the sulfide is found as disseminated anhedral grains that are interstitial to silicate minerals. Grain size of sulfide correlates to the host rock, with a decreasing trend in grain size down-section as the contact with the footwall rock is approached. Generally pyrrhotite is found at the bottom of Unit I whereas chalcopyrite concentration increases toward the top. Sulfur isotope data indicate that the majority of the sulfur is of sedimentary origin, resulting from assimilation of footwall rocks (Ripley, 1981), in this case, the Virginia Formation. Precious metal concentrations generally correlate with the abundance of copper, with average Pd values around 1 ppm (Severson and Hauck, 2003). The average ratio of palladium to platinum is 3:1.

The location of PGE and Au-Ag-enriched horizons directly below ultramafic layers higher in the stratigraphy (Unit VI, Fig. 5) implies that magma recharge and mixing likely caused localized sulfur-saturation leading to the liquation of a chalcophile-scavenging sulfide liquid. As multiple pulses of magma entered the chamber, each pulse is believed to have assimilated Virginia Formation from footwall rocks. This led to earlier magma pulses being sulfur-saturated, then as a new pulse of fertile, precious metal-bearing magma entered the chamber, it came in contact with the underlying sulfur-

saturated magma of the underlying unit, thereby creating a mineralized zone at the top of a respective unit and below or close to the ultramafic base of the overlying unit.

Theriault et al. (2000) distinguished a PGE-rich and PGE-poor variety of sulfide mineralization in the NorthMet deposit. PGE-rich mineralization mainly occurs in Unit I, but also in Unit VI. PGE-poor mineralization occurs in the remaining units. These two ore types imply moderate to high R values (2,500-17,000) and low to moderate R values (100-3,000), respectively. Higher R values are interpreted to be indicative of lower degrees of footwall contamination of PRI magmas by sulfur-rich footwall rocks whereas lower R values correlate to greater degrees of footwall assimilation. These values support the idea that magma-mixing was an important factor during the formation of PGE-rich horizons, which are spatially related to ultramafic layers within the intrusion.

2. METHODS OF INVESTIGATION

The principal analytical tool used for this research was the JEOL JSM-6490LV variable pressure scanning electron microscope (SEM) housed at the University of Minnesota Duluth. The SEM, which is equipped with an energy dispersive spectrometer, was used to image and analyze polished thin sections of ore feed and polished grain mounts of pilot plant concentrates to determine the textural and mineralogical occurrence and compositions of PMM in NorthMet ore. In addition, reflected and transmitted light microscopy was used to further evaluate the textural and mineralogic settings of PMM in many of the polished thin sections (PTS).

2.1 Sample Selection

Seventeen PTS of samples collected from NorthMet drill core were investigated for this study (Table 1). These thin sections were borrowed from the archive at the University of Minnesota Duluth's Natural Resources Research Institute (NRRI). Company assay data compiled by Severson and Hauck (2003) were used to sort through the large volume of archived sections. The NRRI thin sections are labeled based on drill hole number followed by sample depth (for example: 26010-116 = hole 26010, depth 116 feet). Assay data are numbered in a similar way (Table 1). Concentration of Pd was used as the indicator of the presence of PGE, as it has been previously documented as the primary PGE in NorthMet ores (Geerts, 1991; Severson & Hauck, 2003). Samples have been selected from various parts of the deposit focusing on areas with greater than 0.5 ppm Pd to assure success in locating multiple minute grains of PGM. The pilot-plant concentrate studied was PolyMet's C5 sample, which was produced in 2007.

Table 1: Drill-hole number, sample location and assay data of samples investigated in this study (NA=not analyzed).

Drill Hole	Depth (Ft.)	Copper%	Nickel%	Sulfur%	Cobalt-ppm	Pt-ppb	Pd-ppb	Au-ppb	Ag-ppm	Unit	Rock Type	From	To
26010	116	4.89	0.4	11.99	328	96	10386	1926	13.3	1	Anorthositic Troctolite	115	117
26010	117	4.89	0.4	11.99	328	96	10386	1926	13.3	1	Anorthositic Troctolite	116	118
26013	103	0.36	0.09	0.47	32	361	2081	164	1.5	1	Troctolitic Anorthosite	102	104
26013	106	0.36	0.09	0.47	32	361	2081	164	1.5	1	Troctolitic Anorthosite	105	107
26013	110	0.36	0.09	0.47	32	361	2081	164	1.5	1	Troctolitic Anorthosite	109	111
26015	266	0.31	0.08	0.39	41	77	278	24	1.1	1	Augite Troctolite	265	267
26015	346	0.45	0.08	0.36	39	130	302	33	2.1	1	Anorthositic Troctolite	345	347
26017	640	0.43	0.08	0.72	52	98	449	36	1.4	1	Augite Troctolite	639	641
26021	103	0.13	0.05	NA	46	127	446	41	0.6	1	Anorthositic Troctolite	102	104
26031	729	0.96	0.23	1.34	79	512	1999	218	2.6	1	Augite Troctolite	728	730
26031	735	0.27	0.09	0.46	54	81	514	77	1.4	1	Augite Troctolite	734	736
26045	372	0.31	0.11	NA	47	107	589	104	1.3	1	Augite Troctolite	371	373
26057	96	0.37	0.11	0.28	49	262	809	58	1.1	1	Augite Troctolite	95	97
26057	101	0.37	0.11	0.28	49	262	809	58	1.1	1	Augite Troctolite	100	102
26096	717	0.67	0.13	0.81	37	204	1171	60	2.3	1	Augite Troctolite	716	718
26143	320	0.1	0.04	0.16	51	65	154	22	0.6	6	Anorthositic Troctolite	319	321
26143	1205	0.02	0.02	0.1	78	65	286	42	1	2	Troctolite	1204	1206

2.2 SEM Analyses and Imaging of PMM in Ore Samples

The SEM is equipped with an Oxford Instruments X-act silicon drift energy dispersive x-ray spectrometer system controlled by the INCA Energy250 software package. Operating conditions were: 20 keV accelerating voltage, objective aperture: 30 μm , spot size: 60, probe current of approximately 1.3 nanoamps, working distance: 10 mm. INCA software was checked for calibration prior to collecting spectral data using the quant optimization feature, with copper as the standardizing element. A small piece of copper tape was placed on the thin section holder and spectra were collected with the quant optimization function. Quant optimization provides spectra from a reference material with which the software adjusts instrument-related parameters used in EDS quantification calculations. Mineral chemical analyses were conducted on discovered PGM phases and on adjacent phases.

Searching for PMM in the 17 PTS was conducted using two strategies. Because PMM are known to have a strong sulfide association, areas rich in sulfide were first scanned for PMM. The SEM was used in backscatter electron composition mode which creates a grey scale image in which brightness positively correlates to increasing average atomic number and density of the phase. To offset the bias induced by this sulfide-centric approach, a second strategy was employed whereby a uniform grid search was conducted. The grid was composed of three traverses along the long axis of the thin section and five lateral traverses. The stage was able to be moved in a frame-by-frame scan at a fixed magnification at regular intervals along either the X or Y axis. This was a time-consuming task, as the optimal magnification for observing 1-2 μm grains of PMM

was 1000x. In this case, one frame is approximately equal in width to the diameter of a strand of human hair (approximately 100 micrometers).

Because PGE and Au-Ag minerals have high atomic numbers, PMM appear as very bright spots in a black background of filtered-out sulfide and silicate minerals. This effect can be enhanced by increasing the brightness and contrast of the digital image produced by the SEM software. The ideal brightness and contrast setting for scanning purposes filtered out all minerals, except those with high atomic number, producing a blacked-out screen image on the computer monitor in which PMM appear as bright, white spots. In order to facilitate navigation of the sample, the view mode could be enhanced with an auxiliary secondary electron image (SEI) where brightness and contrast could be adjusted independent of the backscatter electron (BSE) image. The result of this arrangement is that two images are produced simultaneously: the first is a black screen in BEC mode with nothing visible (the majority of the time) and the second is the SEI which provides location and proof of movement. Searching for PMM is time consuming and perplexing, with many bright grains observed in SEM images initially believed to represent PMM, turning out to be other minerals with high atomic number cations such as galena, nickeline, zircon, and baddeleyite. Incidentally, apatite was usually visible in black-out brightness and contrast settings due inclusion of high atomic number trace elements.

The small size of PMM (1-2 μm) and the nature of energy dispersive spectrometry (EDS) introduce a degree of uncertainty regarding the precise composition of PMM. When incident electrons interact with the sample, characteristic x-rays are

produced from a volume within the sample. These are then measured and processed by the INCA software and outputted as an energy spectrum, with an associated quantifiable analysis. The problem lies in distinguishing spectra generated out of very small PMM from adjacent/ enclosing phases. This is because the volume of excitation is often larger than the precious metal grain of interest. Therefore, when an analysis is being interpreted, x-rays collected may not have physically originated exclusively from within the PMM grain of interest (Reed, 2005). This problem is inherent to electron beam analysis, regardless of whether the tool is an electron microprobe or a SEM: when the particle of interest is micron-scale, characteristic x-rays can be generated from surrounding phases which are difficult to distinguish from those of the particle of interest (Cabri, 2002). Select, located PMM were also investigated with transmitted and reflected light microscopes to further evaluate textural and mineralogical relationships between PGM and surrounding phases.

2.3 SEM Analyses and Imaging of PMM in Ore Concentrates

Ore concentrates were searched and analyzed with the same SEM operating conditions. These polished sections were prepared by Vancouver Petrographics. A process was used in which the concentrate was mounted in epoxy in a puck using a vacuum to impregnate the material, after which it was applied to a glass slide and polished. A textural and mineralogical context does not exist in the concentrate PTS, as a result, these sections were searched using only a grid pattern in which numerous traverses were executed over a wide area of the sample.

2.4 Reflected and Transmitted Microscopy

Select, located PGM were also investigated with transmitted and reflected light microscopes to further evaluate textural and mineralogical relationships between PGM and surrounding phases. This was necessary because some PGM appeared to be anomalously hosted in primary silicate minerals in SEM images. During review of apparent primary silicate-hosted PGM with a transmitted light microscope, it was evident that these PGM are sulfide-hosted because they are in contact with opaque minerals that are not visible in SEM images of the same location and occurrences.

3. RESULTS

A total of 346 precious metal minerals (PMM) were located by SEM scanning of NorthMet ore in this study. Fourteen different types of PMM are identified in this study, although almost 27% of platinum group minerals (PGM) could not be positively identified (Table 2). Seventy-seven percent (267) of these occurrences are hosted by sulfide minerals as inclusions or at sulfide grain boundaries (Table 2; Fig. 6). The remaining 23% of PMM are found in primary silicates, secondary silicates, and apatite (Table 3; Fig. 7). PMM routinely occur as very small (1-2 μm) grains in sulfide, silicate, and apatite at NorthMet (Fig. 8). Of the 346 PMM grains documented in this study, 72% are less than 2 μm (Fig. 8). Grain shapes are generally anhedral, with some subhedral and very few euhedral occurrences along with a small number of vein occurrences.

One of the most significant results of this study that became obvious as the search for PMM progressed is that the PGM and the Au-Ag minerals have very distinct textural occurrences and mineral associations in NorthMet ore. This became particularly apparent when 33 PGM that appear in SEM images to be hosted in primary silicate minerals were found to be associated with sulfide when investigated with transmitted light microscopes, as will be discussed below. This discovery resulted in the recognition that whereas 55% of Au-Ag minerals are hosted in silicate minerals, only 10% of PGM are, and then only in secondary silicates or apatite (Table 3, Fig. 7). Moreover, whereas most PGM occurrences appear as inclusions in or at the margins of sulfide minerals, many Au-Ag mineral occurrences do not appear as distinct inclusions, but rather as discrete grains in

cleavage and fracture in both sulfide and silicates, suggesting that they may be secondary (Figs. 9a-d). Au-Ag minerals are known to be easily mobilized by secondary processes (Li et al., 2007; Wood, 2002 and references therein), therefore the occurrence of gold and silver compounds in cleavage and fracture of primary silicate minerals is not unexpected. Because of their distinct textural occurrences, mineral associations, and likely paragenesis, the 100 Au-Ag minerals and 246 PGM found in this study are described separately.

Table 2: PMM with sulfide mineral associations; cp=chalcopyrite, pn=pentlandite, cb=cubanite; po=pyrrhotite, tn=talnakhite, bn=bornite.

PMM Name	Formula	Total #	Total PMM In Sulfide	Sulfide Host Mineral						Inclusion in sulfide	At Sulfide Boundary	Boundary adjacent to primary silicate	Boundary adjacent to secondary silicate	<50% Enclosed in sulfide
				cp	pn	cb	po	tn	bn					
Kotulskite	Pd(Bi,Te) ₁₋₂	15	11	10	1	0	0	0	0	2	9	7	2	2
Froodite	PdBi ₂	11	11	4	6	1	0	0	0	10	1	1	0	0
Naldrettite	Pd ₂ Sb	3	3	3	0	0	0	0	0	2	1	1	0	0
Paolovite	Pd ₂ Sn	83	78	51	12	9	4	1	1	41	37	28	9	12
Sobolevskite	PdBi	2	2	1	0	0	0	1	0	0	2	1	1	1
Sperrylite	PtAs ₂	25	23	14	5	3	1	0	0	9	14	10	4	6
Stibiopalladinite	Pd ₅ Sb ₂	11	10	9	1	0	0	0	0	1	9	7	2	1
Taimyrite	(Pd, Pt, Cu) ₃ Sn	2	2	2	0	0	0	0	0	2	0	0	0	0
Telluropalladinite	Pd ₉ Te ₄	1	1	1	0	0	0	0	0	1	0	0	0	0
Undetermined PGM		93	81	42	24	5	4	3	3	38	43	29	14	14
TOTALS		246	222	137	49	18	9	5	4	106	116	84	32	36
%			90%	62%	22%	8%	4%	2%	2%	48%	52%	38%	14%	31%
Gold and Silver Minerals														
Acanthite	AgS	16	11	7	3	1	0	0	0	5	6	1	5	5
Empressite	AgTe	2	2	1	0	0	1	0	0	1	1	0	1	1
Hessite	Ag ₂ Te	3	3	1	1	1	0	0	0	3	0	0	0	0
Electrum	AuAg	62	22	12	3	3	3	1	0	14	8	5	3	3
Gold	Au	17	7	3	1	0	3	0	0	4	3	0	3	3
TOTALS		100	45	24	8	5	7	1	0	27	18	6	12	12
%			45%	53%	18%	11%	16%	2%	0%	60%	40%	13%	27%	27%

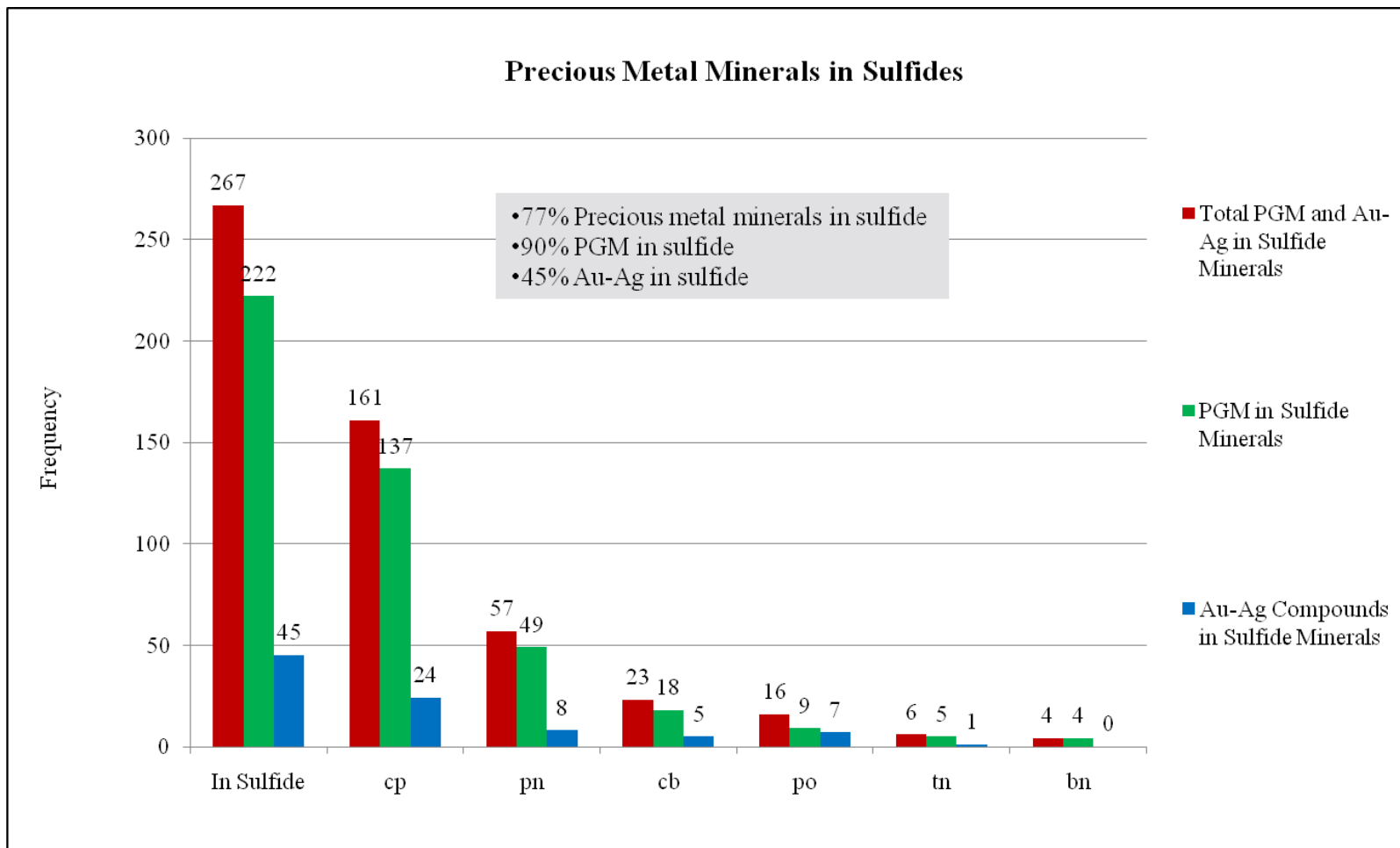


Figure 6: Frequency of sulfide minerals hosting PMM; cp=chalcopyrite, pn=pentlandite, cb=cubanite; po=pyrrhotite, tn=talnakhite, bn=bornite.

Table 3: Non-sulfide mineral associations of PGE minerals distinguished from Au-Ag minerals; High plag=An# >60, Low plag= An# <60, cpx=clinopyroxene, opx=orthopyroxene.

PMM Name	Formula	# Occurrences	In Silicate/ other	High Plag	Low Plag	CPX	OPX	Olivine	Biotite	Chlorite	Sericite	Undetermined Secondary	In Apatite
Kotulskite	Pd(Bi,Te) ₁₋₂	15	4	0	0	0	0	0	0	3	0	0	1
Froodite	PdBi ₂	11	0	0	0	0	0	0	0	0	0	0	0
Naldrettite	Pd ₂ Sb	3	0	0	0	0	0	0	0	0	0	0	0
Paolovite	Pd ₂ Sn	83	5	0	0	0	0	0	2	1	0	0	2
Sobolevskite	PdBi	2	0	0	0	0	0	0	0	0	0	0	0
Sperrylite	PtAs ₂	25	2	0	0	0	0	0	0	1	1	0	0
Stibiopalladinite	Pd ₅ Sb ₂	11	1	0	0	0	0	0	0	1	0	0	0
Taimyrite	(Pd, Pt, Cu) ₃ Sn	2	0	0	0	0	0	0	0	0	0	0	0
Telluro-palladinite	Pd ₉ Te ₄	1	0	0	0	0	0	0	0	0	0	0	0
Undetermined PGM		93	12	0	0	0	0	0	1	4	1	2	4
TOTALS		246	24	0	0	0	0	0	3	10	2	2	7
%			10%	0%	0%	0%	0%	0%	1%	4%	1%	1%	3%
Gold and Silver Minerals													
Acanthite	AgS	16	5	0	1	0	0	1	0	0	1	2	0
Empressite	AgTe	2	0	0	0	0	0	0	0	0	0	0	0
Hessite	Ag ₂ Te	3	0	0	0	0	0	0	0	0	0	0	0
Electrum	AuAg	62	40	5	2	5	0	7	11	3	0	0	7
Gold	Au	17	10	0	0	3	0	2	2	3	0	0	0
TOTALS		100	55	5	3	8	0	10	13	6	1	2	7
%			55%	5%	3%	8%	0%	10%	14%	6%	1%	2%	7%

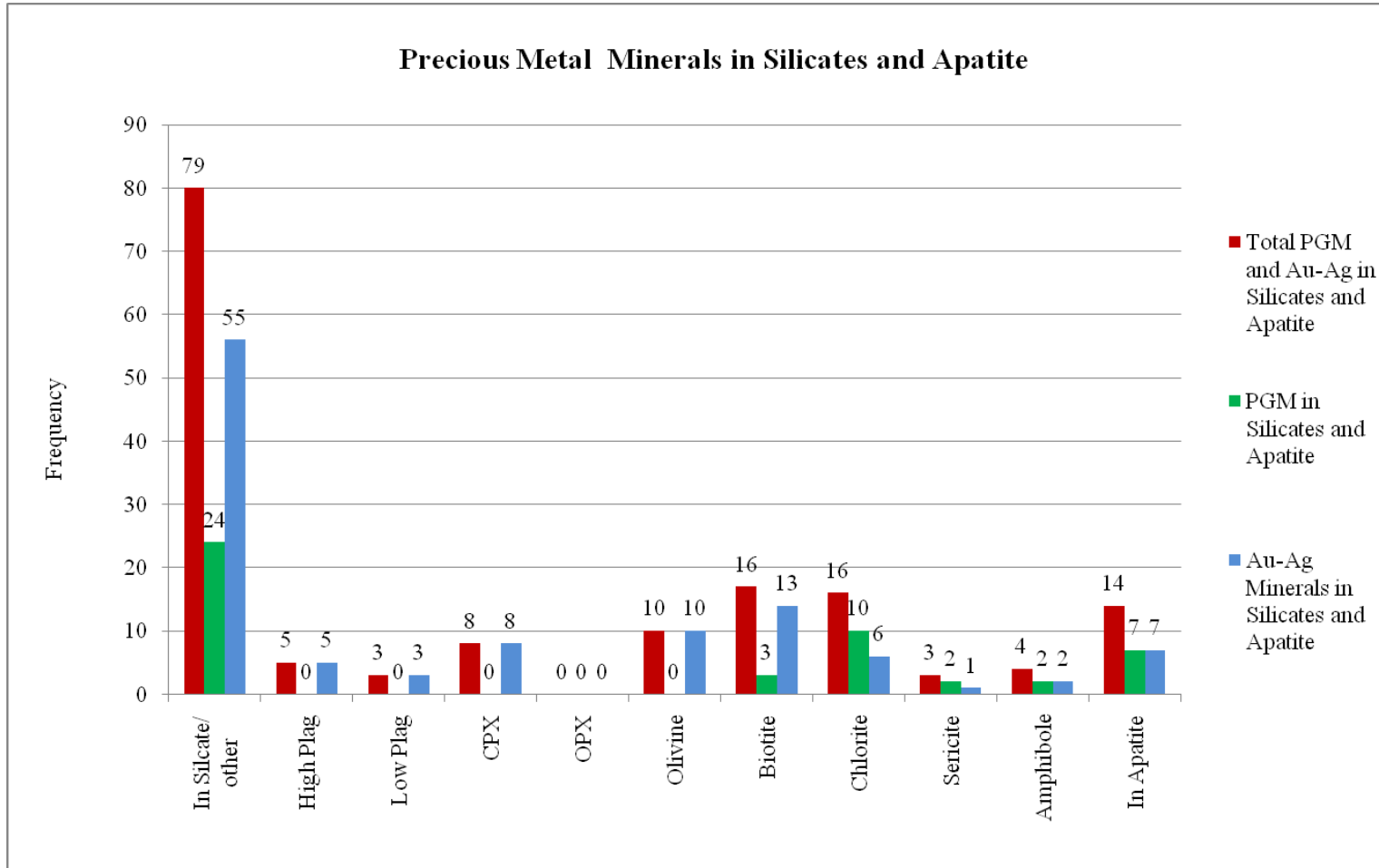


Figure 7: Frequency of silicate minerals hosting PMM (based on SEM EDS data).

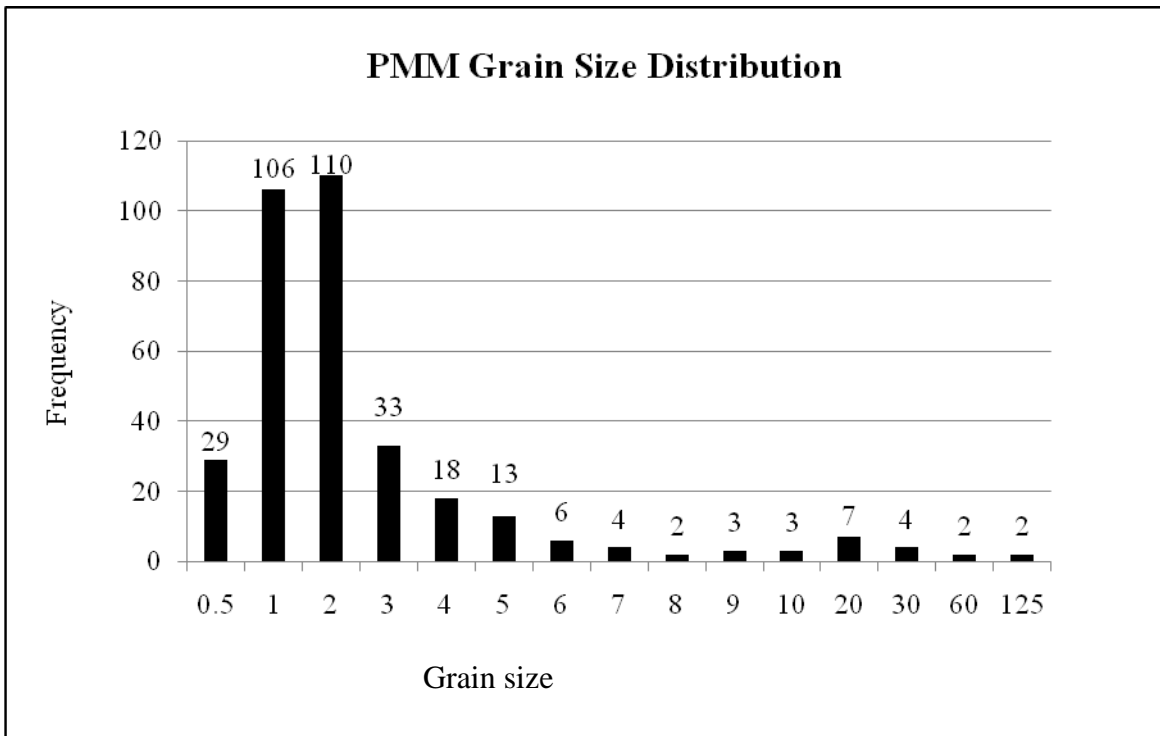


Figure 8: Grain size distribution of 346 PMM.

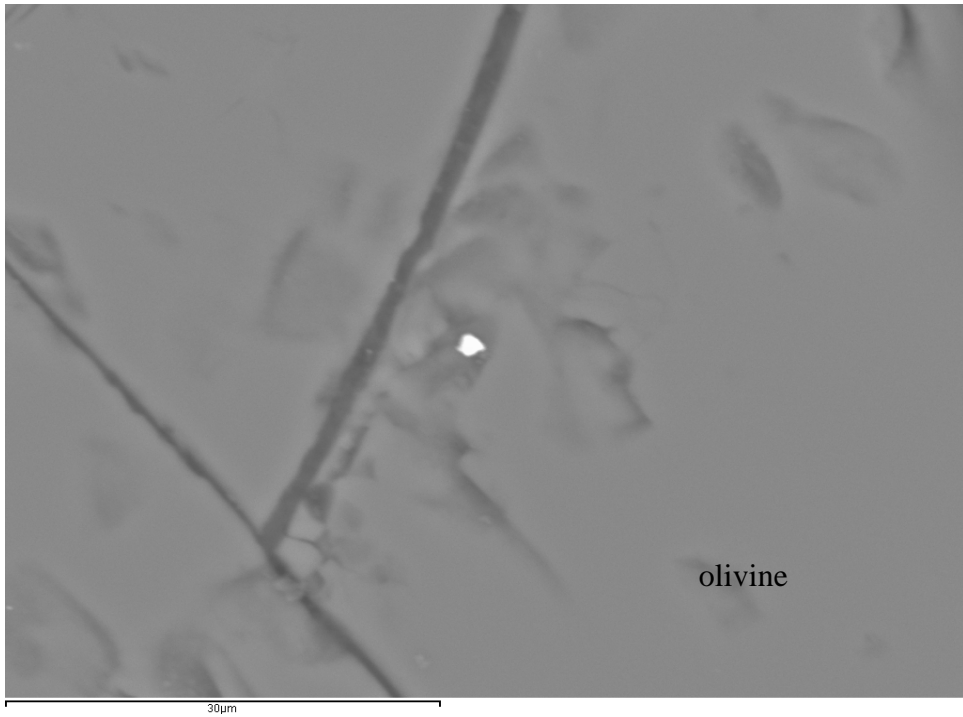


Figure 9a: Gold grain in olivine fracture, scale bar is 30 μm (Site 5: 26015-266)

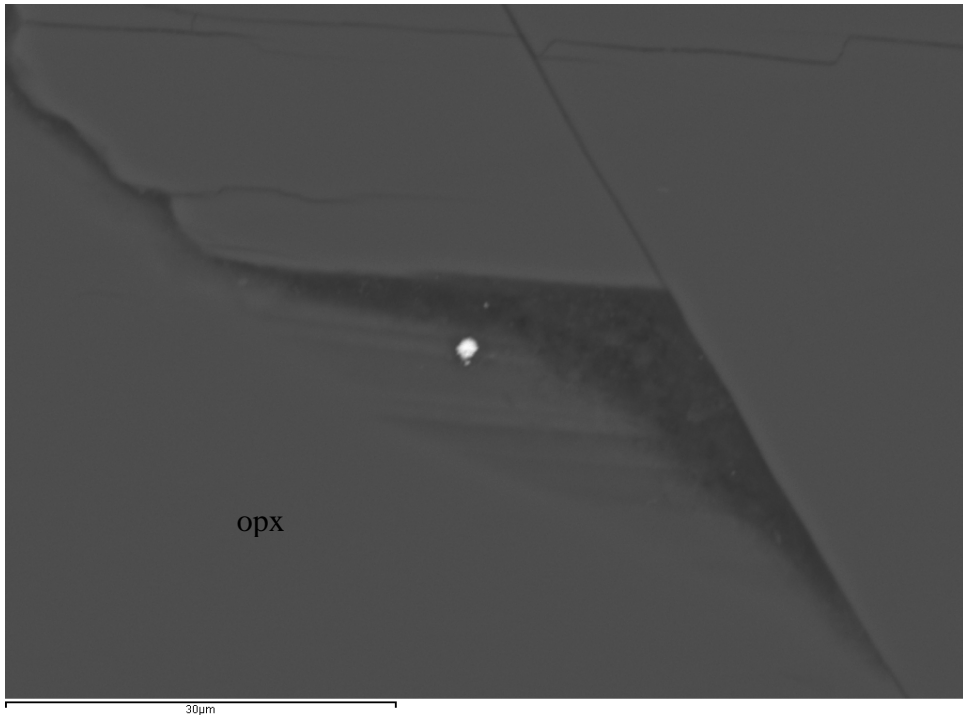


Figure 9b: Electrum grain in orthopyroxene cleavage, scale bar is 30 μm (Site 28: 26015-266).

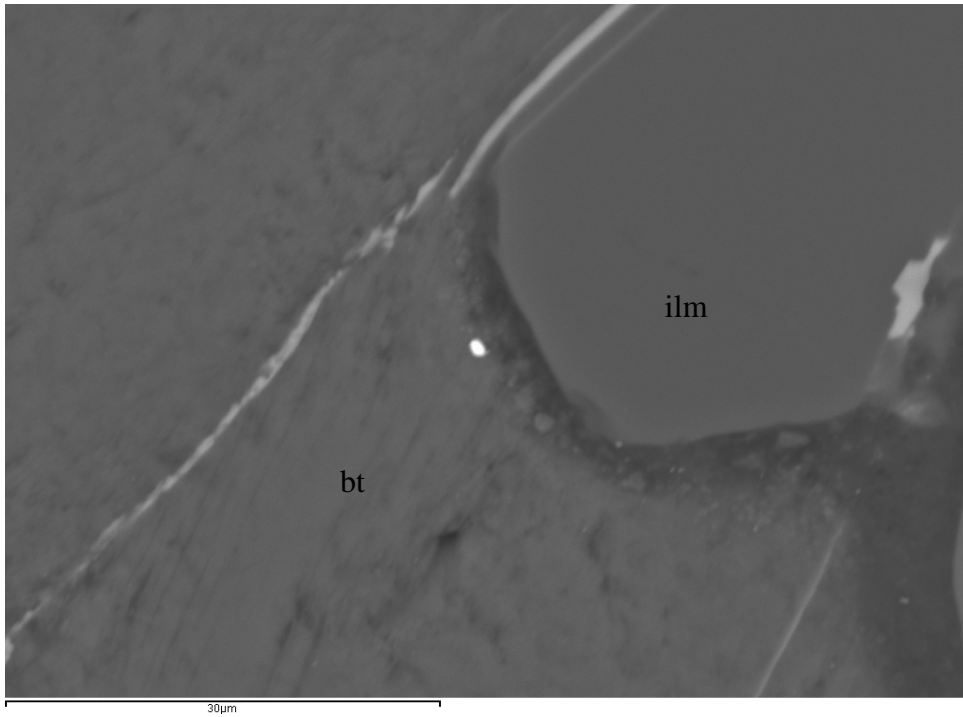


Figure 9c: Electrum grain at boundary between biotite and ilmenite, scale bar is 30 μm (Site 23: 26015-266).

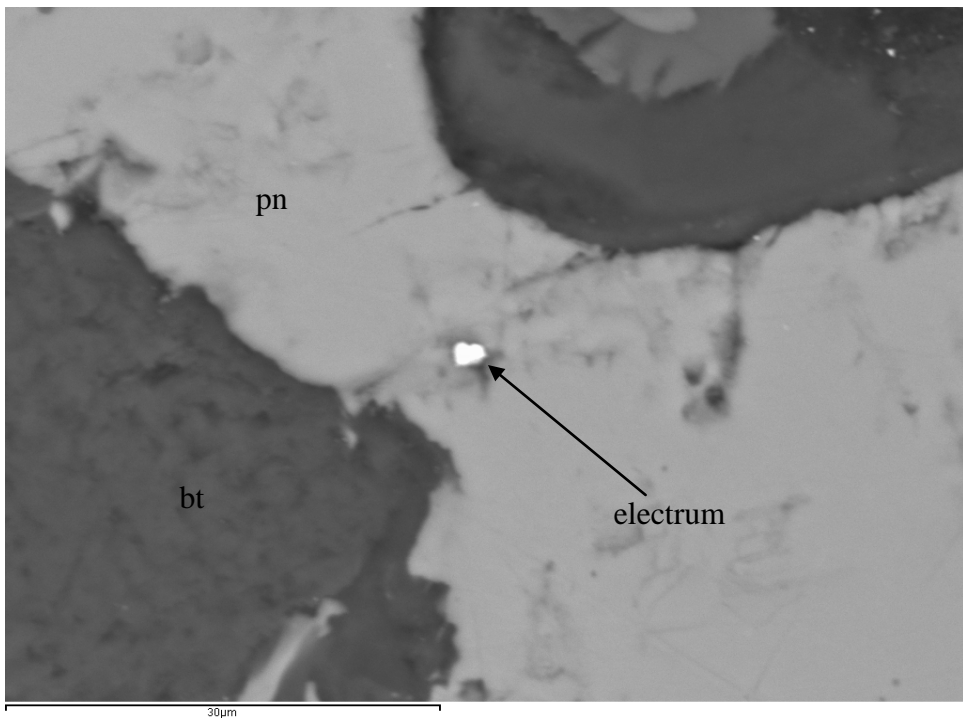


Figure 9d: Electrum grain in pentlandite fracture, scale bar is 30 μm (Site 2: 26015-266).

3.1 Gold and Silver Minerals

Five different gold and silver minerals have been identified in this study. In order of decreasing abundance, these minerals are electrum (AuAg), gold (Au), empressite (AgTe), hessite (Ag₂Te), and acanthite (Ag₂S). The mineralogical occurrences of Au-Ag minerals are distributed almost evenly among sulfides (45%) and silicates (55%, including apatite). Of the Au-Ag in silicates, 47% are located in primary silicates: plagioclase, olivine, clinopyroxene, and orthopyroxene and the remainder are located in secondary silicates and apatite (Table 3, Fig. 7).

There are 26 Au-Ag minerals that occur in primary silicates. Review of SEM BEC photomicrographs of these Au-Ag occurrences indicates that Au-Ag in primary silicates typically occur as discrete grains in fractures and cleavage of these minerals and that the Au-Ag minerals are not distinct inclusions in primary silicates. Frequently, these appear to exist on the surface of the primary silicate (Figs.9a-b). These Au-Ag occurrences were not investigated with reflected or transmitted light microscopes.

Of the 45 Au-Ag minerals with a sulfide association, 27 Au-Ag minerals appear as inclusions and 18 occur at sulfide grain boundaries. Within the inclusion category, five occur as distinct inclusions and these are interpreted as a primary igneous texture, i.e., there is an obvious enclosing relationship between the Au-Ag mineral and the host sulfide (Fig. 10). It is not entirely clear if the remaining twenty-two minerals in the inclusion category are inclusions or are on the surface of sulfides in fractures or recesses, rather than intergrown with the sulfide, as would be expected with coeval crystallizing

minerals. For example, is a PMM an inclusion if it resides in fracture (e.g. Fig. 9d)? This grain could be interpreted as an inclusion or simply that it exists on the surface of the sulfide.

Secondary electron images (SEI) of Au-Ag minerals demonstrate that many Au-Ag minerals are topographically higher than adjacent sulfides and silicates and that Au-Ag grains do not appear to be intergrown with adjacent minerals, but rather, they exist as discrete grains (Fig. 11). Au-Ag minerals that occur as discrete grains in sulfide fracture and cleavage are interpreted to represent secondary mineral occurrences, rather than primary. Interestingly, this type of Au-Ag occurrence is rarely vein-shaped and tends to occur as equant grains at fracture and cleavage of sulfides and silicates or at boundaries between sulfides, silicates, and oxides (Figs. 9a-d).

The wide distribution and apparent mobility of Au-Ag minerals within the samples investigated during this study was exemplified when it was discovered that an electrum grain that had previously existed within pentlandite fracture (Fig. 9d), was no longer present during subsequent investigation of the same location in the sample (Fig. 12). The sequence of events that led up to this discovery provides insight into how this happened. In order to eliminate charge build-up in the samples, they were carbon-coated prior to viewing with the SEM. After that, the carbon was removed with polishing compound and a polishing cloth on some PTS so that the carbon film would not limit light from passing through the sample during additional review of select samples with a light microscope. Subsequent to that, one PTS was re-coated with carbon to facilitate further review (# 26015-266) with the SEM. The electrum that had previously existed

within a recess in cubanite was no longer visible using identical SEM operating conditions to the ones used when the electrum was initially discovered.

This gives significant support to the observation that many Au-Ag minerals appear to exist as grains on the surface of silicates and sulfides and additionally, that they are not well adhered to host minerals. Furthermore, the mineralogical and textural occurrence of Au-Ag minerals within the sample set begs the question: if the electrum grain in Figure 9d was removed as a result of light polishing, how much movement of Au-Ag minerals occurred during the preparation of polished thin sections? This also has implications for beneficiation: if Au-Ag minerals are poorly adhered and possibly widely distributed, they are likely to be separated from sulfide during grinding processes, if in fact they were attached to sulfide in the first place.

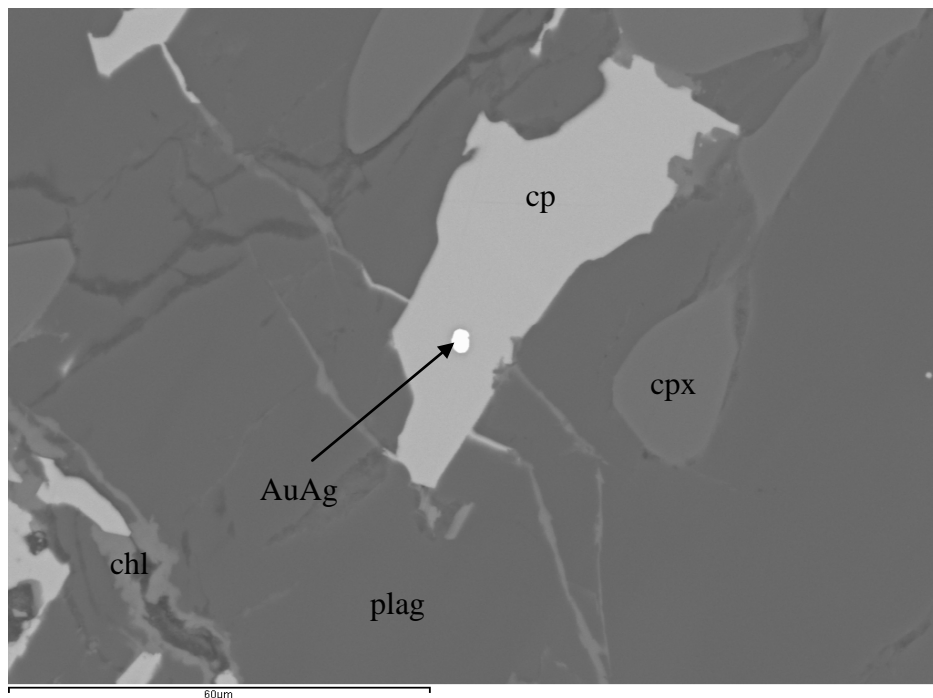


Figure 10: Distinct inclusion of electrum in chalcopyrite, scale bar is 60 μm (Site 1: 26013-106).

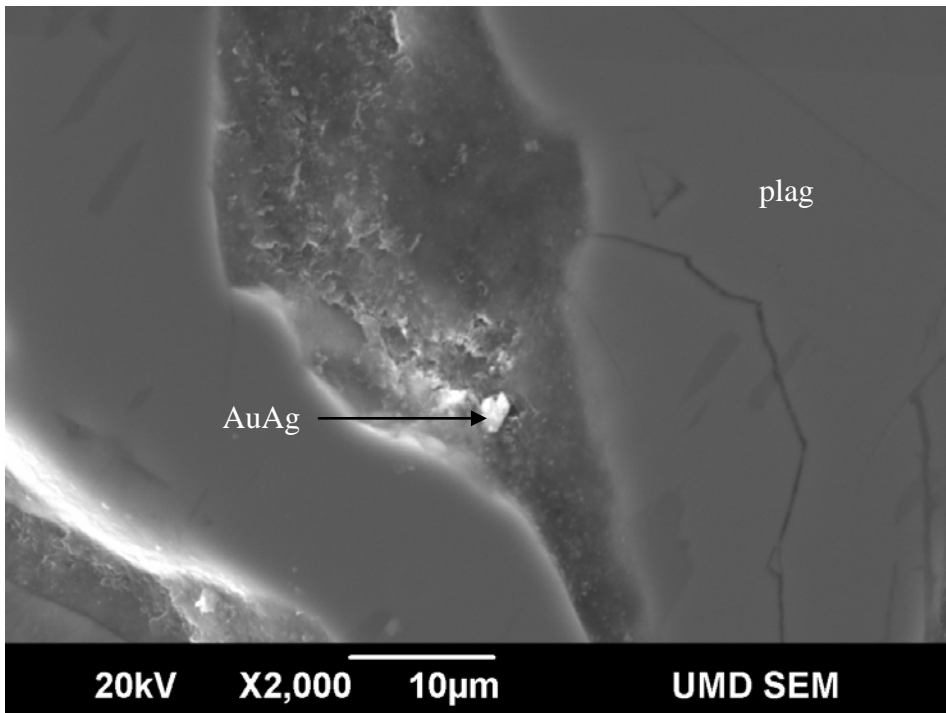


Figure 11: Secondary electron image of electrum grain in recess within plagioclase (Site 33: 26096-717).

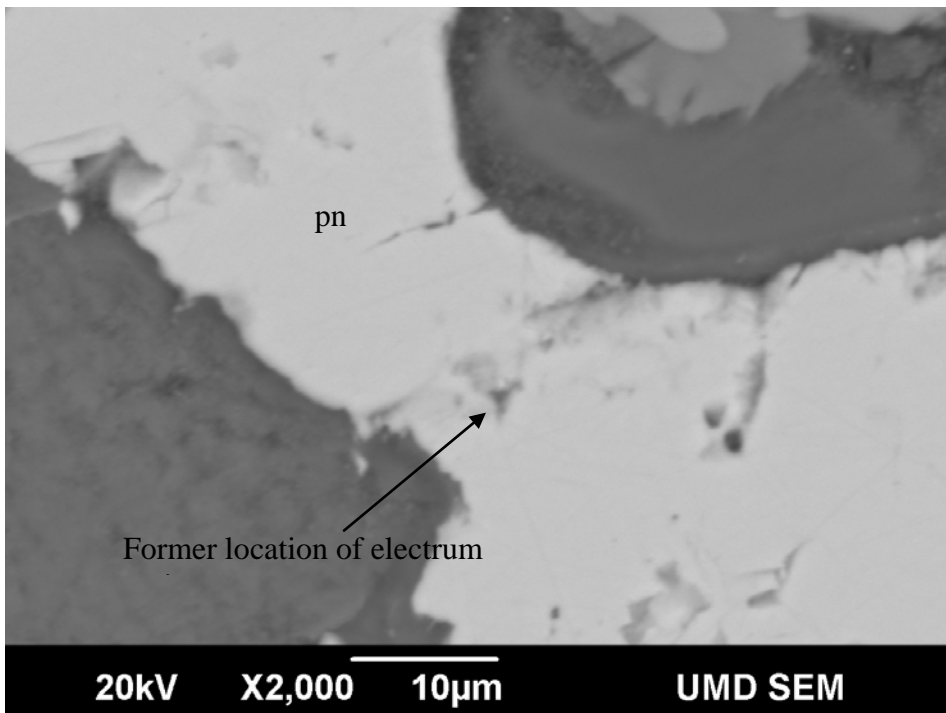


Figure 12: Former location of electrum grain in pentlandite fracture, see figure 12d, (Site 2: 26015-266).

3.2 Platinum Group Minerals

Nine PGM were positively identified by the stoichiometry of their elemental abundances in this study. In order of decreasing abundance, these are: paolovite (Pd_2Sn), sperrylite (PtAs_2), kotulskite ($\text{Pd}(\text{Bi},\text{Te})_{1-2}$), froodite (Pd_2Sb), stibiopalladinite (Pd_5Sb_2), naldrettite (Pd_2Sb), taimyrite ($(\text{Pd}, \text{Pt}, \text{Cu})_3\text{Sn}$), sobolevskite (PdBi), and telluro-palladinite (Pd_9Te_4). Paolovite (Pd_2Sn) is the most common identifiable PGM (24%). The largest category of PGM (27%) is PGM of undetermined or unknown type (Table 2). Elements common in PGM of the undetermined category are: palladium, platinum, tin, antimony, bismuth, and tellurium. Numerous named and un-named PGE minerals are known to exist (Cabri, 2002). Many of the PGM analyses conducted during this study do not represent known PGM stoichiometric ratios. The uncertainty in the type of PGM may result from several causes:

- 1) the PGM grain is a complex alloy, or has unique or complex composition that is not easily attributed to PGM that are documented in the literature;
- 2) the characteristic x-rays generated from the PGM cannot be distinguished from those of surrounding minerals due to the small size of PGM and elements that may exist in both the PGM and the enclosing mineral; and
3. the small size of PGM grains may cause inaccurate ratios of characteristic x-rays to be generated from the grain of interest.

To the last point, Cabri (2002) has noted that microprobe data are sometimes suspect due in part to standardless quantification used in electron beam analysis and the small size of

the PGM grains, which produce unreliable x-ray spectra. Although over a quarter of the PGM analyzed in this study cannot be positively identified, this is of little consequence to the larger goal of this project: to determine the mineralogical and textural context of PGM and Au-Ag in NorthMet ore.

3.3 Platinum Group Mineral Occurrences in Sulfide Minerals

Ninety percent of the PGM located in NorthMet ores are spatially and texturally related to sulfide minerals. Based on SEM BEC imaging, most PGM appear to occur as inclusions in sulfides (e.g., Figs. 15b & 16c) and at sulfide grain boundaries (e.g., Figs. 17c & 18). Inclusions and boundary occurrences represent 48% and 52% of PGM occurrences in sulfide minerals, respectively (Fig. 6, Table 2). The abundance of PGM as inclusions in sulfide may be an overestimate, given recent 3D (Godel et al., 2010: x-ray computed tomography) and 2D imaging studies (Holwell & McDonald 2010: laser ablation inductively coupled plasma mass spectrometry) of PGM in sulfide minerals. Both studies show that PGM grains occur primarily at sulfide grain boundaries. Moreover, the research of Godel et al. (2010) determined that less than seven volume percent of PGM in samples investigated from the Merensky Reef of the Bushveld Complex were totally enclosed in sulfide. Previous 2D studies of the same samples appeared to indicate that 33% of PGM were enclosed in sulfide. This demonstrates the limits of 2D analysis and the high (> 90%) occurrence of PGM at sulfide grain boundaries. If a comparable proportion of NorthMet PGM observed as inclusions in 2D, instead occur at sulfide grain boundaries, then the actual percentage of boundary PGM occurrences may approach 90%.

The potential for 2D imaging by SEM-BEC and reflected light microscopy to result in misleading interpretations was revealed in this study. After the full inventory of PGM occurrences was first tabulated from SEM-BEC imaging, 33 occurrences appeared to be inclusions in primary silicates. Given that platinum group elements are strongly

incompatible in silicates (Naldrett, 2004; Mungall, 2005) this relationship, if true, had profound implications for the metallogensis of PGM and compelled further investigation. As will be discussed at the end of the results section, transmitted and reflected light petrography revealed that all these apparent primary silicate occurrences were actually associated with sulfide boundary occurrences deeper in the section.

Chalcopyrite (CuFeS_2) is the dominant sulfide in NorthMet ore body (Morton and Hauck 1987; Geerts, 1991) and is host to 62% of the sulfide-hosted PGM in this study (Table 2, Fig. 6). PGM occurrences in chalcopyrite are more than double the number of occurrences observed in pentlandite, the next most abundant PGM sulfide host mineral. Other sulfides documented and listed in decreasing order are cubanite (CuFe_2S_3), pyrrhotite (Fe_{1-x}S), talnakhite ($\text{Cu}_9(\text{Fe}, \text{Ni})_8\text{S}_{16}$), and bornite (Cu_5FeS_4) (Table 2). Two PGM occurrences were hosted by nickeline (NiAs). Cu-Fe-S and Fe-Ni-S Compositions of sulfide host minerals are illustrated in Figures 13 and 14, respectively. These sulfides all appear enriched in sulfur and plot above the ideal location of the respective sulfide minerals. This is likely a result of the generic internal standards within the INCA EDS software. EDS analytical data for PMM and host minerals can be found in Appendix A.

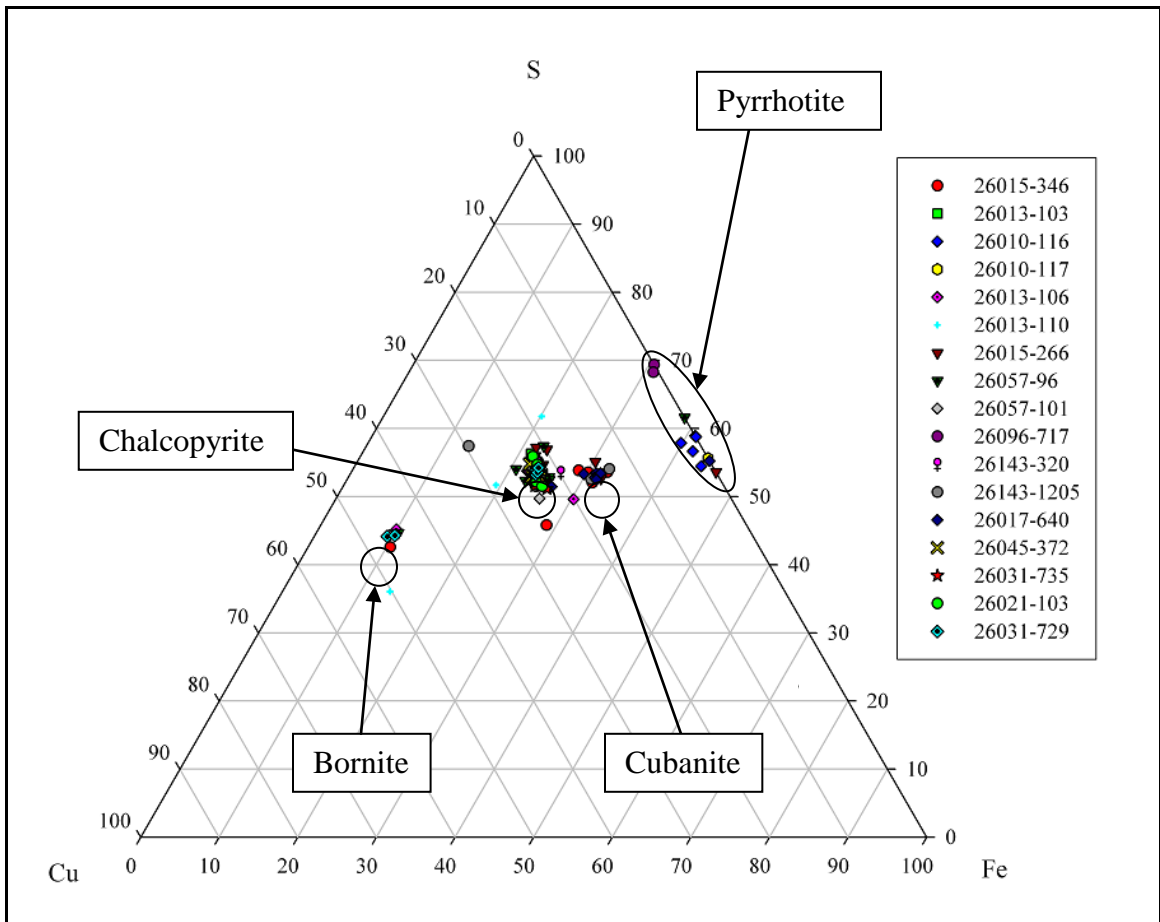


Figure 13: Cu-Fe-S compositions of sulfide minerals hosting PMM (in percent cations).

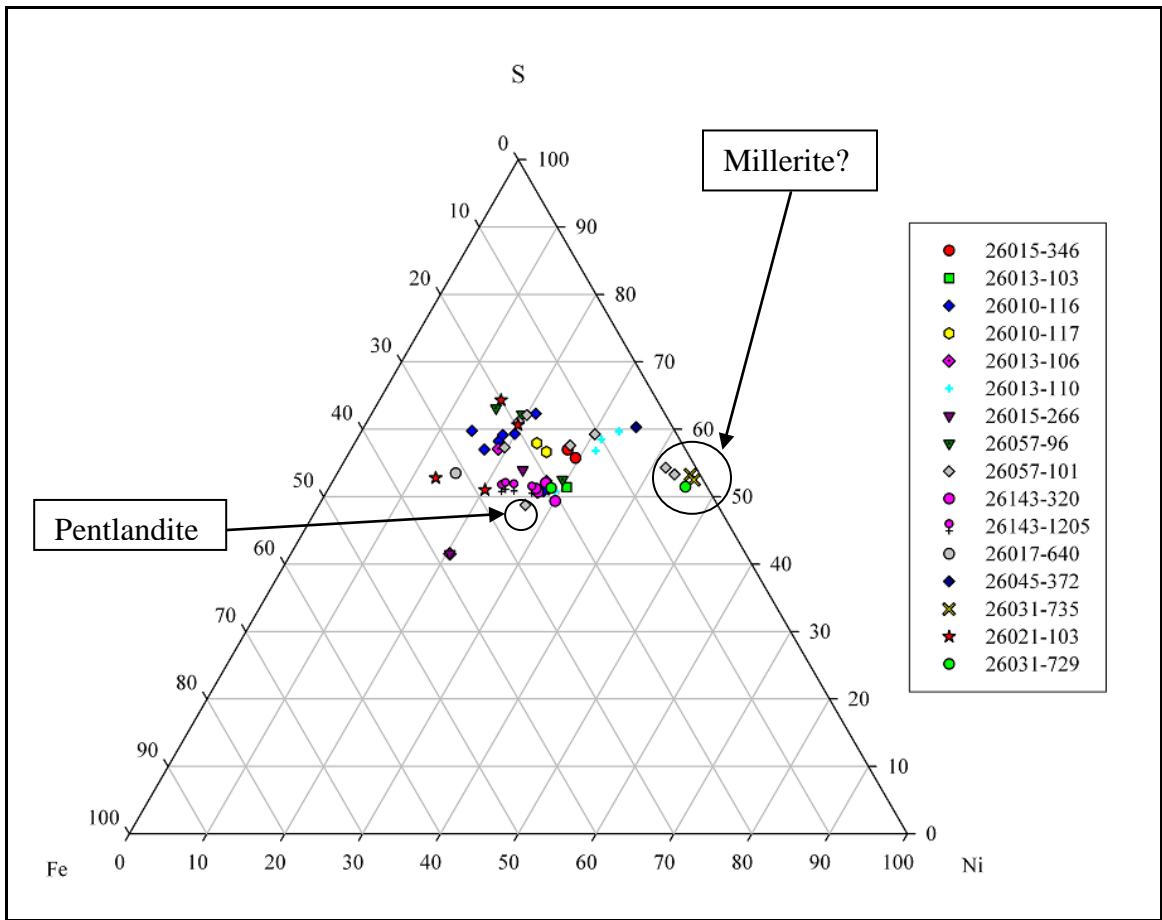


Figure 14: Fe-Ni-S compositions of sulfide minerals hosting PMM (in percent cations).

Sulfide-hosted PGM most commonly occur in areas of fine-grained sulfide inclusions in primary silicate minerals that form halos around larger sulfide grains (Figs. 15a, 16a, & 17a). These halo sulfides are typically enriched in copper relative to the larger sulfides they surround. They are usually chalcopyrite grains with bornite, cubanite, and pentlandite intergrowths (Fig. 15b). Usually the halo sulfide grains are aligned with cleavage or twinning direction of the host silicate, particularly in plagioclase (Fig. 15a). Examples of PGM interpreted to be inclusions in halo sulfides are illustrated in Figures 15b and 16c.

Fine-grained halo sulfides primarily occur in the outer zones of plagioclase grains, but also in rims of clinopyroxene and orthopyroxene, suggesting the possibility that sulfide minerals are a later-forming phase and they become enclosed in the perimeters of adjacent coeval silicate cumulus minerals (Figs. 16a & 17a). Previous studies in the Duluth Complex have documented sulfide halo textures (Foose and Weiblen, 1986; Geerts, 1994; Marma, 2002, Severson and Hauck 2003). Fine-grained sulfide halo texture has been attributed to a combination of primary magmatic processes and chlorine-rich fluids and associated hydrothermal alteration and mobilization/ concentration of PGM (Foose and Weiblen, 1986; Marma, 2002). Other authors suggest that halo textures result from magmatic processes (Geerts, 1994; Komppa, 2002; Severson and Hauck, 2003).

Of the 116 observed PGM sulfide boundary occurrences, 84 are adjacent to primary silicates and 32 were adjacent to secondary silicates (Table 2, Fig. 6). Plagioclase is the most common primary phase in contact with PGM occurrences at sulfide boundaries, followed by clinopyroxene, orthopyroxene, and olivine. Chlorite is

ubiquitous and accounts for the majority of secondary silicate in contact with PGM, followed by amphibole and sericite. Sulfide boundary PGM are usually tenuously connected to the sulfide host (Fig. 18). Based on images of 116 PGM boundary occurrences, 36 (31%) of sulfide boundary occurrences are more than half enclosed in adjacent silicate minerals (Table 2). Of these 36 sulfide boundary PGM occurrences that are mostly enclosed in adjacent silicates, 28 are in primary silicates and 8 are in secondary silicates.

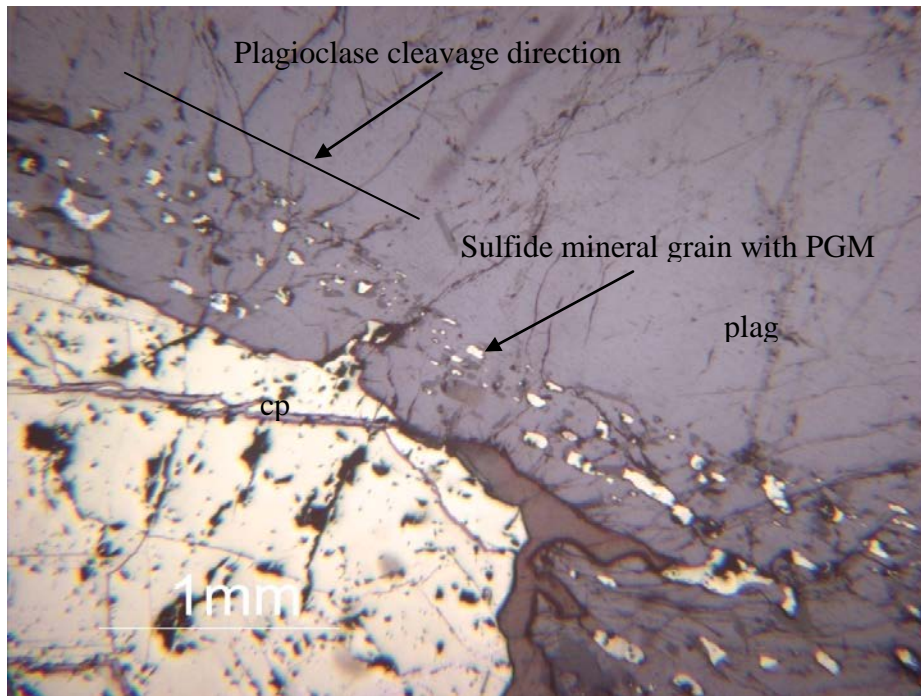


Figure 15a: Fine-grained sulfide minerals as inclusions in plagioclase forming a halo around a larger sulfide grain (reflected light) (Site 20: 26057-101).

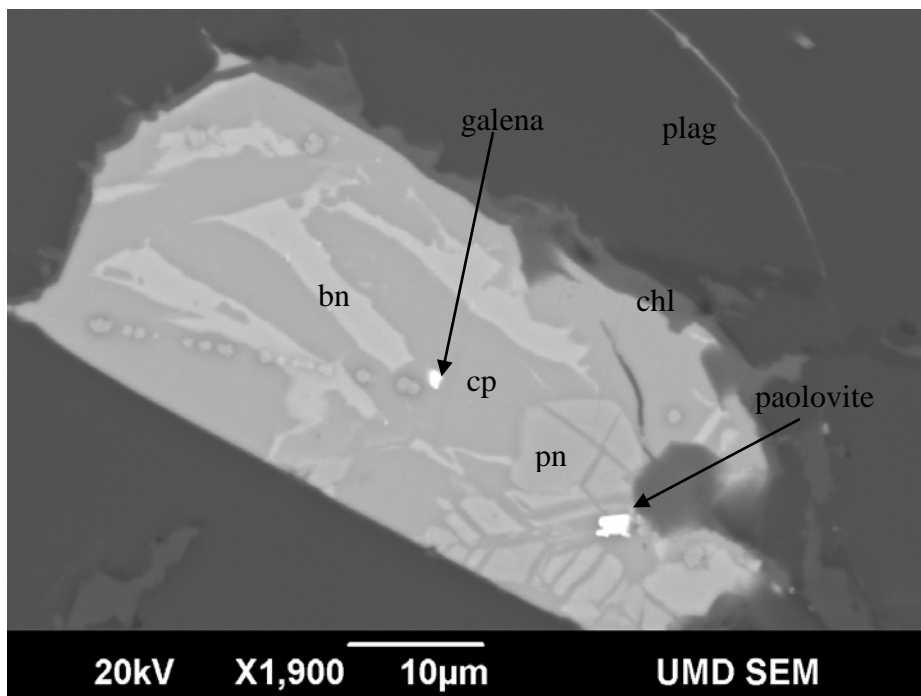


Figure 15b: BEC image of paolovite inclusion in multi-sulfide grain (Site 20: 26057-101).

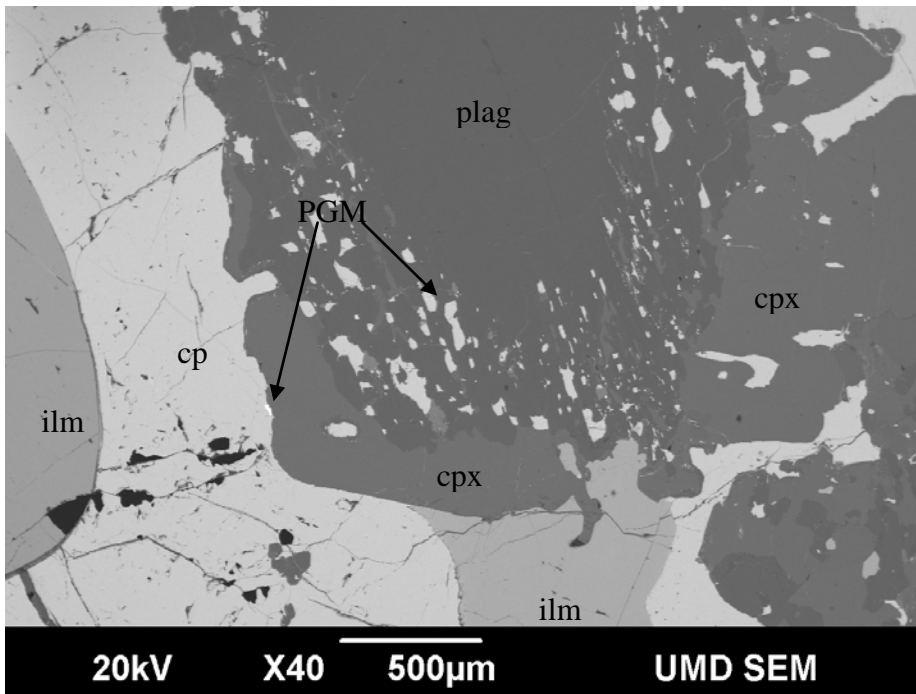


Figure 16a: BEC image of fine-grained sulfide halo with multiple PGM around perimeter of larger sulfide grain; plag=plagioclase, cpx=clinopyroxene, ilm=ilmenite; (Sites 11 and 15: 26013-106).

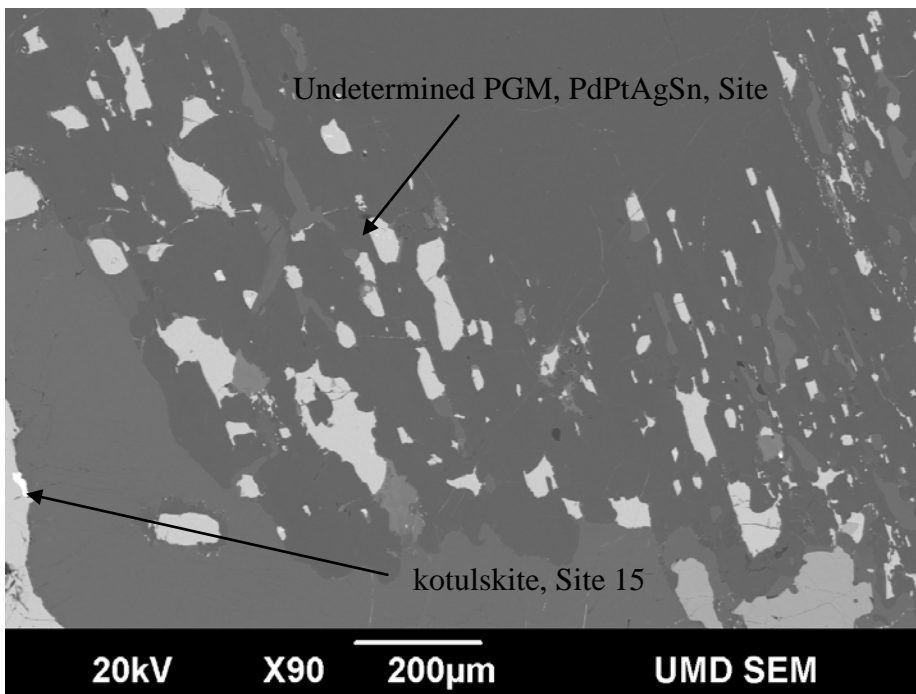


Figure 16b: BEC image of fine-grained sulfides with PGM (Sites 11 and 15: 26013-106).

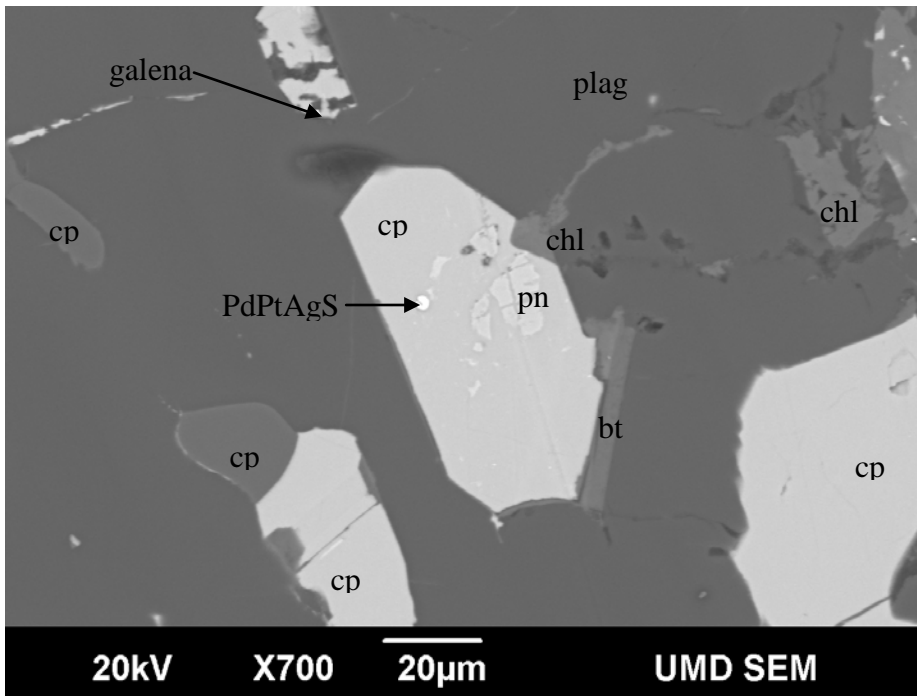


Figure 16c: BEC image of Undetermined PGM inclusion in multi-sulfide grain; bt=biotite, chl=chlorite; (Site 11: 26013-106).

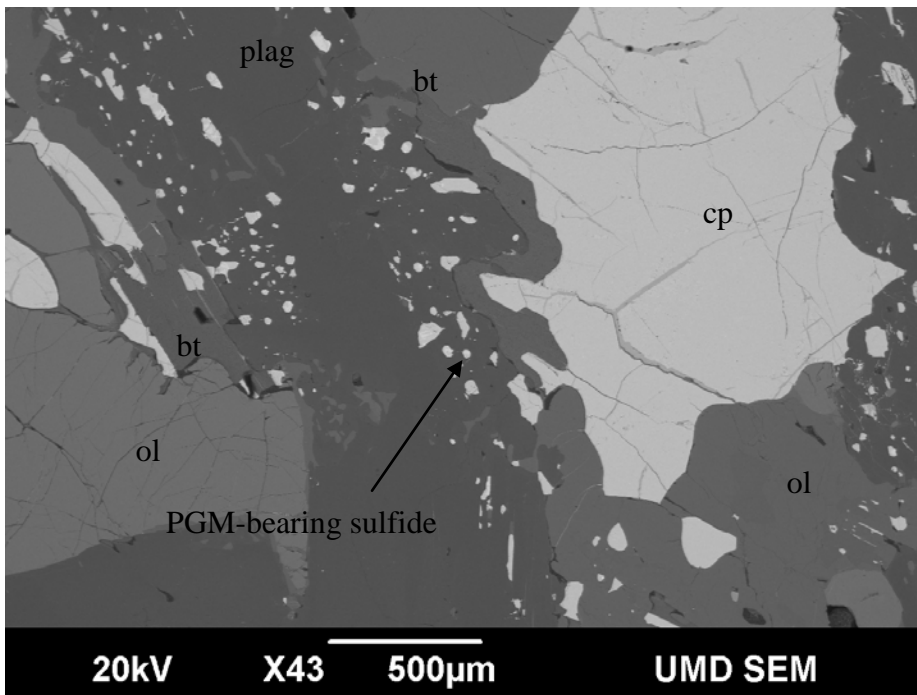


Figure 17a: BEC image of fine-grained interstitial sulfides typical of PGM occurrence (Site 2: 26057-96).

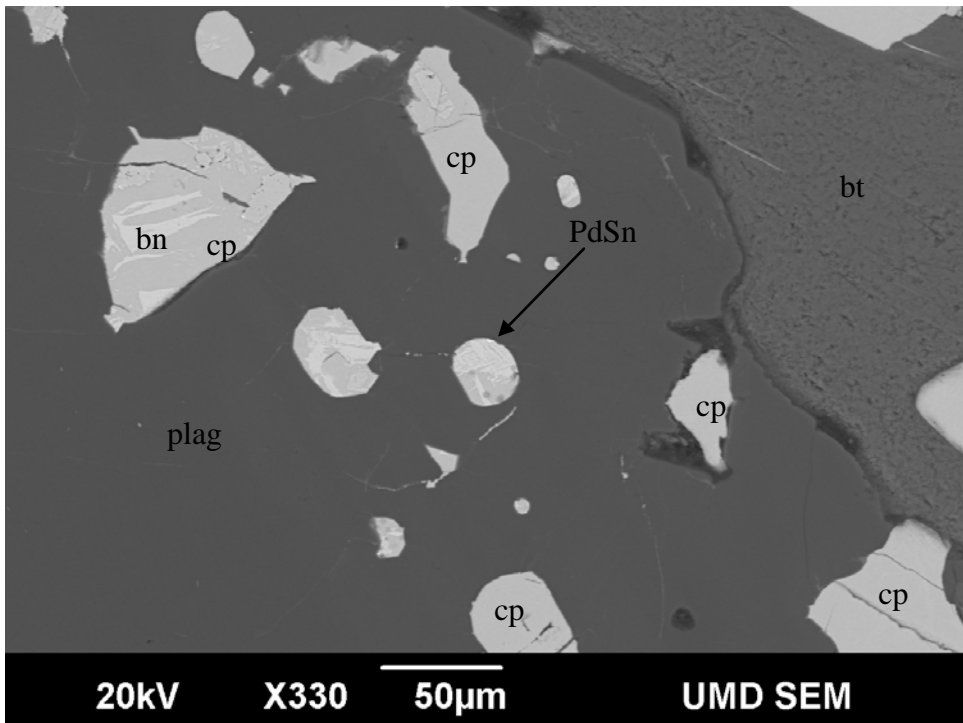


Figure 17b: BEC image of fine-grained sulfides and boundary PGM occurrence (Site 2: 26057-96).

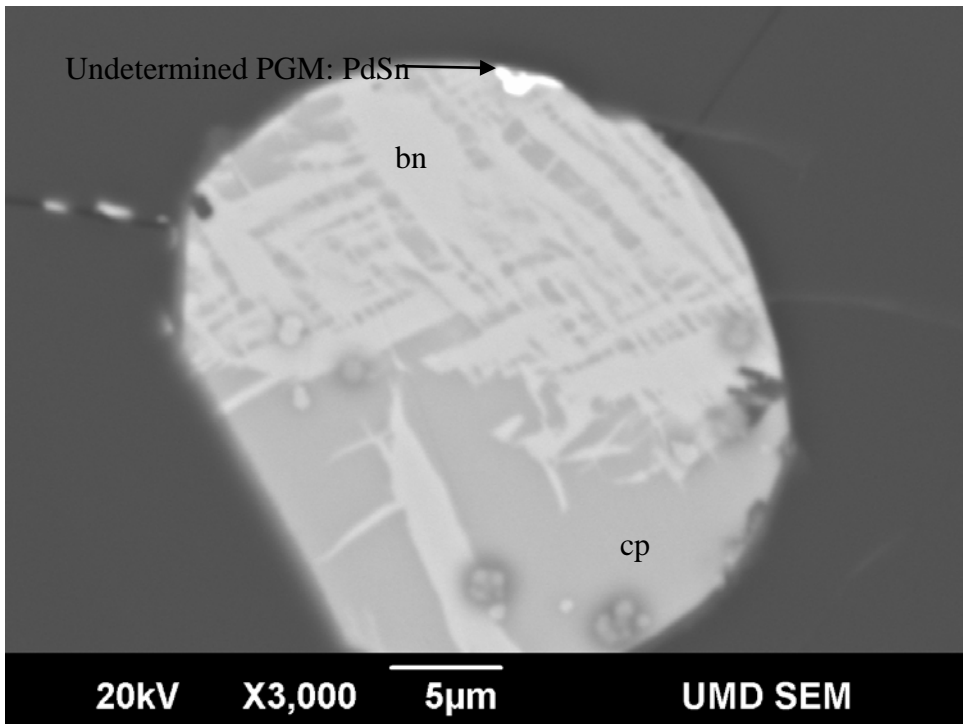


Figure 17c: Sulfide boundary PGM occurrence (Site 2: 26057-96).

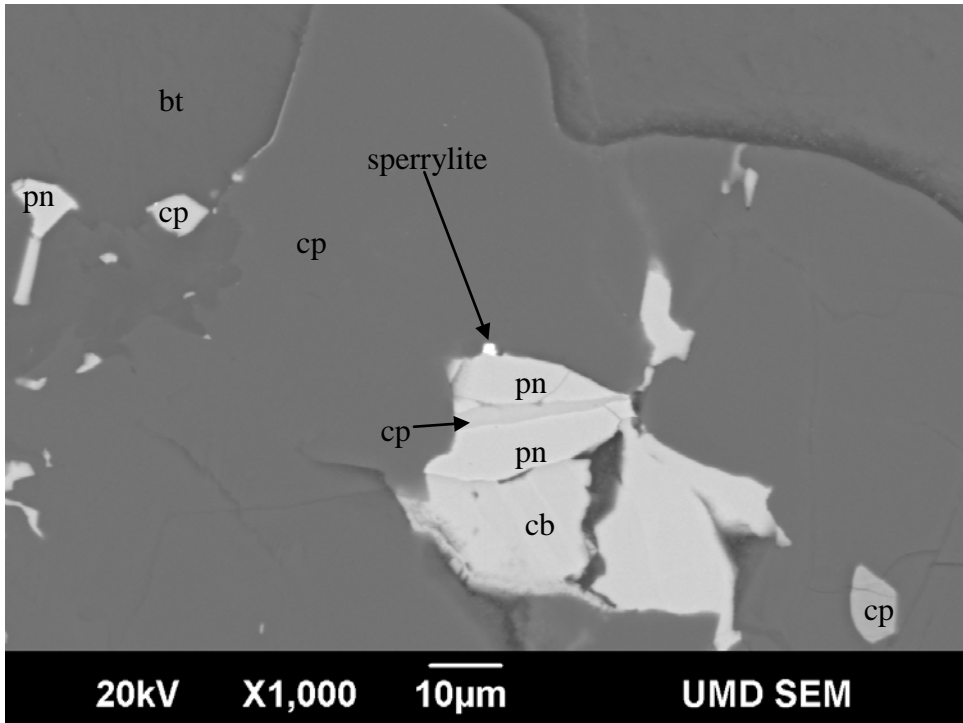


Figure 18: Sulfide boundary PGM occurrence in which PGM is <50% enclosed in sulfide (Site 10: 26013-106).

3.4 Platinum Group Mineral Occurrences in Secondary Silicates and Apatite

PGM in secondary silicates and apatite typically occur in close association with sulfide minerals, usually less than 500 μm distant from sulfides and appear to be isolated from sulfides by dissolution of sulfide and replacement by secondary silicate minerals. Of the secondary minerals that enclose PGM, chlorite is the most abundant, followed by undetermined alteration minerals (most likely actinolite and hornblende), and sericite (Table 2). The physical characteristics of undetermined secondary minerals are mostly clear to pale green in plane light with moderate relief and low to middle second order interference colors, similar to actinolite and tremolite. Like sulfide-hosted occurrences, PGM in secondary silicates and apatite are generally found in areas enriched in sulfide (Figs. 19 and 20a)

The category “In Apatite” in Table 3 was originally created with the intent of identifying PMM that were entirely enclosed in apatite. To interpret and categorize PMM in apatite requires a somewhat subjective decision because mineralogical enclosing relationships are not always obvious. Table 3 indicates that 7 PGM and 7 Au-Ag minerals are in apatite, but even these 14 occurrences are all observed to be close to ($\leq 500 \mu\text{m}$) or in contact with sulfide and are not completely enclosed in apatite. A PMM that is in contact with apatite is notable because apatite is known to be associated with late, chlorine-bearing aqueous liquids in crystallizing magmas (chloro-apatite), and because chlorine-rich fluids have been previously cited as a mechanism for concentrating PMM in Cu-Ni-PGE deposits (Foose and Weiblen, 1986; Boudreau & McCallum, 1992; Severson, 1994).

Figure 19 illustrates an exceptionally large, euhedral sperrylite crystal that is in minor contact with chloro-apatite and chalcopyrite that has been classified as a sulfide boundary occurrence (see Appendix A EDS data for analytical data). Sperrylite accounts for the majority of euhedral PGM occurrences and is also commonly larger than other PGM located during this study. Incidentally, some of the paolovite grains located in this study were euhedral to subhedral but most paolovite did not exhibit a well-formed crystalline shape; all the other PGM did not exhibit euhedral crystal habit. The image in Figure 19 shows a large apatite crystal that is intergrown with chalcopyrite. The sperrylite crystal is mostly enclosed in unaltered plagioclase, indicating that the liquids from which the apatite crystallized did not significantly react with adjacent plagioclase and that deuteric alteration is minimal. This image and others like it do not illustrate any definitive relationship with PGM occurrence and apatite. A total of seven PGM (3% of all PGM) located in this study are in contact with or close (≤ 1 mm) to apatite. This relatively small percentage of apatite associations is overwhelmed by PGM with sulfide associations (90%) and does not support a model in which chlorine-rich fluids are the primary mechanism by which PMM are concentrated in NorthMet.

Dissolution of sulfide and replacement by secondary silicate leading to isolation of seemingly un-reactive PGM is well illustrated in Figures 20(a-c). In this occurrence, fine-grained sulfides are aligned with plagioclase cleavage and occur as a halo surrounding a relatively larger chalcopyrite grain. A network of chlorite alteration veins surround a somewhat rectangular PGM-bearing chalcopyrite grain. The original rectangular shape of the chalcopyrite grain can be discerned by the area of chlorite that

now mantles it. Two of four large PGM grains occur in chlorite sandwiched between plagioclase and chalcopyrite and at the corner of what appears to have originally been the chalcopyrite grain. Interestingly, the two PGM grains in the chlorite have the same subhedral granular shape as the grains still enclosed in sulfide.

Given the prevalence and frequency of sulfide boundary PGM noted in this study (Table 2), it seems likely that hydrothermal alteration and dissolution of sulfide has the potential to result in PGM being isolated from a sulfide host. However, only 7% of all PGM located for this study occur in secondary silicates and of the 36 sulfide boundary PGM occurrences that are greater than 50% enclosed in adjacent silicate, only 8 are located in secondary silicate minerals. It should be noted that, in general, the majority of these samples show low degrees of alteration. One would expect that in more altered ore, that isolation of PGM would be more common. Additionally, sample 26010-116 is from a unique, gabbroic pegmatite: its grain size, degree of alteration, and precious metal contents are rather anomalous (Morton and Hauck, 1987): the concentration of Pd, Au, and Ag are an order of magnitude higher than all other samples that were investigated during this study (see Table 1).

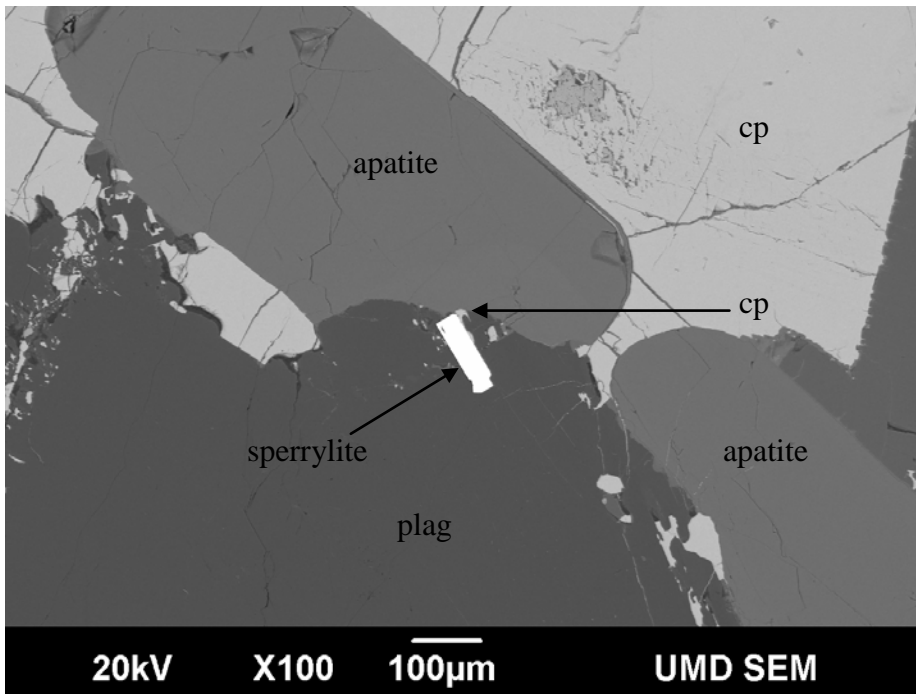


Figure 19: Large, euhedral sperrylite crystal in contact with apatite and chalcopyrite (Site 17: 26057-96).

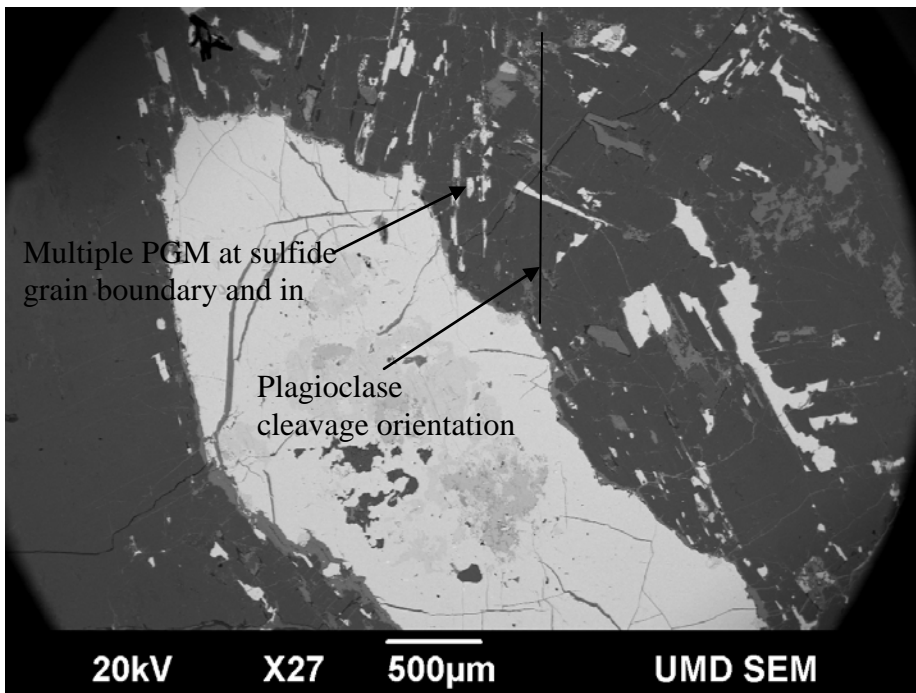


Figure 20a: Fine-grained sulfides at interface between large sulfide grain and plagioclase (Site 1: 26010-116).

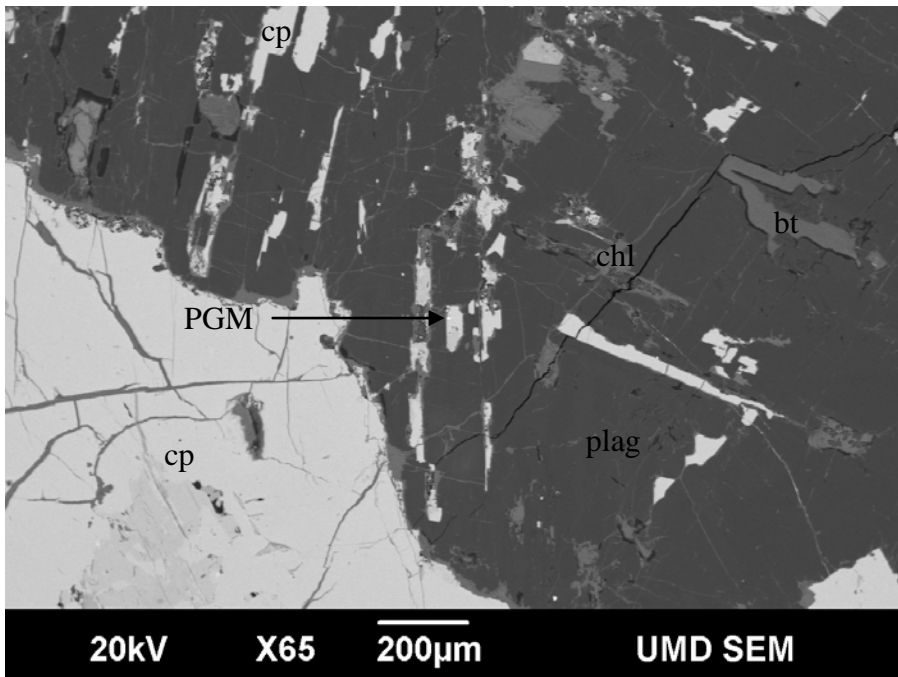


Figure 20b: Fine-grained sulfides aligned with plagioclase cleavage, chlorite in fractures (Site 1: 26010-116).

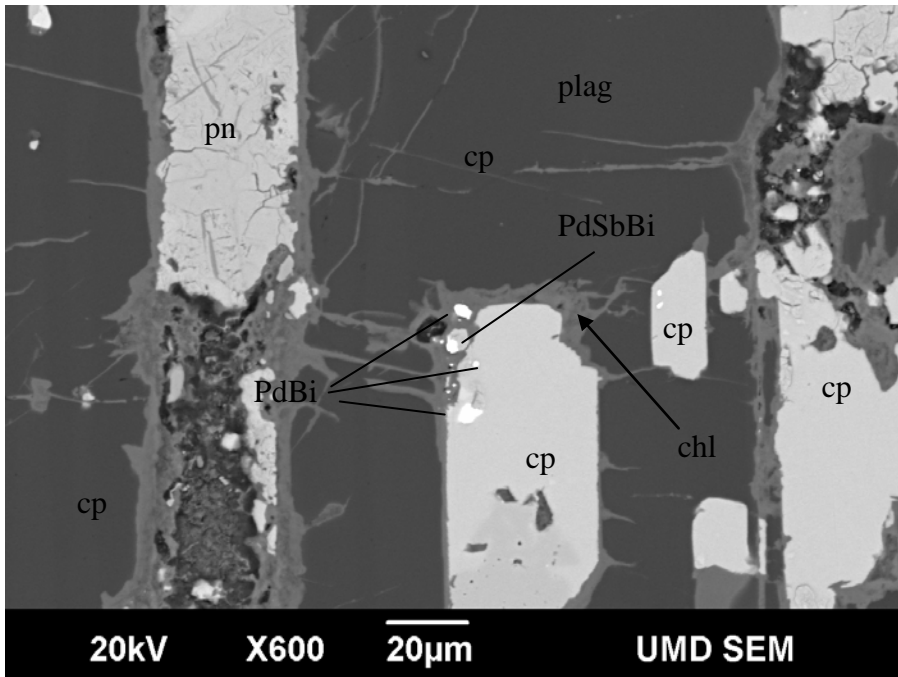


Figure 20c: Undetermined PGM (PdSbBi) at boundary of altered/ mobilized chalcopyrite grain. Bright grains at right center are galena, vein material is chlorite (Site 1: 26010-116).

3.5 Apparent Platinum Group Mineral Occurrences in Primary Silicate Minerals

As noted above, after the initial inventory of 346 PMM occurrences were compiled, it was determined that 33 PGM appeared to be enclosed entirely in primary silicates. This was a significant and surprising result because PGE are known to be strongly incompatible in silicate minerals (Naldrett, 2004; Mungall, 2005). And while some have suggested that PGM micronuggets can be physically collected by adherence to chromite grains (Finnigan et al., 2008, Mungall, 2005) no such process has been suggested for silicate minerals. Indeed, the presence of PGM inclusions in primary silicates strongly contradicts accepted orthomagmatic models of magmatic sulfide ore-forming processes (Naldrett, 2004; Mungall, 2005).

Of the primary silicate minerals that appeared to host PGM in SEM BEC images, plagioclase is the most common followed by clinopyroxene, olivine, and orthopyroxene. Biotite is host to three PGM, however it is not always clear whether biotite is a primary igneous phase or a secondary alteration phase. If it is primary, it is clearly late-stage given its interstitial occurrence to other primary silicates and oxide minerals. Similar to sulfide-hosted occurrences, PGM in primary silicates are found in sulfide-enriched areas, particularly in fine-grained sulfide halos that surround relatively larger sulfide grains (Fig. 21a). Indeed, PGM that appear to be enclosed in silicates are usually within 500 μm of sulfide grains.

Because PGM classified as primary silicate-hosted based on SEM BEC images are anomalous and call into question the orthomagmatic origin of PGM, further investigation of these occurrences was undertaken to verify that the host mineral was

unequivocally silicate. All 33 primary silicate PGM occurrences were reviewed with both transmitted and reflected light microscopy. During this review, when BEC images were compared to transmitted petrographic images, which illuminate phases in a 30 μm thickness of the sample, it became apparent that all of the PGM formerly interpreted as exclusively hosted by primary silicate are, in fact, partially sulfide-hosted, or have sulfide that is located within such a small distance ($<10\ \mu\text{m}$) that a sulfide association is inferred. In light of this recognition, Table 3 shows that no PGM are hosted in primary silicates and only 10% are hosted in secondary silicates.

In BEC images that appear to indicate a PGM is hosted in a primary silicate, the PGM occurs as a bright white spot enclosed in primary silicate (Figs. 21a-b, 22a, 23a). Looking at these same occurrences in transmitted light provides a view through the entire depth of the thin section, as opposed to an SEM BEC image that is produced by electron interaction with a very thin layer near the surface of the sample. In transmitted light, PGM appear as opaque phases that are much larger grains compared to BEC images at similar magnifications. The expanded area of opaque phase is interpreted to indicate that these PGM are in fact partially sulfide-hosted at depth. (Figures 21d, 22b, 23b). In other words, it seems that the PGM are located at the extreme fringe of sulfide that protrudes into an adjacent silicate phase. The plane of section makes it appear that that the PGM is hosted entirely in silicate in BEC images, when in fact, it is partially sulfide-hosted.

That nearby sulfide cannot be detected in SEM BEC imaging is understandable given that electron bombardment of the sample creates characteristic x-rays that are generated and emitted from only the top 2-3 μm of the polished surface of the rock slice,

which is typically 30 μm in thickness (Reed, 2005). Therefore, a sulfide grain that exists deeper than 3 μm below the surface will not be visible in the BEC image. In retrospect, it is evident that over-reliance on SEM BEC images provides only part of the information that is available in the thin section regarding the relationship between sulfides, silicates, and PGM. However, with the exception of anomalously large PGM, locating PGM without a SEM would be nearly impossible, especially in instances in which the goal of the research is to locate a large number of PGM to create a statistically valid data set.

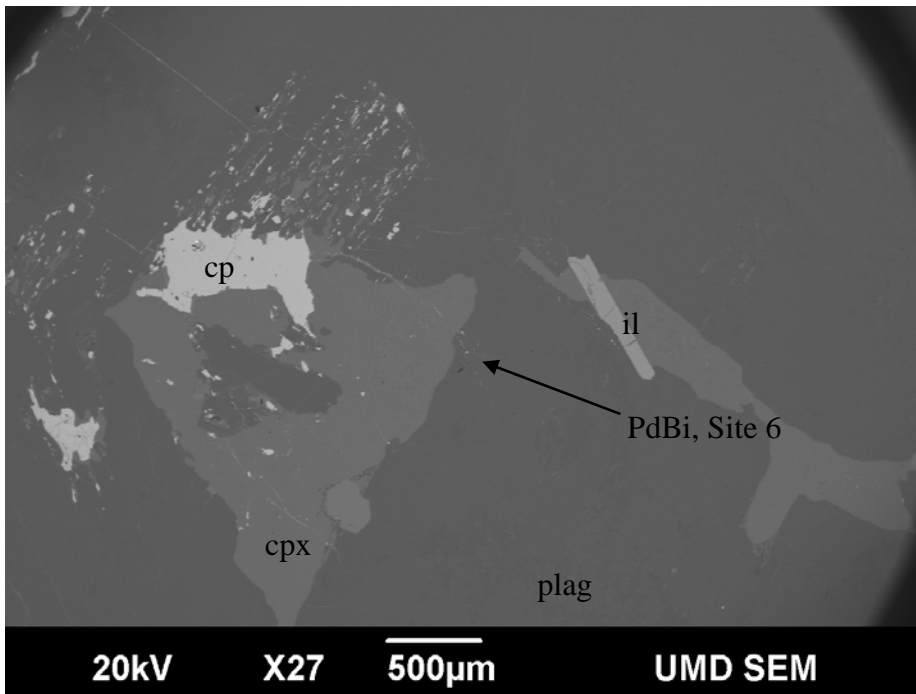


Figure 21a: Fine-grained sulfide halo aligned with plagioclase cleavage, triangular clinopyroxene, and PGM inclusion in plagioclase (Site 6: 26010-117).

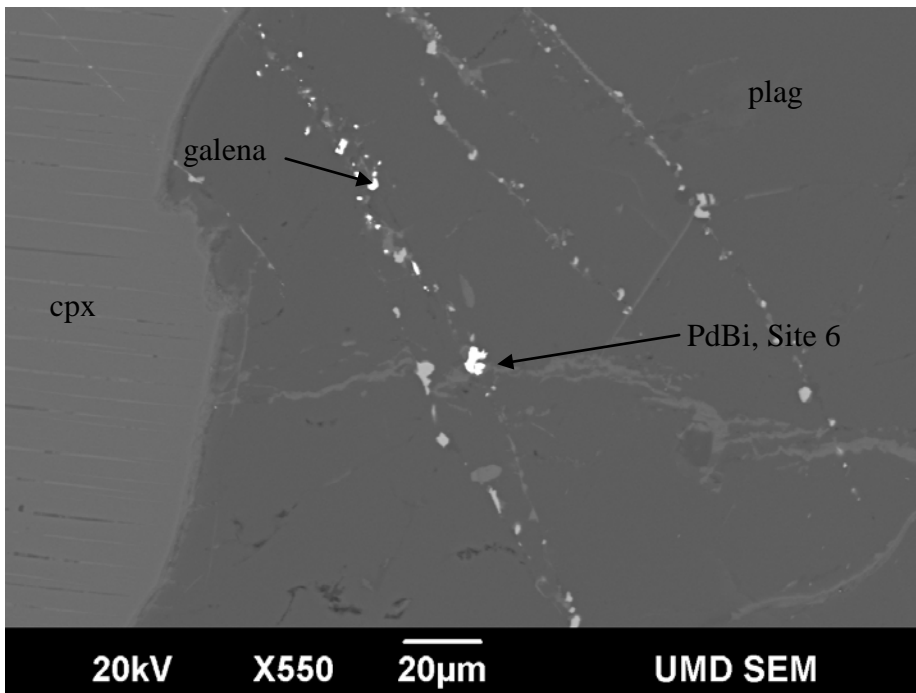


Figure 21b: PGM in plagioclase that does not appear to be sulfide hosted in this BEC image (Site 6: 26010-117).

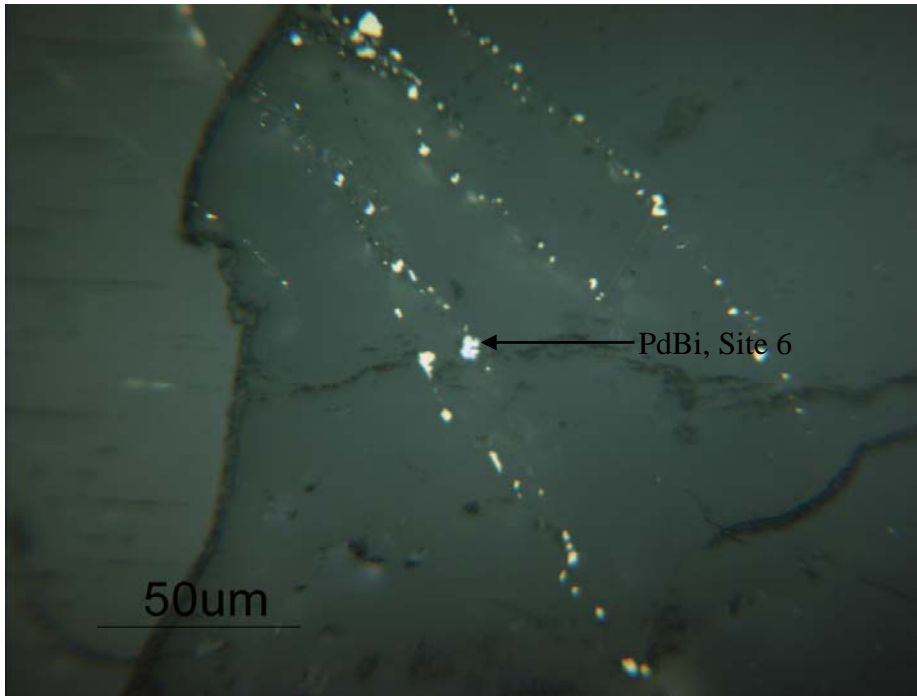


Figure 21c: Linear trend of sulfides and PGM in plagioclase, in reflected light photomicrograph. PGM appears to be enclosed in plagioclase (Site 6: 26010-117).

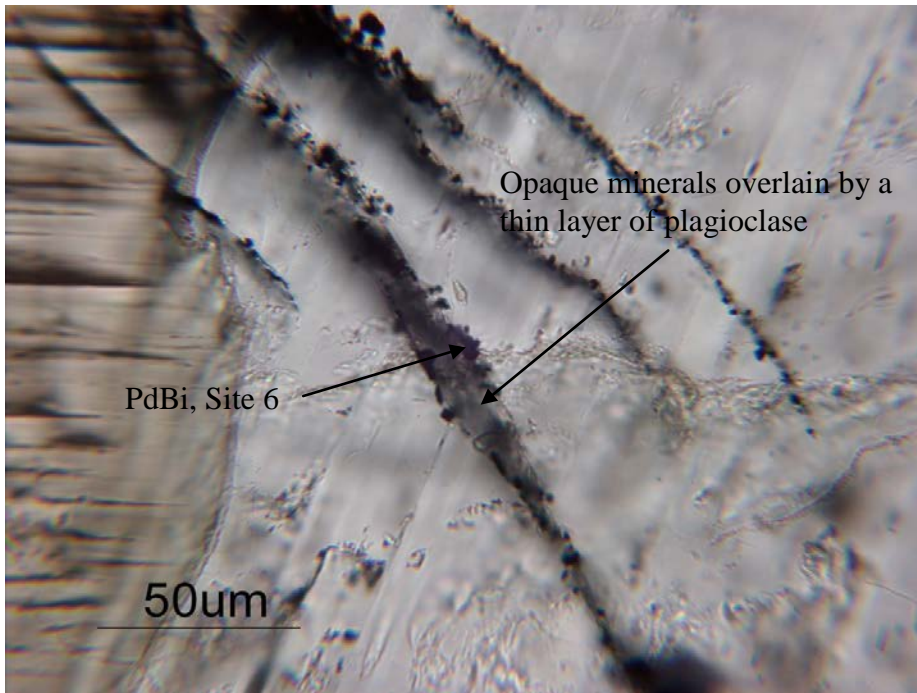


Figure 21d: Transmitted plane light image of Site 6: 26010-117 illustrating how opaque minerals can be obscured and hidden by overlying plagioclase.

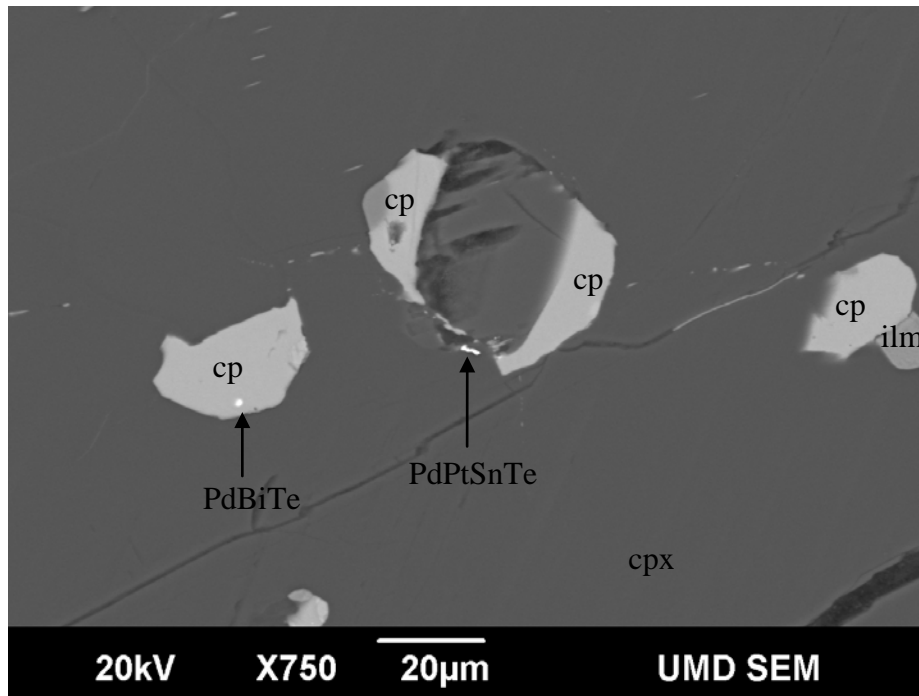


Figure 22a: BEC image of PGM in clinopyroxene (Site 19: 26013-106).

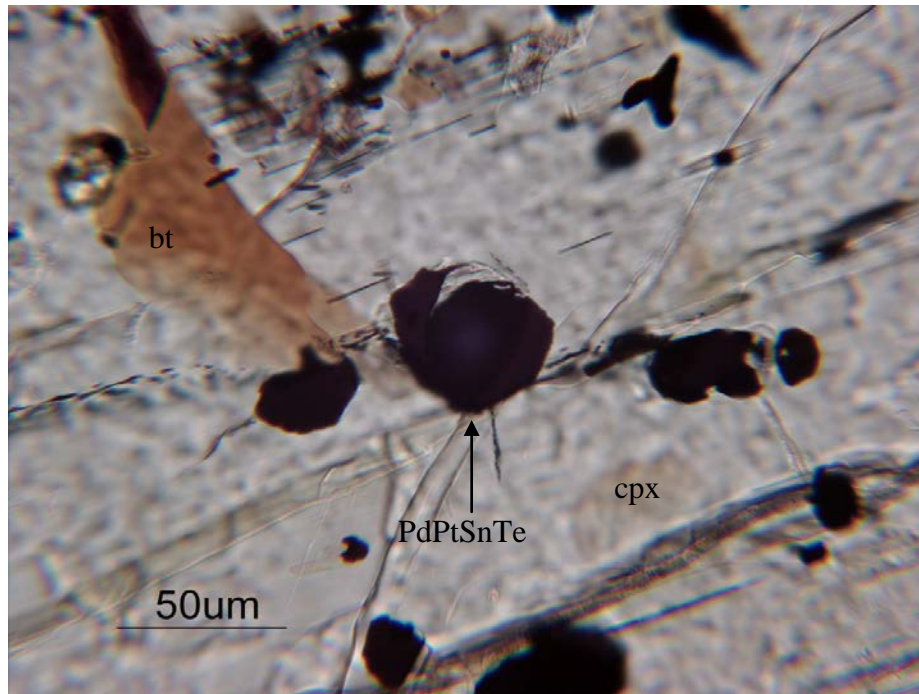


Figure 22b: Transmitted light image of circular, opaque sulfide that is not visible in BEC image, the sulfide is partially covered by a thin layer of clinopyroxene (Site 19: 26013-106).

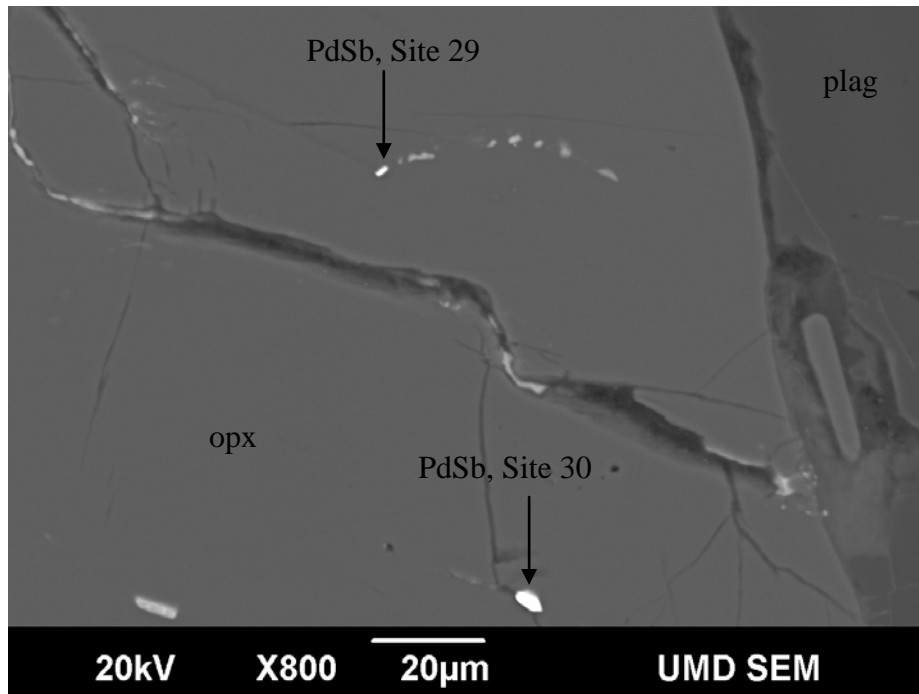


Figure 23a: BEC image of PGM in orthopyroxene (Sites 29 and 30: 26015-266).

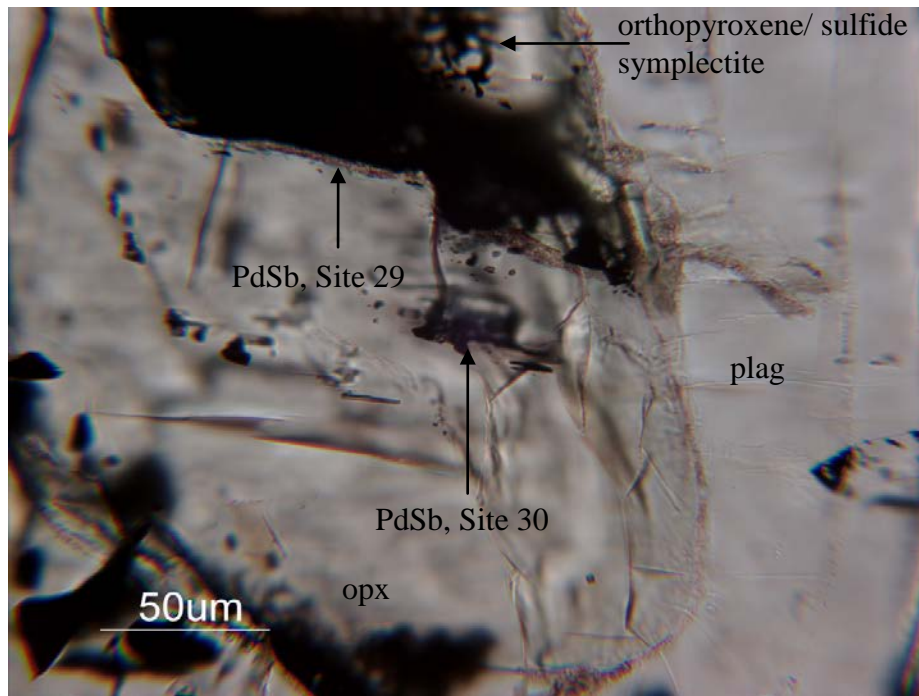


Figure 23b: Plane light image showing that sulfide is present below the orthopyroxene and is in contact with PGM (Sites 29 and 30: 26015-266).

3.6 PolyMet's C5 Concentrate

PolyMet's C5 concentrate was produced during pilot plant test runs using sulfide flotation methods. A total of 54 PGE and Ag minerals were located in concentrate C5 using the same methods that were employed to locate PMM in NorthMet ore (Table 4, Fig. 24). The 54 PMM located in C5 were classified from SEM BEC images and EDS data as occurring: 1) as inclusions in sulfide grains (28%), 2) at sulfide grain boundaries (45%), and 3) as liberated grains (27%). The primary goal of surveying PolyMet's ore concentrate was to determine if a difference exists between PMM that are known to exist in the ore and PMM that are recovered by sulfide flotation methods.

Of the 15 PMM types observed in polished thin sections of ore (including undetermined PGM), 8 were located in C5. These are: paolovite (Pd_2Sn), sperrylite (PtAs_2), stibiopalladinite (Pd_5Sb_2), kotulskite ($\text{Pd}(\text{Bi},\text{Te})_{1-2}$), undetermined PGM, acanthite (AgS), empressite (AgTe), and hessite (Ag_2Te) (Fig. 25). PMM located in the ore but not in C5 are: froodite (Pd_2Sb), naldrettite (Pd_2Sb), sobolevskite (PdBi), taimyrite ($(\text{Pd}, \text{Pt}, \text{Cu})_3\text{Sn}$), telluropalladinite (Pd_9Te_4), gold (Au), and electrum (AuAg). One PGM was located in C5 that was not found in the ore: Insizwaite ($\text{Pt}(\text{Bi},\text{Sb})_2$). Similar to PGM located in ore, PGM of undetermined stoichiometry make up the largest category of PGM (19 occurrences), followed by paolovite (11 occurrences).

PMM located in C5 mostly occur as very small (1-2 μm) grains. Of 54 grains documented in C5, 80% were 2 μm or less (Fig. 26). Grain shapes are generally anhedral, with some subhedral and very few euhedral occurrences. A PMM classified as liberated

from sulfide implies that it is not visibly in contact with a sulfide grain either as an inclusion or as a sulfide boundary occurrence.

In polished thin section, concentrate C5 appears as a dense amalgamation of mostly sulfide clasts along with up to 45% silicate gangue minerals (Fig. 27a). Silicates in C5 mirror the mineralogy of the ore: plagioclase, pyroxene, olivine, and undetermined silicates, most likely chlorite and amphiboles. EDS analyses of some of the mineral clasts observed in C5 produces poor results that do not resemble original mineral compositions. The composition of many of the silicate minerals appears to be altered by the processes of comminution and flotation. The physical effects of grinding and sample preparation combined with the possible compositional alteration resulting from exposure to flotation chemicals may produce poor EDS data.

One way to consider the effectiveness of the beneficiation process and to determine if any PMM are more or less amenable to concentration is to compare the relative abundances of respective PMM in the ore to the concentrate. Most notable is that no gold minerals were observed in C5 and that only five silver minerals were located. As far as PGM, each type of PGM located in C5 occurs approximately in similar abundance to its occurrence in ore. The main exception to this appears to be sperrylite which accounts for 10% of PGM located in ore samples and 20% of PGM located in C5. As noted previously, sperrylite is generally larger than the other PGM in NorthMet, it is also typically euhedral (Fig. 19). These physical characteristics may improve the recovery of sperrylite relative to other PGM.

The five silver minerals identified in C5 all appeared as inclusions in sulfide minerals. No silver minerals were observed liberated from sulfide. PGM as apparent inclusions in sulfide look like occurrences of this type observed in ore and are associated with copper sulfides (Fig. 27b). Sulfide boundary PGM occurrences are also present in C5 and also mostly occur in copper sulfides (Fig. 27c). PGM that are liberated from sulfide also exist in C5 (Fig. 27d), indicating that some PGM may be amenable to flotation processes even without a connection to sulfide.

Table 4: Precious metal minerals in PolyMet's C5 concentrate.

PMM Name	Formula	Total #	cp	pn	cb	po	tn	bn	Inclusion in sulfide	At sulfide boundary	Liberated from sulfide
Kotulskite: Pd(Bi,Te) ₁₋₂	Pd(Bi,Te) ₁₋₂	4	0	2	0	0	1	0	0	3	1
Froodite: PdBi ₂	PdBi ₂	0	0	0	0	0	0	0	0	0	0
Naldrettite: Pd ₂ Sb	Pd ₂ Sb	0	0	0	0	0	0	0	0	0	0
Paolovite: Pd ₂ Sn	Pd ₂ Sn	11	5	3	1	0	1	0	5	5	1
Sobolevskite: PdBi	PdBi	0	0	0	0	0	0	0	0	0	0
Sperrylite: PtAs ₂	PtAs ₂	10	4	0	1	1	2	0	4	4	2
Stibiopalladinite: Pd ₅ Sb ₂	Pd ₅ Sb ₂	4	2	0	0	0	0	0	0	2	2
Taimyrite: (Pd, Pt, Cu) ₃ Sn	(Pd, Pt, Cu) ₃ Sn	0	0	0	0	0	0	0	0	0	0
Telluropalladinite: Pd ₉ Te ₄	Pd ₉ Te ₄	0	0	0	0	0	0	0	0	0	0
Insizwaite: Pt(Bi,Sb) ₂	Pt(Bi, Sb) ₂	1	0	0	0	0	0	0	0	0	1
Undetermined PGM		19	8	2	2	0	1	0	5	8	6
Total PGM		49	19	7	4	1	5	0	14	22	13
%			39%	14%	8%	2%	10%	0%	28%	45%	27%
			cp	pn	cb	po	tn	bn			
Acanthite	AgS	2	0	1	0	0	1	0	2	0	0
Empressite	AgTe	1	1	0	0	0	0	0	1	0	0
Hessite	Ag ₂ Te	2	0	0	1	0	1	0	2	0	0
Electrum	AuAg	0	0	0	0	0	0	0	0	0	0
Gold	Au	0	0	0	0	0	0	0	0	0	0
Total Ag		5	1	1	1	0	2	0	5	0	0
%			20%	20%	20%	0%	40%	0%	100%	0%	0%
Total Con PMM		54	20	8	5	1	7	0	19	22	13

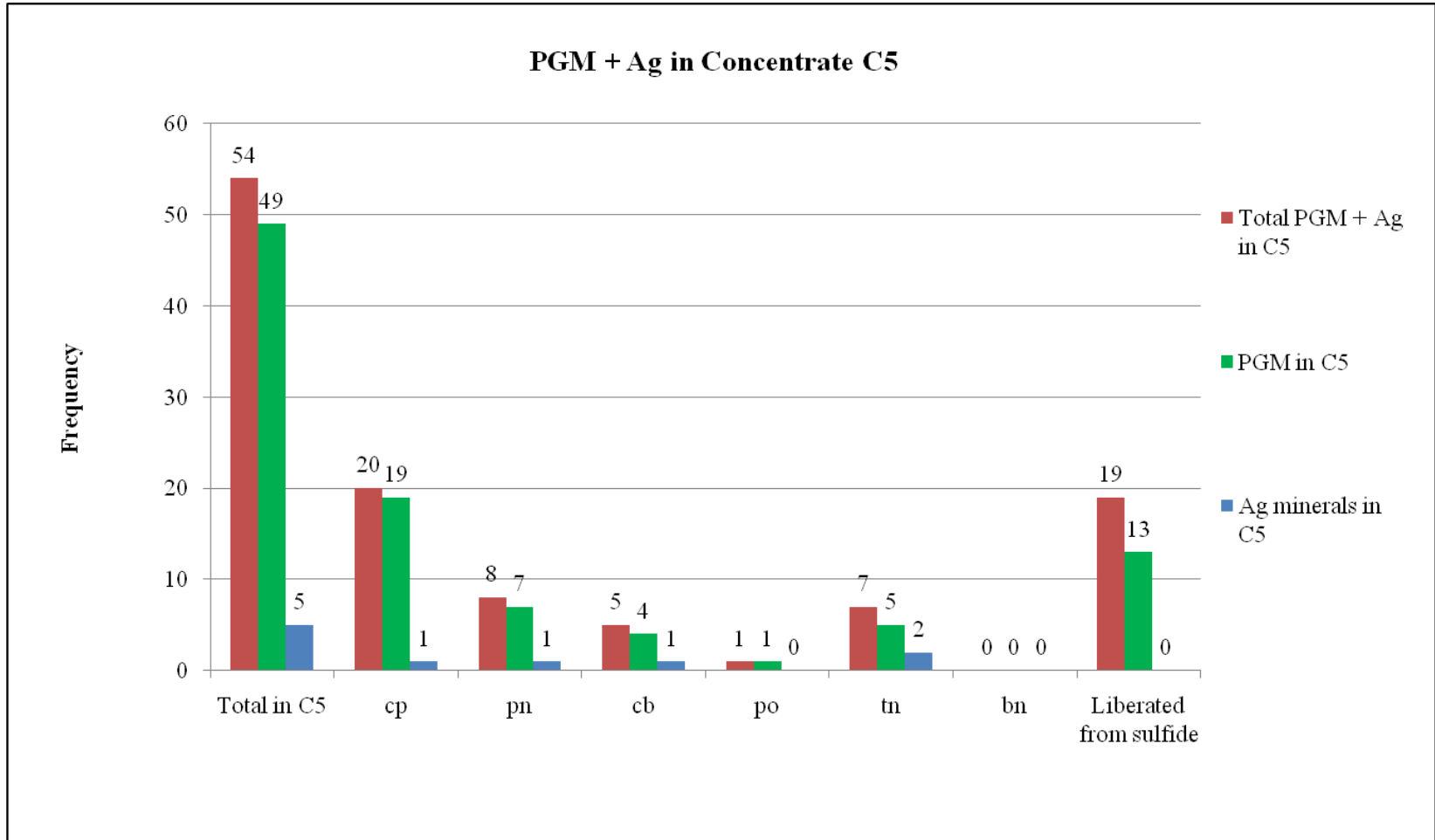


Figure 24: Frequency of sulfide minerals hosting PMM in C5; cp=chalcopyrite, pn=pentlandite, cb=cubanite; po=pyrrhotite, tn=talnakhite, bn=bornite.

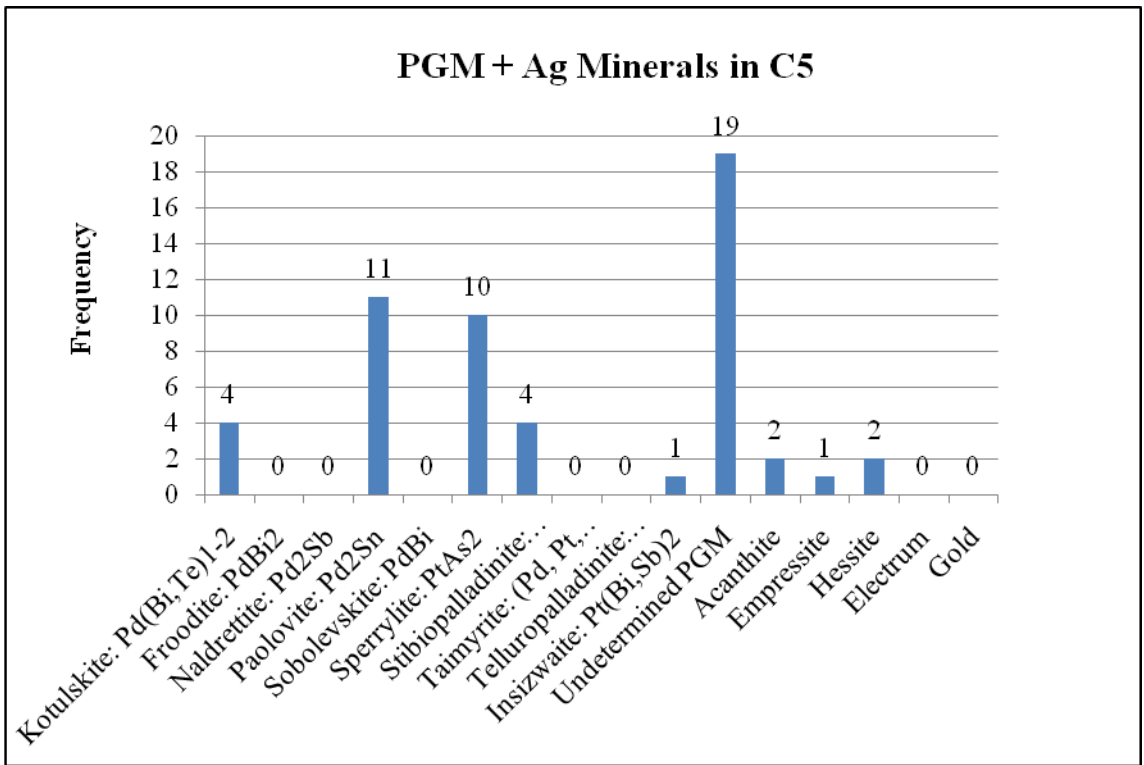


Figure 25: PMM in C5.

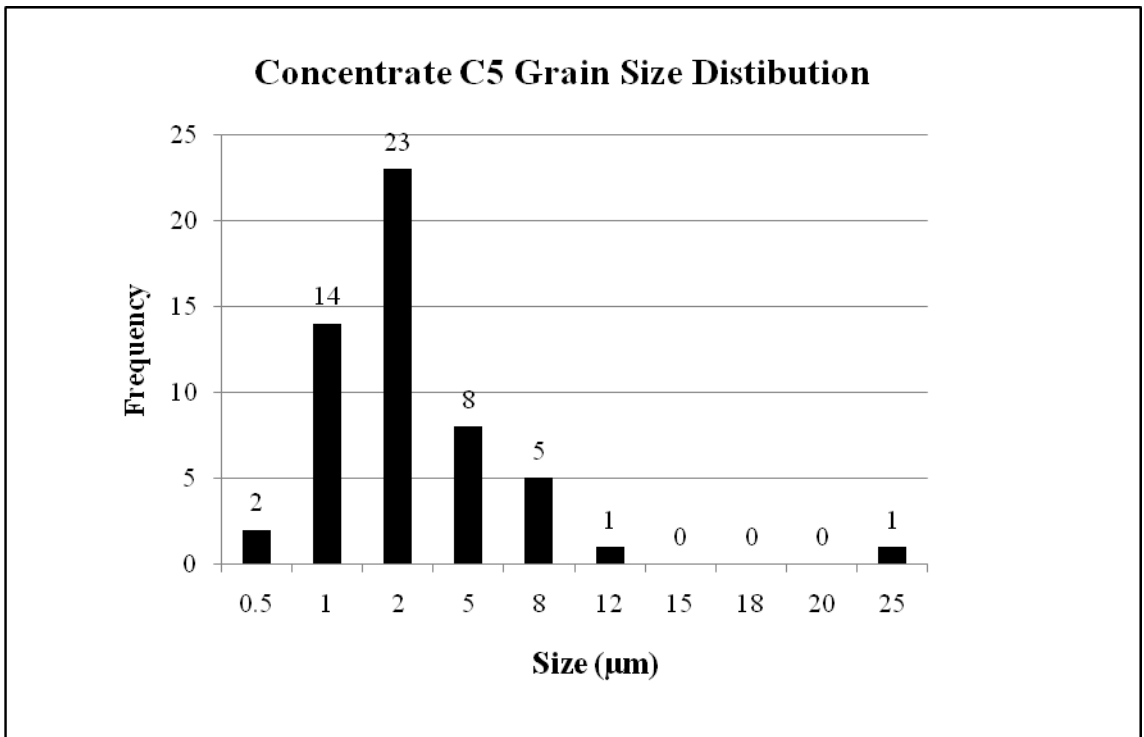


Figure 26: Grain size distribution of 54 PMM in C5.

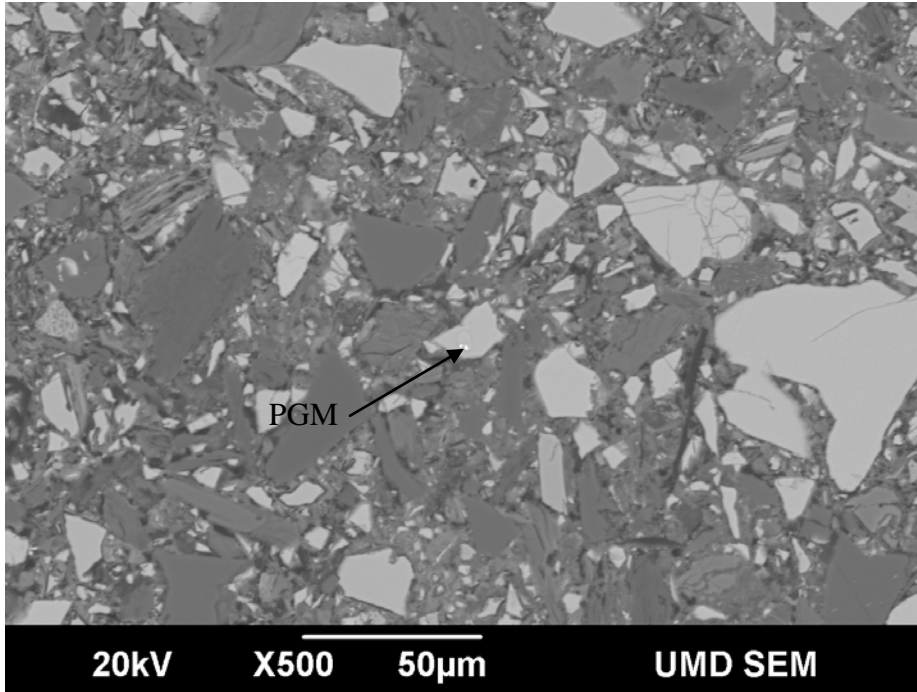


Figure 27a: SEM BEC image showing the texture of concentrate C5 with PGM-bearing sulfide grain (Site 10).

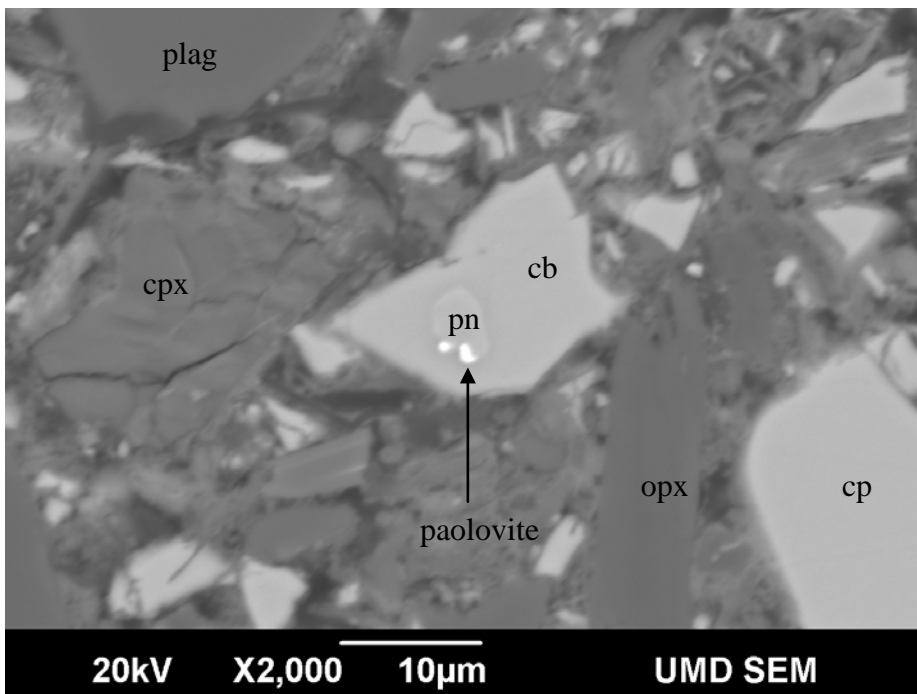


Figure 27b: SEM BEC image of PGM as inclusion in sulfide grain in concentrate C5 (Site 10).

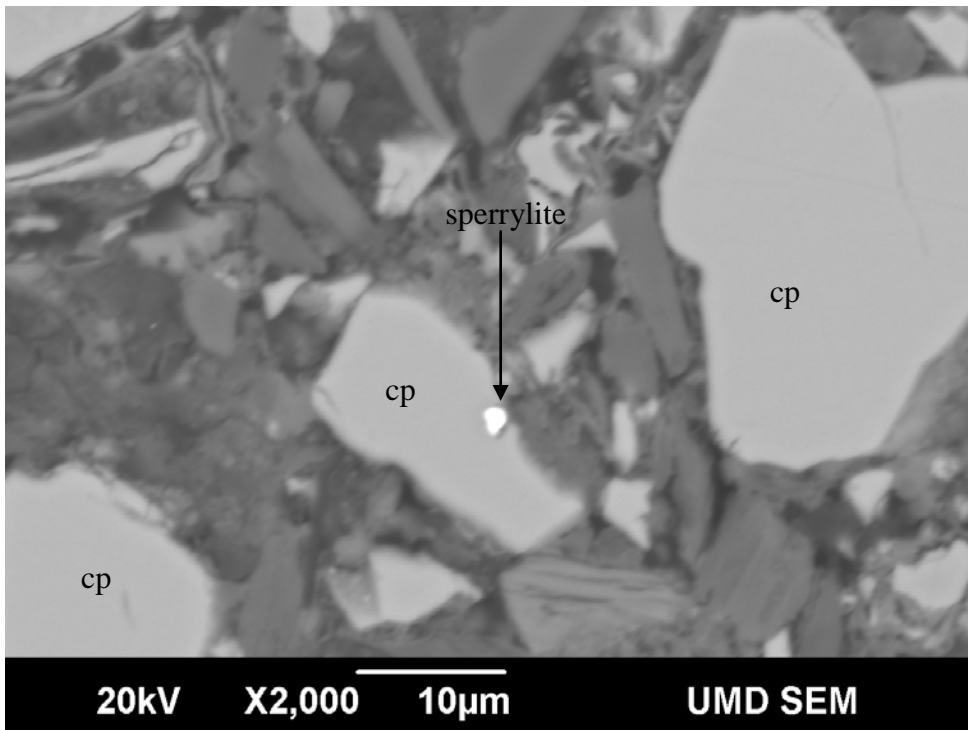


Figure 27c: SEM BEC image of boundary PGM occurrence in sulfide grain in concentrate C5 (Site 8).

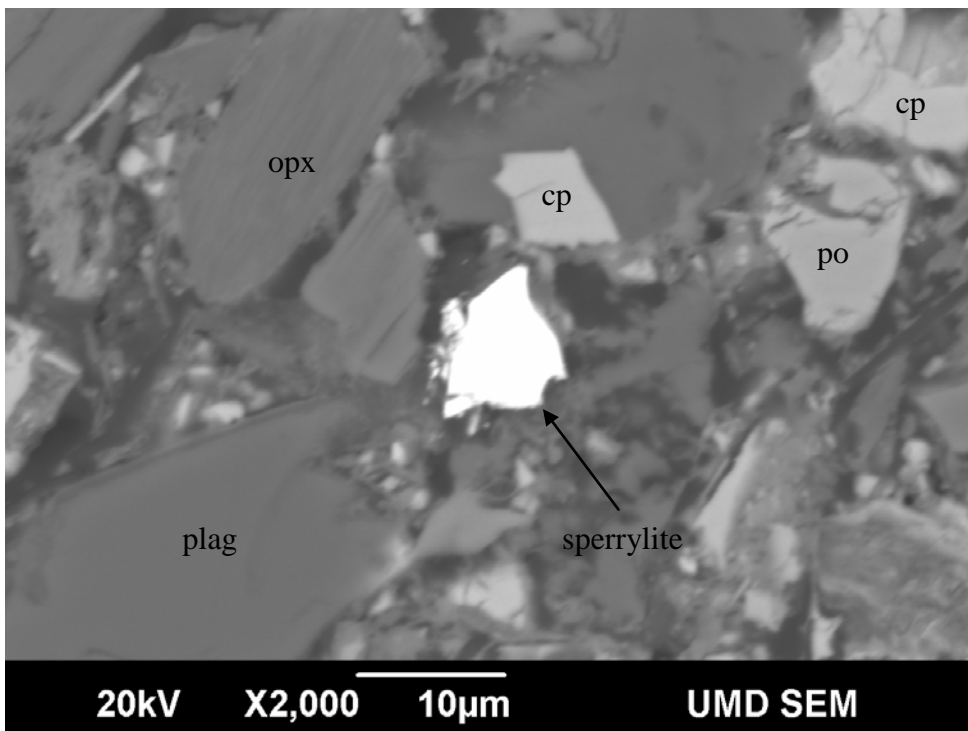


Figure 27d: SEM BEC image of liberated PGM occurrence in concentrate C5 (Site 6).

3.7 Results Summary

In this study, 346 PMM were located in ore samples and 54 PMM were located in concentrate C5 samples. Of the PMM in ore samples, 246 are PGM and 100 are Au-Ag minerals; 77% of PMM located in ore samples have a sulfide association. Of the PMM in concentrate C5, 49 are PGM and 5 are silver minerals, no Au minerals were located in concentrate C5. Grain size of PMM in ore and concentrate is mostly in the range of 1-2 μm .

Gold and silver minerals occur differently than do the PGM, 55% of Au-Ag minerals are in primary and secondary silicates. Au-Ag minerals in primary silicates occur in fracture and cleavage and often appear to exist as discrete, equant grains on the surface of host minerals (e.g. Figs. 9a-b, 9d, 11). Au-Ag minerals also occur at grain boundaries between silicates, oxides, and sulfides (Fig. 9c). With the exception of five Au-Ag minerals that appear as distinct inclusions in sulfide (Fig. 10), the location of Au-Ag minerals is interpreted to result from secondary, hydrothermal processes and redistribution of weakly bonded grains during sample preparation (Figs. 9d, 12). The difference in the mineral distribution and textural occurrence of Au-Ag minerals compared to PGM is believed to be the result of the higher mobility of Au-Ag compared to PGM (Li et al., 2007; Wood, 2002 and references therein).

PGM exhibit a stronger sulfide association than Au-Ag minerals with 90% of PGM having a sulfide association. Most PGM occur as inclusions or at grain boundaries of sulfide minerals and are particularly concentrated near fine-grained sulfide halos

surrounding larger sulfide grains. Some PGM that appear to be included in primary silicates are shown by transmitted light microscopy to be in contact with or close (≤ 500 μm) to sulfide minerals, therefore a sulfide association is assumed. Inclusions and boundary occurrences represent 48% and 52%, respectively, of PGM occurrences in sulfide minerals based on the 2D data of this research. Studies by Godel et al., (2010) and Holwell and McDonald, (2010), suggest that most PGM that appear as inclusions in 2D studies may, in fact, be sulfide boundary occurrences, implying that up to 90% of all sulfide-hosted PGM located in this study occur at sulfide grain boundaries. Seven percent of PGM are enclosed in secondary silicates, primarily chlorite, amphibole, and plagioclase alteration minerals; three percent of PGM have an apatite association, typically chloro-apatite. Given that these two mineralogical and textural occurrences are not abundant, a hydrothermal model of PGM concentration is not well-supported.

All of the PMM identified in ore concentrate samples occur in roughly similar proportions in ore samples. The PMM located in C5 occur in relatively lower concentrations in C5 than they exist in ore, with the exception of sperrylite, which represents 10% of PGM located in the ore and 20% of PGM located in C5 indicating the possibility that sperrylite is more amenable to flotation than other PGM in NorthMet. Notably, gold and electrum, which are common in the ore, were not found in the C5 concentrate. One PGM, insizwaite ($(\text{Pt}(\text{Bi},\text{Sb})_2)$), was identified in C5 but not in ore samples. PGM also occur as grains liberated from sulfide in C5 and may indicate that some PGM are recoverable by sulfide flotation even if they are not physically connected

to sulfide grains (e.g. sperrylite). Concentrate C5 also contains silicate gangue minerals which mirror those found of the ore samples.

4. DISCUSSION

4.1 Metallogensis of Au-Ag Minerals in NorthMet

Gold and silver minerals exhibit a much weaker sulfide association than do the PGM, with 56% of Au-Ag minerals being located in silicates and apatite (Table 3, Figure 7), the remaining 44% of Au-Ag minerals appear to be sulfide-hosted. Additionally, Au-Ag minerals are not well adhered to sulfides or silicate “host” minerals. In contrast to PGM, which do not occur in primary silicates in NorthMet, 26 of the 100 Au-Ag mineral occurrences discovered in this study are located in primary silicates. However, these Au-Ag occurrences were not investigated with transmitted light microscopy to determine if sulfides are located at depth, as found with some PGM. That Au-Ag minerals hosted by primary silicates tend to occur at grain boundaries and in fracture and cleavage planes suggests that these occurrences are not inclusions or intergrowths with silicates and that sulfide host minerals are not obscured by overlying silicates.

The minor occurrence of primary Au-Ag minerals as distinct inclusions in sulfide and at sulfide grain boundaries only minimally supports the magmatic sulfide model. The fact that only five Au-Ag minerals occur as distinct inclusions (Fig. 10) and that the majority of Au-Ag minerals with a sulfide association appear to exist on the surface of sulfides (e.g. Figs. 9d and 12) suggests that the primary igneous mineralogical and textural settings of Au-Ag minerals no longer exists in these samples. The predominant occurrence of secondary Au-Ag minerals in primary silicates and sulfides as well as the surficial, poorly-adhered nature of almost all the Au-Ag minerals observed during this

study highlights the mobility of gold and silver. Wood (2002) suggests that oxidizing, chlorine-rich hydrothermal/ deuteritic fluids are responsible for mobilizing precious metals, especially Au-Ag, this may also apply to the occurrence and concentration of Au-Ag in NorthMet. The source of the gold and silver, being so mobile, is unclear. It may have been brought in with the original magma or it may have come in with sulfur from the footwall rocks. If Au and Ag came from footwall rocks, this could explain why Au-Ag minerals occur with PGE: footwall-sourced fluids brought both the sulfur (causing sulfur-saturation) and the gold and silver. It is not evident whether gold and silver were initially concentrated in the NorthMet ore by the liquated sulfide melt that concentrated the PGE, or if aqueous fluids fluxed from footwall rocks transported and precipitated the Au-Ag-minerals.

The original source of gold and silver was probably from sulfide, given that both elements, like PGEs, are chalcophile (Wood, 2002). It is clear from the occurrences documented here that the Au-Ag minerals have a sulfide association, yet it is also evident that this association has been diminished by the dissolution effects of hydrothermal fluids. Wood (2002) showed with experimental data that the solubility of gold in oxidizing chlorine-rich fluids is much higher than that of Pt or Pd and that gold frequently occurs in Pt and Pd deposits but that Pd and Pt are rarely associated with most gold deposits. He suggests that this may reflect solubility differences between these precious metals. Sample preparation of thin sections may have re-distributed grains of Au-Ag. This was demonstrated by the ease with which the electrum grain in Figure 9 was removed by light polishing during removal and replacement of carbon coating (Fig. 12).

4.2 Orthomagmatic Origin of Platinum Group Minerals in NorthMet

After discovering that no PGM located in this study are primary silicate-hosted and re-calculating sulfide and silicate-hosted PGM and Au-Ag, it became evident that 90% of PGM are sulfide-hosted. Additionally, distinguishing PGM from Au-Ag minerals highlights the difference in distribution of these two types of mineral groups (Tables 2 & 3 and Figs. 6 & 7). The seven percent of PGM that are located in secondary silicates are interpreted to have been originally associated with sulfide minerals and were subsequently isolated from a sulfide host by hydrothermal dissolution. The remaining 3% of PGM are spatially associated with apatite and they too have a strong sulfide association and are not completely locked in apatite. PGM in contact with or very close to chloro-apatite could possibly indicate that PGE concentration by chlorine-bearing fluids occurred in NorthMet. Considering the relatively unaltered nature of the samples investigated in this study, that only 3% of all PGM have an apatite association, and that PGM have a 90% sulfide association, it seems unlikely that a hydrothermal mechanism is responsible for concentration of PGM in NorthMet.

Given that effectively all PGM located in this study are or were originally sulfide-hosted and that these occurrences appear to represent primary igneous textures, the results of this study support an orthomagmatic model for concentration of PGE in the magmatic sulfide deposit at NorthMet. In other words, the PGE were partitioned into a liquated sulfide melt by scavenging base and precious metals from silicate magma.

These PGE eventually crystallized from the sulfide melt to form PGM, most commonly, if not in all cases, at the interface between sulfide melt and silicate melt or minerals.

The occurrence of PGM in sulfides, particularly at sulfide grain boundaries has implications for the concentration of PGE and the formation of PGM. As previously noted, 48% of PGM occurrences are found as apparent inclusions and 52% at sulfide grain boundaries. However, the results of the Godel et al. (2010) study using 3D x-ray computed tomography demonstrate that most PGM observed as inclusions in 2D studies are in fact located at sulfide grain boundaries, has profound implications for this study. It suggests that as much as 90% of all the sulfide-hosted PGM located in this study actually occur at sulfide grain boundaries.

The predominant occurrence of PGM at sulfide grain boundaries has been attributed by Holwell and McDonald (2010) to the chalcophile nature of PGE and the increased concentration of Cu and PGE due to fractional crystallization of sulfide liquid. Godel et al. (2010) speculated that crystallization of PGM from the sulfide melt is favored at sulfide-chromite-silicate triple interfaces. The PGM in NorthMet ore show attributes of both processes by occurring mostly in Cu-rich sulfide and occurring at the interface between sulfide and silicate minerals (Figs. 17c, 18, and 20c). One departure from the observations of Godel et al. is that chromite is not present in NorthMet. Ilmenite and chromium-bearing magnetite were occasionally observed in the vicinity of PGM, but a pattern was not recognized or noted. Empirical observations alone may not be able to resolve the reason that PGM form at sulfide grain boundaries, but it does establish a distinct mineralogical and textural occurrence of PGM at sulfide grain boundaries and as

sulfide as a collector. Experimental evidence suggests that PGM tend to crystallize at the margin of sulfide minerals, further supporting the inferred predominant location of PGM at sulfide grain boundaries in NorthMet (Holwell and McDonald, 2010 and references therein)

4.3 Origin of PGM-enriched Sulfide Halos

The preferential occurrence of PGM in fine-grained, silicate-hosted sulfides that form halos around larger sulfide grains is a curious observation and is enigmatic in terms of the origin of the sulfide texture, as well as the increased concentration of PGM in these sulfides. Similar halo textures have been previously recognized in the ores of the Partridge River Intrusion (PRI) and the South Kawishiwi Intrusion (SKI).

Foose and Weiblen (1986) did not use the term halo, but describe one of four types of sulfide textures evident in the SKI ores that appear to be similar to the halo sulfides observed in this study. They termed this sulfide texture “included sulfides.” Their “included sulfides” could represent sulfide halos, as sulfide halos are certainly included in primary silicates. Previous studies of NorthMet (Geerts, 1991; Geerts, 1994) recognized Foose and Weiblen’s four sulfide textures, but did not describe any of the four sulfide texture types with the term halo. None-the-less it seems reasonable to conclude that the halo textures in this study were recognized by Geerts.

Foose and Weiblen (1986) attributed sulfide mineralization of the SKI to hydrothermal processes. The main evidence they cited is that sulfide mineralization in the SKI is associated with reversely zoned plagioclase and with hydrous mineral phases (biotite and amphibole). They suggest that precipitation of sulfides and cation exchange between cumulus minerals and volatile-rich fluids can explain all sulfide textures and the reverse zoning in cumulus silicates within sulfide enriched zones of the SKI. Marma (2002) applies the term halo to fine-grained sulfides in the Birch Lake deposit of the SKI

occurring at rims of larger sulfide grains and within adjacent silicates. He too invokes a hydrothermal origin for concentration of sulfides and PGM though gave no interpretation for the halo texture. Severson and Hauck (2003) noted sulfide halo textures in the Duluth Complex as a whole, but interpret this texture to result from primary magmatic processes, suggesting a complex intergrowth between sulfide melt and crystallizing silicates as the origin of this texture. Geerts (1994) attributes sulfide mineralization in NorthMet to magmatic processes, suggesting that rare earth element compositions of Unit I imply a mantle source and that Unit I is comprised of multiple injections of magma. Similarly to Foose and Weiblen's study of the SKI, Geerts (1994) indicated that plagioclase near the top of Unit I (Geerts' Red zone) is reversely zoned and also called on cation exchange between plagioclase and aqueous fluids to explain calcic rims on plagioclase adjacent to sulfides.

The two characteristics of the SKI sulfide that Foose and Weiblen (1986) cite as evidence for a hydrothermal origin for all sulfide mineralization are not obvious in the NorthMet ores in general and in the sulfide halos in particular. Although biotite and amphibole are present in Duluth Complex sulfide ores, they tend to be homogeneous grains that fill interstitial void spaces. Therefore, they appear to be late magmatic and not the result of subsolidus hydrothermal alteration. The alteration that is present is a low to moderate degree of solidus deuteric alteration that locally forms iddingsite from olivine, sericite from plagioclase, and uralite/actinolite and chlorite from pyroxene (Severson and Hauck, 2003). Most deuteric alteration is focused along grain boundaries, cleavage, or fractures. The degree of alteration is no greater or weaker in the vicinity of the PGM-

bearing sulfide halo textures (Figs. 16a, 17a, & 18). Therefore, a hydrothermal alteration origin for the halos does not seem to be supported by the minor late deuteric alteration observed in the NorthMet ores. If anything, hydrothermal fluids appear to cause late sulfide dissolution rather than precipitation within silicate minerals. That these fluids do not appear to remobilize PGE from already crystallized PGM (Figs. 20a-c), suggests that aqueous fluids may serve to slightly upgrade the PGM to sulfide ratio by preferentially dissolving sulfide.

The other evidence cited by Foose and Weiblen (1986) for a hydrothermal origin for the SKI sulfides is the presence of more calcic plagioclase along plagioclase rims. They interpreted this reversed zoning as possibly resulting from an increase in P_{H_2O} . With sulfide halos typically concentrated in plagioclase rim areas, one would expect to observe increased An contents in these sulfide-enriched plagioclase rims. Microprobe analyses of plagioclase core in lower PRI rocks by Chalokwu and Grant (1990) show that most core compositions range between An₆₀ and An₇₀. Geerts (1994) microprobed 78 plagioclase grains from troctolitic rocks within and around the Red zone, or the top of Unit I and found that plagioclase in Unit II averaged An₆₅, and plagioclase from un-mineralized portion of Unit I below the Red zone, averaged An₇₁. This correlates with the work of Chalokwu and Grant (1990). Plagioclase within the Red zone had average cores of An₆₄ and average rims of An₇₆, indicating that plagioclase in sulfide enriched zones within the Red zone of Unit I is reversely zoned (Geerts, 1994).

Systematic plagioclase analyses were not conducted as part of this study, however 27 plagioclase EDS analyses were executed for PMM in plagioclase that host Au-Ag

minerals (8) or were formerly interpreted as PGM host minerals (19). Of the 27 plagioclase analyses, eighteen were $An > 60$ and nine were $An < 60$ (Fig. 28). With a significant number of these analyses being less than average PRI plagioclase core compositions (Chalokwu and Grant, 1990; Geerts, 1994) and the remainder being equivalent to core compositions, this does not obviously indicate reverse zoning.

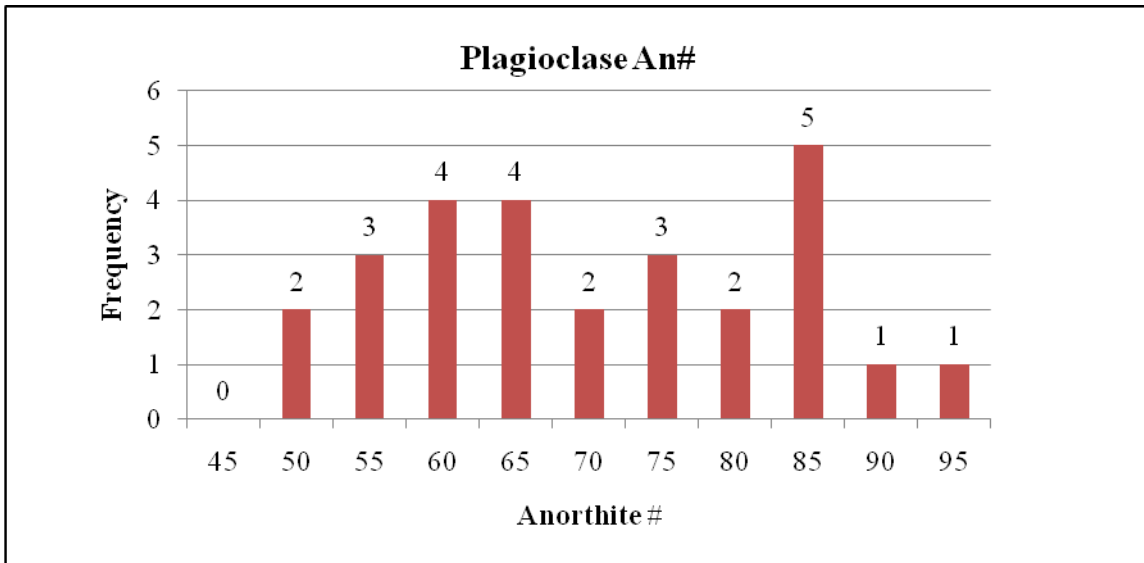


Figure 28: Histogram demonstrating range of anorthite content of 27 plagioclase EDS analyses.

As Severson and Hauck (2003) argued, a primary magmatic origin seems a more reasonable explanation for the PGM-bearing, fine-grained sulfide halos in NorthMet. In this case, the halos are likely the result of complex intergrowth of sulfide melt and silicate minerals and melts (Figs.15a, 16a-b, 17a-b, 18, 19, 20a-c, 21a-d, 22a-b, 23a-b). Why this intergrowth occurs is not clear, but that the halos mantle larger masses of sulfide, that the sulfide occurs along crystallographic planes in the silicate (usually plagioclase) host, and that they tend to be copper and PGE enriched must be a clue to its origin.

One possible explanation is that as large blebs of sulfide melt fractionally crystallize MSS sulfide, the residual sulfide melt becomes enriched in Cu and PGE (Fig. 3). As crystallization of the immiscible sulfide and silicate melts continues, the diminishing porosity of the crystal mush perhaps forces silicate minerals growing adjacent to now Cu-PGE enriched sulfide melt to incorporate the sulfide melt. The presence of sulfide melt adjacent to a growing plagioclase crystal likely impedes the diffusion of chemical constituents from the silicate melt necessary for continued growth of the plagioclase. In addition, perhaps the presence of the sulfide melt creates crystallographic flaws in the slow-growing plagioclase, which then envelop the sulfide to form inclusions.

4.4 Cause of Low Precious Metal Element Recoveries in PolyMet Ores

PolyMet's pilot plant produced a 75% a combined recovery of Pd, Pt, and Au, whereas the base metals of copper and nickel were recovered at a 90% recovery rate (Patelke, 2009, unpublished data). Because base and precious metals are generally assumed to be sulfide-hosted, the immediate question is: why there is a difference in recovery rates when using sulfide flotation recovery methods? Based on the observations made in this study, the principal explanations to this issue are related to the distinctive textural and mineralogical occurrence of PGM and Au-Ag minerals relative to sulfide minerals.

This study has determined that 77% of all PMM have a sulfide association, which correlates well with PolyMet's 75% recovery of combined Pd, Pt, and Au. The main reason for the relatively lower recovery of precious metals appears to be that Au-Ag compounds have a weaker sulfide association than do the PGM: 56% of Au-Ag are not sulfide-hosted, whereas 90% of PGM are sulfide-hosted. The implication is that 56% of Au-Ag compounds will not be recovered by sulfide flotation methods because they are not physically in contact with sulfide. Furthermore, the weak physical connection between Au-Ag minerals and adjacent minerals (e.g. Figs 9a-d, 11, 12) indicates that many Au-Ag mineral grains are likely lost to tailings. It may be that Au-Ag minerals that appear as inclusions in sulfide (e.g. Fig. 10) have a stronger physical connection with the sulfide grain and that these Au-Ag minerals are more likely to be recovered by flotation processes. Notably, the five silver minerals observed in C5 all occur as apparent inclusions in sulfide grains (Table 4), i.e. there is an intergrown relationship between the

minerals. The low gold recovery is highly evident considering that out of fifty-four PMM located in the C5 concentrate, none were gold minerals, suggesting that within the ore that was processed, perhaps even more than 56% of Au-Ag minerals were not physically associated with, or strongly connected to sulfide.

Visual inspection of sulfide-hosted PGM indicates that 48% of these occur as apparent inclusions in sulfide and 52% occur at sulfide grain boundaries. Godel et al. (2010) show that most PGM in Bushveld ore that appear as inclusions in 2D studies are in fact boundary occurrences that appear as inclusions due to the limited perspective of 2D studies. Applying the same proportional distortion implies that up to 90% of all the PGM located in NorthMet ores might actually occur at sulfide grain boundaries. The common occurrence of PGM at sulfide boundaries may limit the recovery of PGE at NorthMet. Boundary PGM are susceptible to isolation from sulfide through dissolution of sulfide by hydrothermal fluids and replacement by secondary silicates. This isolation would be expected to negate recovery of PGM with the use of sulfide flotation methods.

With 31% of all boundary PGM being less than 50% enclosed in sulfide, many PGM would tend to be susceptible to detachment from their sulfide host minerals during the grinding stage of beneficiation,. This implies that many boundary PGM have at best, a 50/50 chance of remaining bonded to sulfide during grinding processes and that some of these PGM may separated from sulfide and then be lost to tailings during flotation processes.

Merkle and McKenzie (2002) indicate that the greatest losses of PGM in South African ore occur during grinding and concentration processes and that the balance

between liberating PGM and over-grinding is difficult to achieve. This is largely a factor of the exceedingly small size of PGM. PGM at NorthMet are also small in size: 62% of all precious metals located in ore samples for this study are $\leq 2 \mu\text{m}$.; 80% of PMM located in C5 are $\leq 2\mu\text{m}$. A balance between over-grinding and liberation of precious metals is critical for PolyMet as well.

5. CONCLUSION

The difference in the occurrence and distribution of PGM vs. Au-Ag has implications for both ore-forming processes and beneficiation of precious metals from NorthMet ore. Au-Ag minerals frequently occur in fracture and cleavage of primary silicate minerals and at grain boundaries between silicates, sulfides, and oxides. Additionally, most Au-Ag minerals appear to be weakly attached to adjacent minerals, appearing to reside on the surface of adjacent minerals, i.e., an intergrown relationship is absent. These textural locations suggest that Au-Ag has been re-mobilized and that many of these occurrences do not represent primary igneous textures. Despite the fact that Au-Ag is frequently isolated from sulfide, it does occur in sulfide-enriched rock and likely was collected by sulfide prior to re-mobilization by hydrothermal fluids or possibly sample preparation. Differences in the solubilities of Pd and Pt vs. Au-Ag in aqueous fluids may explain why Au-Ag was mobilized in NorthMet, whereas PGE appear immobile.

The relatively low sulfide association of Au-Ag combined with the weak physical connection between sulfides and Au-Ag minerals makes these elements difficult to recover from NorthMet ores with sulfide flotation processes. The low sulfide association of Au-Ag minerals is the principal reason that there is a difference in recovery rates between base and precious metals. Seventy-seven percent of all PMM located in this study occur in contact with sulfide, which is very close to PolyMet's 75% average

recovery rate of Pd, Pt, and Au, indicating that sulfide flotation processes are efficiently recovering sulfide-hosted PMM from NorthMet ores.

Platinum group minerals have a strong sulfide association, with as much as 90% occurring in contact with sulfide minerals. PGM primarily occur at sulfide grain boundaries in sulfide halo textures, usually in plagioclase. Sulfide halos are interpreted to result from magmatic processes involving interactions between a Cu-PGE-enriched sulfide melt and silicate minerals during the late stages of crystallization of the crystal mush. PGM occur in secondary silicates (7%) and in association with apatite (3%) in contact with, or close to sulfides. PGM do not occur as inclusions in primary silicate minerals.

It is difficult to over-emphasize the small size of PMM in NorthMet ores. The scale is hard to comprehend and is easy to overlook or underestimate. Also, the complexity of the rock textures, even at 1000-2000x magnifications, lures the observer into a false sense of size. The electron beam microscope produces very fine imagery and after reviewing hundreds of images, it is easy to overlook the small and limited extent of the 2D perspective that these images provide. An example of this is how some PGM located during this study were perceived to be hosted in primary silicate minerals. But with simple transmitted light petrography imaging the entire 30 micron thickness of the thin section, it became evident that sulfide was lurking just below the surface.

Apparent primary silicate-hosted PGM occurrences are, in actuality, sulfide boundary PGM that are intimately intergrown with adjacent silicate minerals. The SEM is a powerful tool for locating multiple precious metal minerals in polished thin sections.

However, it provides only part of the picture. Apparent primary silicate-hosted PGM are PGM that are intimately intergrown with silicates, protrude through adjacent primary silicates, and are partially covered by a thin layer of silicate that obscures underlying sulfide host minerals. The view is so small that even the 30 μm thickness of the sample becomes huge and is not available for viewing with the SEM.

The principal line of evidence in NorthMet ores of formation by orthomagmatic processes is the strong sulfide association of PGM, the indirect sulfide association of Au-Ag, the general paucity of hydrous, secondary minerals in PGM-bearing sulfide halo textures, and the mostly well-preserved primary igneous textures.

Bibliography

- Andersen, J.C.O., 2006, Postmagmatic Sulphur Loss in the Skaergaard Intrusion: Implications for the Formation of the Platinova Reef, *Lithos*, v. 92, pp.198-221.
- Arndt, N.T., Leshar, C.M., and Czamanske, G.K., 2005, Mantle-Derived Magmatic Ni-Cu-(PGE) Deposits; *Economic Geology* 100th Edition, pp 5-23.
- Barnes, S. J., and Lightfoot, P., 2005, Formation of Magmatic Nickel Sulfide Ore Deposits and Processes Affecting Their Platinum Group Element Contents: *Economic Geology* 100th Anniversary Volume, pp. 179-213.
- Barnes, S.J., and Maier, W.D., 2002, Platinum Group Element Distributions in the Rustenberg Layered Suite of the Bushveld Complex, South Africa: *Canadian Institute of Mineralogy and Metallurgy*, Special volume 54, pp. 431-458.
- Boudreau, A.E., and McCallum, I.S., 1992, Concentration of Platinum Group Elements by Magmatic Fluids in Layered Intrusions; *Economic Geology*, v. 87, pp. 1830-1848.
- Cabri, L. J., 2002, *Geology, Geochemistry, Mineralogy and Mineral Beneficiation of Platinum Group Elements*, Canadian Institute of Mining, Metallurgy, and Petroleum, 852 p.
- Campbell, I.H., and Naldrett, A.J., 1979, Influence of Silicate: Sulfide Ratios on the Geochemistry of Magmatic Sulfides; *Economic Geology*, v. 74, pp. 1503-1505.
- Chalokwu, C.I., and Grant, N.K., 1990, Petrology of the Partridge River intrusion, Duluth Complex, Minnesota: Relationships between mineral compositions, density, and trapped liquid abundance. *J. Petrology* 31, 265-93
- Eckstrand, O.R., and Hulbert, L. 2007, Magmatic nickel-copper-platinum group element deposits. In *Goodfellow, W.D., ed., Mineral Deposits of Canada: A Synthesis of Major Deposit-types*, District Metallogeny, the Evolution of Geological Provinces, and Exploration Models, Geological Association of Canada Special Publication 5, p. 205-222.
- Finnigan, C.S., Brenan, J.M., Mungall, J.E., and McDonough, 2008, Experiments and Models Bearing on the Role of Chromite as a Collector of Platinum Group Minerals by Local Reduction, *Journal of Petrology*, 49, pp. 1647-1665

- Foose, M.P., and Weiblen, P.W., 1986, The physical and chemical setting and textural and compositional characteristics of sulfide ores from the South Kawishiwi Intrusion, Duluth Complex, Minnesota, USA: in 27th Int. Geol. Congress (Moscow), Special Copper Symposium, Springer-Verlag, New York, pp. 8-24.
- Geerts, S. D., 1991, Geology, Stratigraphy, and Mineralization of the Dunka Road Cu-Ni Prospect, Northeastern Minnesota, Natural Resources Research Institute Technical Report NRRI/TR-91/14, University Minnesota Duluth, 74 p.
- Geerts, S. D., 1994, Petrography and Geochemistry of a Platinum Group Element-Bearing Mineralized Horizon in the Dunka Road Prospect (Keweenaw) Duluth Complex, Northeastern Minnesota, unpublished M.S. thesis, University Minnesota Duluth, 184 p.
- Godel, B., Barnes, Sara J., Barnes, Stephen J., and Maier, W.D., 2010, Platinum Ore in Three Dimensions: Insights from High Resolution X-ray Computed Tomography; *Geology*, v. 38, no. 12, pp.1127-1130.
- Holwell, D.A., and McDonald, I, 2010, A Review of the Behavior of Platinum Group Elements Within Natural Magmatic Sulfide Ore Systems; The Importance of Semi-metals in Governing Partitioning Behavior; *Platinum Metals Review*, v. 54, pp. 26-36.
- Joslin, G.D., 2004, Stratiform palladium–platinum–gold mineralization in the Sonju Lake Intrusion, Lake County, Minnesota, unpublished MS thesis, University of Minnesota–Duluth, p 185.
- Komppa, U.E., 2002, Oxide, sulphide and platinum mineralogy of the South Kawishiwi and Partridge River Intrusions of the Duluth Layered Intrusion Complex, Minnesota, U.S.A., Natural Resources Research Institute Report of Investigation NRRI/RI-2002/02
- Li, C., Barnes, S.J., Makovicky, E., Rose-Hansen, J., and Makovicky, M., 1995, Partitioning of Nickel, Copper, Iridium, Rhenium, Platinum, and Palladium Between Monosulfide Solid Solution and Sulfide Liquid: Effects of Composition and Temperature; *Geochemica et Cosmochimica Acta*, v. 60, no. 7, pp.1231-1238.
- Li, C., Ripley, E.M., Merino M., and Maier W.D., 2004, Replacement of Base Metal Sulfides by Actinolite, Epidote, Calcite and Magnetite in the UG2 and Merensky Reef of the Bushveld Complex, South Africa, *Economic Geology*, v. 99, pp. 173-184.

- Li, C., Ripley, E.M., Oberthür, T., Miller, J.D., Jr., and Joslin, G.D., 2007, Textural, mineralogical and stable isotope studies of hydrothermal alteration in the main sulfide zone of the Great Dyke, Zimbabwe and the precious metals zone of the Sonju Lake Intrusion, Minnesota, USA. *Miner Deposita*, v. 43, p. 97-110
- Listerud, W.H., and Meineke, D.G., 1977, Mineral resources of a portion of the Duluth Complex and adjacent rocks in St. Louis and Lake Counties, northeastern Minnesota: Hibbing, Minn., Minnesota Department of Natural Resources, Division of Minerals Report 93, 74p.
- Marma, J.C., 2002, Magmatic and hydrothermal PGE mineralization of the Birch Lake Cu-Ni-PGE deposit in the South Kawishiwi intrusion, Duluth Complex, northeastern Minnesota: unpublished M.S. thesis, University of Wisconsin: Natural Resources Research Institute, University of Minnesota, Duluth, Technical Report, NRRI/TR-2003/39.
- Mavrogenes, J.A., and O'Neill, H.S.C., 1999, The Relative Effects of Pressure, Temperature, and Oxygen Fugacity on the Solubility of Sulfide in Mafic Magmas: *Geochemica Cosmochimica Acta*, v. 63, pp. 1173-1180.
- Merkle, R. K. W., and McKenzie, A.D., 2002, Mining and Beneficiation of South African Ores – An Overview, *In* Cabri, L. J., ed., *Geology, Geochemistry, Mineralogy and Mineral Beneficiation of Platinum Group Elements*, Canadian Institute of Mining, Metallurgy, and Petroleum, pp.793-807.
- Miller, J.D. Jr., and Severson, M.J., 2002, Geology of the Duluth Complex *in* *Geology and mineral potential of the Duluth Complex and related rocks of northeastern Minnesota*: Minnesota Geological Survey Report of Investigations 58, pp.106 – 143.
- Miller, J.D., Jr., Green, J.C., Severson, M.J., Chandler, V.W., Hauck, S.A., Peterson, D.M., and Wahl, T.E., 2002, Geology and mineral potential of the Duluth Complex and related rocks of northeastern Minnesota: Minnesota Geological Survey Report of Investigations 58, 207p.
- Morton, P., and Hauck, S. 1987, PGE, Au and Ag Contents of Cu-Ni Sulfides Found at the Base of the Duluth Complex, Northeastern Minnesota, Natural Resources Research Institute Technical Report NRRI/GMIN-TR-87-04, University Minnesota Duluth, 94 p.
- Mungall, J.E., 2005, Magmatic Geochemistry of the Platinum Group Elements, *Min. Assoc. of Canada*, v. 35, pp. 1-34.

- Naldrett, A.J., 2004, Magmatic Sulfide Deposits: Geology, Geochemistry and Exploration, Springer Verlaag, 728 p.
- Naldrett, A.J., and Duke, J.M., 1980, Platinum Metals in Magmatic Sulfide Ores, *Science*, v. 208 number 4451, pp 1417-1424.
- Peregoedova, A.V., 1998, The Experimental Study of Pt-Pd Partitioning Between Monosulfide Solid Solution and Cu-Ni Sulfide Melt at 900-840 C, *In* "The 8th International Platinum Symposium," Rustenberg, South Africa, The South African Institute of Mining and Metallurgy, Johannesburg, South Africa, pp. 325-373.
- Reed, S., J., 2005, Electron Microprobe Analysis and Scanning Electron Microscopy in Geology, Cambridge University Press, 189 p.
- Ripley, E. M., 1981, Sulfur Isotopic Abundances of the Dunka Road Cu-Ni Deposit, Duluth Complex, Minnesota; *Economic Geology*, v. 246, pp. 103-107.
- Severson, M. J., and Hauck, S.A., 1990, Geology, Geochemistry, and Stratigraphy of a portion of the Partridge River Intrusion, Natural Resources Research Institute Technical Report NRRI/GMIN-TR-89-11, University Minnesota Duluth, 151 p.
- Severson, M. J., 1994, Igneous Stratigraphy of the South Kawishiwi Intrusion, Duluth Complex, Northeastern Minnesota, Natural Resources Research Institute Technical Report NRRI/TR-93/34, University Minnesota Duluth, 227 p.
- Severson, M., and Hauck, S., 2003, Platinum Group Elements and Platinum Group Minerals in the Duluth Complex, Natural Resources Research Institute Technical Report NRRI/TR-2003/37, University Minnesota Duluth, 312 p.
- Severson, M.J., and S.A. Hauck, 2008, Finish Logging of Duluth Complex Drill Core (And a Reinterpretation of the Geology at the Mesaba (Babbitt) Deposit), University of Minnesota Duluth, Natural Resources Research Institute, Technical Report NRRI/TR-2008/17, 68 p. + 94 plates.
- Therriault, R.D., Barnes, S.J., and Severson, M.J., 2000, Origin of Cu-Ni-PGE Sulfide Mineralization in the Partridge River Intrusion, Duluth Complex, Minnesota, *Economic Geology*, v. 95, no. 5, pp. 929-943.
- Wood, S.A., 2002, The Aqueous Geochemistry of Platinum Group Elements With Applications to Ore Deposits, *In* Cabri, L. J., ed., Geology, Geochemistry, Mineralogy and Mineral Beneficiation of Platinum Group Elements, Canadian Institute of Mining, Metallurgy, and Petroleum, pp.211-249.

Appendix A
Precious Metal Minerals in Ore Samples
Energy Dispersive Spectrometry Data

PTS #26015-346									
Site #	Spectrum #	Mineral name	Element	Weight%	Weight% sigma	Atomic%	Compound%	Formula	# Ions
1	1	Electrum	Ag	19.7	1.83	31			
			Au	80.3	1.83	69			
			Totals	100					
1	2	Cubanite	S	38.89	0.4	54			
			Fe	41.23	0.44	33			
			Cu	19.88	0.49	14			
			Totals	100					
2	1	Paolovite	Pd	61.39	1.03	64			
			Sn	38.61	1.03	36			
			Totals	100					
2	2	Cubanite	S	38.7	0.77	54			
			Fe	37.96	0.83	30			
			Cu	23.33	0.93	16			
			Totals	100					
3	1	Paolovite	Pd	63.05	1.18	66			
			Sn	36.95	1.18	34			
			Totals	100					
3	2	Cubanite	S	38.5	0.97	53			
			Fe	39.93	1.06	32			
			Cu	21.57	1.17	15			
			Totals	100					
4	1	Paolovite	Pd	60.65	1.07	63			
			Sn	39.35	1.07	37			
			Totals	100					
4	2	Cubanite	S	37.3	1.07	52			
			Fe	39.25	1.18	31			
			Cu	23.45	1.32	17			
			Totals	100					
5	1	Electrum	Ag	82.38	19.09	90			
			Au	17.62	19.09	10			
			Totals	100					
5	2	Cubanite	S	38.89	0.78	54			
			Fe	36.22	0.84	29			
			Cu	24.88	0.95	17			
			Totals	100					
6	1	Sperrylite	As	43.84	0.61	66			
			Rh	3.23	0.5	4			
			Pt	52.93	0.65	31			
			Totals	100					
6	2	Pentlandite	S	42.35	0.7	57			
			Fe	19.7	0.62	15			
			Ni	37.95	0.81	28			
			Totals	100					
6	3	Chlorite	Al	10.69	0.27	9.91	20.19	Al2O3	4.64
			Si	16.43	0.33	14.64	35.14	SiO2	6.85
			Fe	33.96	0.49	15.22	43.69	FeO	7.13
			O	38.23	0.47	59.8			28
			Cation sum	18.83					
7	1	Undetermined PGM	Pd	41.49	0.73	54.29			
			Sb	14.09	0.55	16.11			
			Bi	44.42	0.76	29.60			
			Totals	100					
7	2	Orthopyroxene	Mg	12.54	0.23	11.52	20.79	MgO	1.14
			Si	26.25	0.28	20.88	56.15	SiO2	2.07
			Fe	17.92	0.33	7.17	23.06	FeO	0.71
			O	43.29	0.34	60.44			6
			Cation sum	3.93					

PTS #26015-346									
Site #	Spectrum #	Mineral name	Element	Weight%	Weight% sigma	Atomic%	Compound%	Formula	# Ions
8	1	Undetermined PGM	Pd	41.85	0.79	54.77			
			Sb	13.59	0.59	15.54			
			Bi	44.56	0.82	29.69			
			Totals	100					
8	2	Orthopyroxene	Mg	12.74	0.22	11.65	21.12	MgO	1.16
			Si	26.51	0.27	20.99	56.72	SiO2	2.08
			Fe	17.23	0.31	6.86	22.16	FeO	0.68
			O	43.52	0.33	60.5			6
			Cation sum	3.92					
9	1	Undetermined PGM	Pd	42.46	1.03	54.44			
			Sb	17.1	0.82	19.16			
			Bi	40.44	1.09	26.40			
			Totals	100					
9	2	Orthopyroxene	Mg	12.29	0.41	11.37	20.37	MgO	1.13
			Si	25.79	0.5	20.65	55.16	SiO2	2.05
			Fe	19.02	0.59	7.66	24.47	FeO	0.76
			O	42.91	0.61	60.32			6
			Cation sum	3.95					
10	1	Sperrylite	As	40.94	0.6	61.62			
			Rh	7.09	0.52	7.77			
			Sb	1.63	0.35	1.51			
			Pt	50.34	0.68	29.10			
			Totals	100					
10	2	Chalcopyrite	S	38.54	0.42	53.98			
			Fe	28.53	0.41	22.94			
			Cu	31.13	0.51	22.00			
			As	1.81	0.3	1.08			
			Totals	100					
11	1	Sperrylite	As	34.11	0.75	55.69			
			Rh	5.32	0.79	6.33			
			Pt	60.57	0.9	37.98			
			Totals	100					
11	2	Chalcopyrite	S	37.09	0.91	52.34			
			Fe	29.2	0.93	23.66			
			Cu	33.7	1.15	24.00			
			Totals	100					
12	1	Acanthite	S	10.57	0.21	28.46			
			Ag	89.43	0.21	71.54			
			Totals	100					
12	2	Secondary (after plag and cp)	Na	2.8	0.23	2.77	3.78	Na2O	1.11
			Mg	3.24	0.2	3.04	5.38	MgO	1.22
			Al	11.66	0.27	9.83	22.03	Al2O3	3.95
			Si	19.84	0.34	16.08	42.44	SiO2	6.45
			Ca	0.96	0.12	0.55	1.34	CaO	0.22
			Fe	19.46	0.43	7.93	25.03	FeO	3.18
			O	42.04	0.47	59.8			24
			Cation sum	16.13					
12	4	Chalcopyrite	S	31.31	0.74	45.81			
			Fe	34.2	0.86	28.72			
			Cu	34.49	1.02	25.46			
			Totals	100					
13	1	Acanthite	S	9.12	0.21	25.24			
			Ag	90.88	0.21	74.76			
			Totals	100					
13	2	Secondary (after plag and cp)	Mg	3.84	0.2	3.99	6.37	MgO	1.61
			Al	8.29	0.23	7.75	15.66	Al2O3	3.13
			Si	12.46	0.26	11.19	26.65	SiO2	4.52
			S	2.33	0.14	1.83	5.82	SO3	0.74
			Ca	0.61	0.1	0.38	0.85	CaO	0.15
			Fe	30.27	0.45	13.68	38.94	FeO	5.53
			Cu	4.56	0.35	1.81	5.71	CuO	0.73
			O	37.64	0.46	59.37			24
			Cation sum	16.43					
13	5	Chalcopyrite	S	38.35	0.7	53.64			
			Fe	29.2	0.71	23.45			
			Cu	32.45	0.88	22.91			
			Totals	100					

PTS #26015-346								
Site #	Spectrum #	Mineral name	Element	Weight%	Weight% sigma	Atomic%	Compound%	Formula # Ions
14	1	Sperrylite	As	43.55	0.85	65.68		
			Rh	3.14	0.65	3.45		
			Pt	53.31	0.9	30.87		
			Totals	100				
14	2	Chalcopyrite	S	38.81	0.4	54.10		
			Fe	29.42	0.4	23.55		
			Cu	31.77	0.5	22.35		
			Totals	100				
15	1	Sperrylite	As	45.21	0.55	68.24		
			Pt	54.79	0.55	31.76		
			Totals	100				
15	2	Pentlandite	S	41.13	0.4	55.72		
			Fe	19.01	0.35	14.79		
			Ni	39.86	0.46	29.50		
			Totals	100				
16	1	Electrum	Ag	30.4	1.72	44.36		
			Au	69.6	1.72	55.64		
			Totals	100				
16	2	Chalcopyrite	S	39.81	0.57	55.14		
			Fe	28.87	0.57	22.96		
			Cu	31.33	0.7	21.90		
			Totals	100				
17	1	Undetermined PGM	Pd	56.74	0.71	59.21		
			Ag	11.41	0.68	11.75		
			Sb	31.84	0.62	29.04		
			Totals	100				
17	2	Bornite	S	27.68	0.35	42.58		
			Fe	11.83	0.29	10.45		
			Cu	60.49	0.43	46.96		
			Totals	100				
18	1	Electrum	Ag	29.56	2.24	43.38		
			Au	70.44	2.24	56.62		
			Totals	100				
18	2	Chalcopyrite	S	38.05	0.42	53.29		
			Fe	29.95	0.42	24.08		
			Cu	32.01	0.52	22.62		
			Totals	100				
19	1	Electrum	Ag	41.04	6.06	55.97		
			Au	58.96	6.06	44.03		
			Totals	100				
19	2	Chalcopyrite	S	38.37	0.38	53.64		
			Fe	29.69	0.38	23.83		
			Cu	31.93	0.47	22.53		
			Totals	100				
19	3	Pyrite	S	56.52	0.35	69.37		
			Fe	43.48	0.35	30.63		
			Totals	100				
20	1	Paolovite	Pd	64.65	0.51	67.11		
			Sn	35.35	0.51	32.89		
			Totals	100				
20	2	Chalcopyrite	S	38.96	0.61	54.28		
			Fe	28.95	0.61	23.16		
			Cu	32.09	0.75	22.56		
			Totals	100				

PTS #26015-346									
Site #	Spectrum #	Mineral name	Element	Weight%	Weight% sigma	Atomic%	Compound%	Formula	# Ions
21	1	Paolovite	Pd	63.55	0.59	66.05			
			Sn	36.45	0.59	33.96			
			Totals	100					
21	2	Chalcopyrite	S	38.11	0.51	53.41			
			Fe	29.09	0.52	23.41			
			Cu	32.79	0.64	23.19			
			Totals	100					
22	1	Undetermined PGM	Pd	64.87	0.61	67.64			
			Sn	15.01	0.51	14.03			
			Sb	20.12	0.53	18.34			
			Totals	100					
22	2	Orthopyroxene	Mg	12.31	0.21	11.38	20.41	MgO	1.13
			Si	25.65	0.26	20.52	54.87	SiO2	2.04
			Ca	0.87	0.08	0.49	1.21	CaO	0.05
			Fe	18.27	0.3	7.35	23.51	FeO	0.73
			O	42.9	0.32	60.26			6
			Cation sum	3.96					
23	1	Naldrettite	Pd	56.98	1.3	60.25			
			Sb	43.02	1.3	39.75			
			Totals	100					
23	2	Chalcopyrite	S	37.38	0.73	52.60			
			Fe	30.11	0.76	24.33			
			Cu	32.5	0.92	23.08			
			Totals	100					
24	1	Naldrettite	Pd	68.12	1.48	70.97			
			Sb	31.88	1.48	29.03			
			Totals	100					
24	2	Chalcopyrite	S	38.36	0.37	53.65			
			Fe	29.42	0.38	23.62			
			Cu	32.21	0.47	22.73			
			Totals	100					
25	1	Gold	Au	100	0	100.00			
			Totals	100					
25	2	Biotite	Mg	9.25	0.21	8.6	15.34	MgO	3.21
			Al	7.71	0.19	6.46	14.58	Al2O3	2.41
			Si	19.14	0.25	15.41	40.95	SiO2	5.75
			K	7.72	0.17	4.47	9.3	K2O	1.67
			Ti	3.32	0.15	1.57	5.53	TiO2	0.58
			Fe	11.12	0.28	4.5	14.3	FeO	1.68
			O	41.74	0.35	58.99			22
			Cation sum	15.3					
26	1	Undetermined PGM	Ni	1.32	0.34	3.29			
			Cu	9.41	0.57	21.69			
			Zn	1.96	0.54	4.40			
			Ag	9.28	0.72	12.60			
			Au	78.02	0.99	58.01			
			Totals	100					
26	2	Olivine	Mg	16.51	0.26	16.07	27.38	MgO	1.12
			Si	17.93	0.25	15.1	38.37	SiO2	1.05
			Mn	0.49	0.12	0.21	0.63	MnO	0.01
			Fe	26.13	0.36	11.07	33.62	FeO	0.77
			O	38.93	0.35	57.55			4
			Cation sum	2.95					

PTS #26013-103						
Site #	Spectrum #	Mineral name	Element	Weight%	Weight% sigma	Atomic%
1	1	Unnamed PGM	Pd	48.91	0.31	57.03
			Sn	22.96	0.25	24
			Sb	2.81	0.26	2.87
			Pt	25.32	0.27	16.1
1	2	Chalcopyrite	S	38.54	0.18	53.85
			Fe	28.99	0.18	23.26
			Cu	32.46	0.22	22.89
2	1	Unnamed PGM	As	7.54	0.24	11.35
			Pd	52.65	0.43	55.84
			Sn	26.23	0.36	24.95
			Pt	13.58	0.38	7.86
2	3	Chalcopyrite	S	38.74	0.19	54.06
			Fe	25.77	0.18	20.65
			Ni	5.21	0.14	3.97
			Cu	30.27	0.23	21.32
5	1	Unnamed PGM	As	5.75	0.22	8.29
			Pd	72	0.57	73.1
			Sn	10.48	0.31	9.54
			Te	9.04	0.31	7.66
			Bi	2.73	0.55	1.41
5	2	Chalcopyrite	S	37.68	0.25	52.96
			Fe	29.09	0.26	23.47
			Cu	33.23	0.32	23.56
6	1	Kotulskite	Pd	40.02	0.3	53.23
			Te	14.23	0.21	15.78
			Bi	45.76	0.32	30.99
6	3	Chalcopyrite	S	38.12	0.18	53.37
			Fe	29.94	0.18	24.06
			Cu	31.94	0.23	22.57
7	1	Undetermined PGM (in cp)	Fe	1.35	0.08	2.61
			Cu	7.49	0.16	12.75
			Pd	53.48	0.27	54.39
			Sn	26.21	0.23	23.89
			Pt	11.48	0.22	6.37
8	1	Undetermined PGM	Pd	31.54	0.65	44.87
			Sn	7.15	0.4	9.12
			Te	3.24	0.38	3.85
			Pt	22.4	0.62	17.38
			Bi	21.22	0.85	15.37
			Th	14.44	0.68	9.42
8	2	Pentlandite	S	37.04	0.26	51.4
			Fe	22.67	0.25	18.06
			Ni	40.29	0.31	30.54
9	1	Naldrettite	Se	1.88	0.31	3.22
			Pd	52.39	0.7	66.82
			Pb	45.74	0.7	29.96
9	3	Chalcopyrite	S	38.22	0.26	53.5
			Fe	29.24	0.26	23.5
			Cu	32.55	0.33	22.99

PTS #26010-116									
Site #	Spectrum #	Mineral name	Element	Weight%	Weight% sigma	Atomic%	Compound%	Formula	# Ions
1	3	Undetermined	F	2.5	0.37	18.95			
		PGM	Pd	20.89	0.41	28.27			
			Bi	76.61	0.5	52.78			
1	4	Chlorite	Mg	0.73	0.1	0.77	1.21	MgO	0.37
			Al	9.1	0.15	8.7	17.2	Al2O3	4.13
			Si	14.87	0.18	13.65	31.81	SiO2	6.48
			Fe	38.69	0.29	17.87	49.78	FeO	8.48
			O	36.6	0.27	59			28
			Cation sum	19.46					
1	6	Undetermined	Pd	41.85	0.42	49.62			
		PGM	Sb	35.33	0.39	36.61			
			Bi	22.81	0.46	13.77			
1	1	Chalcopyrite	S	38.05	0.26	53.31			
			Fe	29.63	0.26	23.84			
			Cu	32.32	0.32	22.85			
1	7	Undetermined	Pd	35.23	0.46	51.65			
		PGM	Bi	64.77	0.46	48.35			
1	1	Chalcopyrite	S	38.05	0.26	53.31			
			Fe	29.63	0.26	23.84			
			Cu	32.32	0.32	22.85			
1	8	Undetermined	Pd	86.41	3.65	92.59			
		PGM	Bi	13.59	3.65	7.41			
3	1	Gold	O	23.92	0.48	69.43			
			Al	3.8	0.09	6.53			
			Ca	5.48	0.12	6.35			
			Fe	3.27	0.13	2.72			
			Au	63.54	0.47	14.98			
3	3	Undet. Secondary	Al	7.26	0.16	7.29	13.71	Al2O3	3.38
		Chlorite within 1 um	Ca	56.13	0.29	37.96	78.54	CaO	17.58
			Fe	6.02	0.23	2.92	7.75	FeO	1.35
			O	30.59	0.26	51.82			24
			Cation sum	22.31					
4	1		Ag	10.97	0.49	18.37			
			Au	89.03	0.49	81.63			
4	5	Undet. Secondary	Al	12	0.16	11.18	22.67	Al2O3	4.53
		Chlorite within 1 um	Si	14.55	0.17	13.03	31.14	SiO2	5.27
			Ca	2.22	0.08	1.39	3.1	CaO	0.56
			Fe	33.49	0.27	15.08	43.09	FeO	6.1
			O	37.73	0.26	59.31			24
			Cation sum	16.46					
5	1	Electrum	Ag	19.8	0.84	31.08			
			Au	80.2	0.84	68.92			
5	3	Chlorite	Mg	9.49	0.14	8.32	15.74	MgO	3.87
			Al	19.55	0.18	15.43	36.94	Al2O3	7.18
			Si	16.61	0.18	12.6	35.54	SiO2	5.86
			Fe	9.16	0.19	3.49	11.78	FeO	1.63
			O	45.19	0.24	60.16			28
			Cation sum	18.54					
6	1	Electrum	Ag	15.63	0.84	25.28			
			Au	84.37	0.84	74.72			
6	3	Biotite	Mg	4.51	0.12	4.42	7.48	MgO	1.64
			Al	8.54	0.14	7.54	16.14	Al2O3	2.8
			Si	17.22	0.17	14.6	36.84	SiO2	5.42
			Cl	0.9	0.07	0.61	0		0.23
			K	7.66	0.12	4.66	9.22	K2O	1.73
			Ti	3.72	0.11	1.85	6.2	TiO2	0.69
			Fe	18.04	0.23	7.69	23.21	FeO	2.86
			O	39.41	0.25	58.64			21.77
			Cation sum	15.13					

PTS #26010-116									
Site #	Spectrum #	Mineral name	Element	Weight%	Weight% sigma	Atomic%	Compound%	Formula	# Ions
8	1	Electrum	Ag	15.86	0.48	25.6			
			Au	84.14	0.48	74.4			
8	2	Biotite	Mg	4.84	0.12	4.73	8.02	MgO	1.75
			Al	7.87	0.13	6.94	14.88	Al2O3	2.57
			Si	17.39	0.17	14.72	37.2	SiO2	5.46
			Cl	1.02	0.07	0.68	0		0.25
			K	7.99	0.12	4.86	9.62	K2O	1.8
			Ti	3.86	0.11	1.92	6.44	TiO2	0.71
			V	0.39	0.09	0.18	0.7	V2O5	0.07
			Fe	17.2	0.23	7.33	22.13	FeO	2.72
			O	39.44	0.25	58.64			21.75
		Cation sum	15.09						
10	1	Undetermined PGM	As	3.53	0.25	6.28			
			Pd	30.17	0.47	37.81			
			Sb	11.63	0.41	12.74			
			Te	20.35	0.43	21.27			
		Bi	34.33	0.54	21.91				
10	7	Nickeline	Fe	2.21	0.12	2.61			
			Ni	45.64	0.35	51.38			
			As	52.15	0.35	46.01			
10	8	Undetermined PGM	Mo	24.33	0.51	35.58			
			Pd	21.03	0.5	27.74			
			Bi	54.64	0.62	36.68			
10	6	Chalcopyrite	S	38.34	0.27	53.61			
			Fe	29.77	0.27	23.89			
			Cu	31.89	0.33	22.5			
11	1	Undetermined PGM	Fe	2.32	0.24	6.55			
			Pd	27.5	0.7	40.65			
			Bi	70.18	0.72	52.81			
11	8	Pentlandite	S	43.5	0.58	57.93			
			Fe	26.54	0.55	20.29			
			Co	3.24	0.42	2.35			
			Ni	26.71	0.63	19.43			
12	1	Undetermined PGM	Pd	27.44	0.82	42.61			
			Bi	72.56	0.82	57.39			
11	8	Pentlandite	S	43.5	0.58	57.93			
			Fe	26.54	0.55	20.29			
			Co	3.24	0.42	2.35			
			Ni	26.71	0.63	19.43			
12	3	Undetermined PGM	Pd	35.66	0.67	52.12			
			Bi	64.34	0.67	47.88			
11	8	Pentlandite	S	43.5	0.58	57.93			
			Fe	26.54	0.55	20.29			
			Co	3.24	0.42	2.35			
			Ni	26.71	0.63	19.43			
13	1	Undetermined PGM	Pd	13.67	1.61	23.72			
			Bi	86.33	1.61	76.28			
13	4	Pyrrhotite	S	40.63	0.39	54.48			
			Fe	57.23	0.42	44.07			
			Cu	2.14	0.32	1.45			
15	1	Electrum	Ag	19.19	1.2	30.24			
			Au	80.81	1.2	69.76			
15	2	Pyrrhotite	S	44.38	0.35	58.19			
			Fe	53.87	0.37	40.55			
			Ni	1.75	0.23	1.25			
16	1	Gold	Ag	0.04	0.41	0.08			
			Au	99.96	0.41	99.92			
16	2	Chlorite	Al	12.71	0.23	11.62	24.02	Al2O3	5.43
			Si	16.09	0.25	14.13	34.42	SiO2	6.6
			Fe	32.31	0.38	14.27	41.56	FeO	6.66
			O	38.89	0.36	59.97			28
		Cation sum	18.69						

PTS #26010-116									
Site #	Spectrum #	Mineral name	Element	Weight%	Weight% sigma	Atomic%	Compound%	Formula	# Ions
16	4	Gold	Ag	0.59	0.74	1.07			
			Au	99.41	0.74	98.93			
16	2	Chlorite	Al	12.71	0.23	11.62	24.02	Al2O3	5.43
			Si	16.09	0.25	14.13	34.42	SiO2	6.6
			Fe	32.31	0.38	14.27	41.56	FeO	6.66
			O	38.89	0.36	59.97			28
			Cation sum	18.69					
17	1	Froodite	Pd	20.99	0.58	34.28			
			Bi	79.01	0.58	65.72			
17	3	Pentlandite	S	36.94	0.36	51.26			
			Fe	24.85	0.35	19.8			
			Co	2.69	0.26	2.03			
			Ni	35.52	0.43	26.92			
17	2	Froodite	F	3.23	0.55	23.71			
			Pd	18.26	0.59	23.93			
			Bi	78.51	0.73	52.36			
17	3	Pentlandite	S	36.94	0.36	51.26			
			Fe	24.85	0.35	19.8			
			Co	2.69	0.26	2.03			
			Ni	35.52	0.43	26.92			
18	1		Ag	0.35	0.7	0.64			
			Au	99.65	0.7	99.36			
18	2	Pyrrhotite	S	42.02	0.39	55.94			
			Fe	54.16	0.42	41.4			
			Ni	1.69	0.23	1.23			
			Cu	2.13	0.28	1.43			
19	1	Electrum	Ag	11.39	1.03	19.01			
			Au	88.61	1.03	80.99			
19	2	Pyrrhotite	S	43.9	0.38	57.86			
			Fe	52.61	0.4	39.82			
			Cu	3.49	0.31	2.32			
20	1	Gold	Ag	-0.01	0.63	-0.02			
			Au	100.01	0.63	100.02			
20	2	Chalcopyrite	S	38.17	0.4	53.44			
			Fe	29.67	0.41	23.84			
			Cu	32.16	0.5	22.72			
21	1	Electrum	Ag	21.01	2.66	32.69			
			Au	78.99	2.66	67.31			
21	2	Chalcopyrite	S	37.58	0.4	52.82			
			Fe	29.65	0.41	23.93			
			Cu	32.78	0.5	23.25			
22	1	Electrum	Ag	16.02	0.8	25.84			
			Au	83.98	0.8	74.16			
22	2	Undet. Secondary	Mg	1.19	0.2	1.68	1.98	MgO	0.91
			Si	2.34	0.17	2.85	5.01	SiO2	1.55
			Ca	0.33	0.1	0.29	0.47	CaO	0.15
			Fe	70.94	0.5	43.48	91.27	FeO	23.55
			Br	1.28	0.32	0.55	0		0.3
			O	23.91	0.41	51.15			27.7
			Cation sum	26.16					
23	1	Undetermined PGM	Pd	10.75	1.36	19.12			
			Bi	89.25	1.36	80.88			
23	2		S	38.19	0.38	53.48			
			Fe	29.25	0.39	23.51			
			Cu	32.56	0.48	23.01			
23	3	Pentlandite	S	42.76	0.41	57.13			
			Fe	29.97	0.41	22.98			
			Co	2.56	0.29	1.86			
			Ni	24.71	0.45	18.03			

PTS #26010-116									
Site #	Spectrum #	Mineral name	Element	Weight%	Weight% sigma	Atomic%	Compound%	Formula	# Ions
24	1	Undetermined	Pd	38.94	0.76	55.6			
		PGM	Bi	61.06	0.76	44.4			
24	2	Pyrrhotite	S	44.1	0.36	57.92			
			Fe	53.92	0.37	40.66			
			Ni	1.98	0.23	1.42			
25	1	Undetermined	Pd	31.27	1.2	47.2			
		PGM	Bi	68.73	1.2	52.8			
25	2	Pentlandite	S	43.45	0.42	57.84			
			Fe	28.67	0.4	21.91			
			Co	3.08	0.29	2.23			
			Ni	24.79	0.45	18.02			
26	1	Undetermined	Pd	45.95	2.31	62.54			
		PGM	Bi	54.05	2.31	37.46			
26	2	Pentlandite	S	42.03	0.44	56.73			
			Fe	31.94	0.44	24.76			
			Co	5.82	0.34	4.27			
			Ni	18.21	0.44	13.42			
			Pd	2	0.35	0.82			
27	1	Froodite	Pd	21.21	0.62	34.58			
			Bi	78.79	0.62	65.42			
27	2	Pentlandite	S	36.15	0.38	50.4			
			Fe	25.33	0.37	20.28			
			Co	2.75	0.28	2.09			
			Ni	35.77	0.45	27.24			
28	1	Froodite	Pd	20.37	0.7	33.44			
			Bi	79.63	0.7	66.56			
28	2	Pentlandite	S	40.65	0.46	54.97			
			Fe	32.13	0.47	24.94			
			Co	4.82	0.36	3.54			
			Ni	22.41	0.5	16.55			
29	1	Froodite	Pd	21.82	0.85	35.4			
			Bi	78.18	0.85	64.6			
29	2	Pentlandite	S	44.39	0.68	58.93			
			Fe	20.58	0.59	15.69			
			Co	7.51	0.53	5.43			
			Ni	27.52	0.73	19.95			
30	1	Undetermined	Pd	38.08	0.62	50.1			
		PGM	Sb	17.55	0.46	20.18			
			Bi	44.37	0.65	29.72			
30	2	Pentlandite	S	35.74	0.37	49.96			
			Fe	25.04	0.37	20.1			
			Co	2.86	0.28	2.17			
			Ni	36.36	0.45	27.76			
31	1	Undetermined	Pd	32.17	0.63	43.95			
		PGM	Sb	17.78	0.48	21.23			
			Bi	50.05	0.67	34.82			
31	2	Pentlandite	S	35.51	0.53	49.7			
			Fe	26.01	0.54	20.9			
			Co	2.82	0.4	2.15			
			Ni	35.66	0.65	27.25			

PTS #26010-117										
Site #	Spectrum #	Mineral name	Element	Weight%	Weight% sigma	Atomic%	Compound%	Formula	# Ions	An#
3	1	Undetermined PGM	S	12.85	0.4	39.09				
			Fe	11.49	0.37	20.07				
			Cu	1.88	0.33	2.89				
			Se	1.39	0.47	1.72				
			Ag	5.55	0.46	5.02				
3	2	Chalcopyrite	S	38.36	0.32	53.6				
			Fe	30.34	0.32	24.34				
			Cu	31.3	0.4	22.07				
4	1	Undetermined PGM	Pd	40.73	0.52	51.6				
			Sb	22	0.42	24.36				
			Bi	37.27	0.55	24.04				
4	2	Chalcopyrite	S	38.31	0.33	53.59				
			Fe	29.44	0.33	23.65				
			Cu	32.25	0.41	22.76				
5	1	Electrum	Ag	1.19	1.44	2.16				
			Au	98.81	1.44	97.84				
5	2	Pentlandite	S	43.46	0.33	57.92				
			Fe	24.4	0.31	18.67				
			Ni	32.14	0.37	23.4				
6	1	Undetermined PGM	Pd	34.48	0.94	50.82				
			Bi	65.52	0.94	49.18				
6	6	Plagioclase	Na	3.81	0.13	3.45	5.14	Na2O	0.45	
			Al	14.29	0.17	11.02	27.01	Al2O3	1.43	
			Si	26.69	0.22	19.78	57.1	SiO2	2.56	
			K	0.57	0.07	0.3	0.68	K2O	0.04	
			Ca	7.2	0.14	3.74	10.07	CaO	0.48	
			O	47.44	0.25	61.71			8	
		Cation sum	4.96							
8	1	Gold	Ag	-0.32	0.76	-0.59				
			Au	100.32	0.76	100.59				
8	2	Chalcopyrite	S	37.28	0.36	52.5				
			Fe	29.98	0.38	24.24				
			Cu	32.74	0.46	23.26				
10	1	Electrum	Ag	5.86	5.93	10.21				
			Au	94.14	5.93	89.79				
10	2	Pentlandite	S	40.24	0.42	55.63				
			Fe	22.35	0.37	17.74				
			Co	1.44	0.25	1.08				
			Ni	32.91	0.46	24.85				
11	1	Froodite	Pd	20.71	0.75	33.9				
			Bi	79.29	0.75	66.1				
11	2	Plagioclase	Na	4.23	0.16	3.82	5.71	Na2O	0.5	An#
			Al	14.36	0.2	11.05	27.14	Al2O3	1.43	48
			Si	26.73	0.26	19.76	57.18	SiO2	2.56	
			K	0.39	0.08	0.21	0.48	K2O	0.03	
			Ca	6.79	0.16	3.52	9.5	CaO	0.46	
			O	47.49	0.3	61.64			8	
		Cation sum	4.98							
12	1	Electrum	Ag	42.71	7.97	57.65				
			Au	57.29	7.97	42.35				
12	2	Chalcopyrite	S	38.59	0.97	53.91				
			Fe	28.78	0.97	23.08				
			Cu	32.63	1.19	23				
13	1	Electrum	Ag	23.77	2.64	36.27				
			Au	76.23	2.64	63.73				
13	2	Chalcopyrite	S	37.97	1.01	53.19				
			Fe	30.33	1.03	24.4				
			Cu	31.7	1.26	22.41				

PTS #26010-117										
Site #	Spectrum #	Mineral name	Element	Weight%	Weight% sigma	Atomic%	Compound%	Formula	# Ions	An#
14	1	Gold	Ag	-3.63	-4.88	-6.84				
			Au	103.63	-4.88	106.84				
14	2	Pyrrhotite	S	41.85	0.37	55.63				
			Fe	58.15	0.37	44.37				
15	1	Electrum	Ag	36.83	5.19	51.56				
			Au	63.17	5.19	48.44				
15	2	Chalcopyrite	S	37.82	0.38	53.07				
			Fe	29.62	0.39	23.86				
			Cu	32.57	0.47	23.06				
16	1	Electrum	Ag	50.74	6.85	65.29				
			Au	49.26	6.85	34.71				
16	3	Plagioclase	Na	3.65	0.16	3.3	4.92	Na2O	0.43	An#
			Al	14.48	0.2	11.16	27.37	Al2O3	1.44	52
			Si	26.76	0.26	19.81	57.25	SiO2	2.56	
			K	0.55	0.08	0.29	0.67	K2O	0.04	
			Ca	7	0.16	3.63	9.8	CaO	0.47	
			O	47.55	0.3	61.8			8	
			Cation sum	4.95						

PTS #26013-106										
Site #	Spectrum #	Mineral name	Element	Weight%	Weight% sigma	Atomic%	Compound%	Formula	# Ions	An#
1	1	Electrum	Ag	68.32	0.6	79.75				
			Au	31.68	0.6	20.25				
1	2	Chalcopyrite	S	38.42	0.37	53.72				
			Fe	29.15	0.37	23.4				
2	1	Undetermined PGM	Cu	32.43	0.46	22.88				
			As	12.96	0.4	19.33				
			Pd	49.82	0.63	52.32				
			Sn	19.07	0.51	17.95				
2	2	Chalcopyrite	Pt	18.16	0.58	10.4				
			S	39	0.37	54.34				
			Fe	28.71	0.37	22.96				
2	3	Bornite	Cu	32.29	0.46	22.7				
			S	29.83	0.35	45.17				
			Fe	11.44	0.28	9.95				
3	1	Undetermined PGM	Cu	58.73	0.42	44.88				
			Pd	60.27	0.74	63.37				
			Sn	27.23	0.66	25.67				
3	2	Cubanite	Te	12.5	0.62	10.96				
			S	38.44	0.36	53.18				
			Fe	39.96	0.4	31.74				
4	1	Empressite	Cu	21.6	0.44	15.08				
			Ag	55.04	0.61	59.15				
			Te	44.96	0.61	40.85				
4	2	Pyrrhotite	S	13.94	0.27	22.14				
			Fe	80.48	0.43	73.38				
			Cu	5.58	0.38	4.47				
5	1	Paolovite	Pd	65.5	0.47	67.93				
			Sn	34.5	0.47	32.07				
5	2	Chalcopyrite	S	38.62	0.37	53.93				
			Fe	28.94	0.37	23.2				
			Cu	32.44	0.46	22.86				
6	1	Electrum	Ag	59.21	0.61	72.61				
			Au	40.79	0.61	27.39				
6	2	Pentlandite	S	37.15	0.35	51.41				
			Fe	27.94	0.36	22.2				
			Ni	34.91	0.43	26.39				
7	1	Empressite	Ag	58.62	0.76	62.63				
			Te	41.38	0.76	37.37				
7	2	Chalcopyrite	S	37.06	0.41	52.22				
			Fe	30.87	0.43	24.97				
			Cu	32.08	0.52	22.81				
8	1	Undetermined PGM	Pd	49.21	0.99	53.91				
			Ag	9.49	0.72	10.26				
			Sn	28.93	0.77	28.42				
			Pt	15.58	0.76	9.31				
8	3	Chalcopyrite	S	38.72	0.38	54.01				
			Fe	29.41	0.38	23.56				
			Cu	31.87	0.47	22.43				
9	1	Undetermined PGM	Pd	41.97	0.7	46.38				
			Ag	21.63	0.65	23.57				
			Sn	20.91	0.58	20.71				
			Pt	15.49	0.63	9.34				
9	3	Plagioclase	Na	0.91	0.11	0.84	1.23	Na2O	0.11	An#
			Al	17.96	0.21	14.12	33.94	Al2O3	1.83	89
			Si	22.2	0.24	16.77	47.5	SiO2	2.17	
			Ca	12.39	0.19	6.56	17.33	CaO	0.85	
			O	46.54	0.28	61.71			8	
10	1	Undetermined PGM	Cation sum	4.96						
			As	17.58	0.73	25.39				
			Pd	45.45	0.96	46.2				
			Sn	22.16	0.79	20.2				
10	5	Pentlandite	Pt	14.81	0.95	8.21				
			S	36.46	0.36	50.68				
			Fe	27.77	0.37	22.17				
			Ni	35.77	0.43	27.15				

PTS #26013-106										
Site #	Spectrum #	Mineral name	Element	Weight%	Weight% sigma	Atomic%	Compound%	Formula	# Ions	An#
11	1	Undetermined PGM	Pd	53.64	0.7	57.53				
			Ag	10.85	0.65	11.48				
			Sn	27.18	0.57	26.13				
			Pt	8.32	0.49	4.87				
11	2	Chalcopyrite	S	38.59	0.38	53.88				
			Fe	29.58	0.39	23.7				
			Cu	31.83	0.48	22.42				
12	1	Paolovite	Pd	65.02	0.63	67.46				
			Sn	34.98	0.63	32.54				
12	2	Chalcopyrite	S	38.25	0.38	53.52				
			Fe	29.76	0.38	23.91				
			Cu	31.98	0.47	22.58				
13	1	Undetermined PGM (in cp)	Pd	46.6	0.8	53.98				
			Ag	8.21	0.66	9.38				
			Sn	21.13	0.6	21.94				
			Pt	11.97	0.57	7.56				
			Bi	12.09	0.73	7.13				
14	1	Kotulskite	Pd	39.49	0.79	52.25				
			Te	16.29	0.58	17.97				
			Bi	44.22	0.84	29.79				
14	2	Chlorite	Al	9.51	0.22	9.02	17.96	Al2O3	4.19	
			Si	12.15	0.24	11.07	26	SiO2	5.14	
			S	3.11	0.16	2.48	7.76	SO3	1.15	
			Fe	35.02	0.42	16.05	45.05	FeO	7.45	
			Ni	2.54	0.25	1.11	3.23	NiO	0.51	
			O	37.68	0.41	60.27			28	
			Cation sum		18.46					
15	1	Paolovite	Pd	64.98	0.48	67.42				
			Sn	35.02	0.48	32.58				
15	3	Chalcopyrite	S	37.98	0.38	53.22				
			Fe	30.2	0.39	24.29				
			Cu	31.82	0.48	22.49				
15	2	Kotulskite	Pd	40.21	0.62	53.1				
			Te	15.61	0.44	17.19				
			Bi	44.18	0.65	29.71				
15	3	Chalcopyrite	S	37.98	0.38	53.22				
			Fe	30.2	0.39	24.29				
			Cu	31.82	0.48	22.49				
16	1	Undetermined PGM	Pd	46.52	0.87	58.97				
			Sn	7.09	0.53	8.06				
			Te	7.38	0.57	7.8				
			Bi	39.01	0.9	25.18				
16	2	Clinopyroxene	Mg	8.94	0.18	8.15	14.83	MgO	0.81	
			Al	0.6	0.1	0.49	1.12	Al2O3	0.05	
			Si	25.69	0.25	20.28	54.95	SiO2	2.02	
			Ca	14.61	0.21	8.08	20.44	CaO	0.8	
			Ti	0.37	0.09	0.17	0.62	TiO2	0.02	
			Fe	6.25	0.23	2.48	8.03	FeO	0.25	
			O	43.55	0.31	60.35			6	
		Cation sum		3.94						

PTS #26013-106										
Site #	Spectrum #	Mineral name	Element	Weight%	Weight% sigma	Atomic%	Compound%	Formula	# Ions	An#
17	1	Kotulskite	Pd	38.94	0.65	51.54				
			Te	17.01	0.48	18.77				
			Bi	44.05	0.69	29.68				
25	3	Chlorite	Mg	12.21	0.27	10.64	20.24	MgO	5	
			Al	19.26	0.32	15.12	36.4	Al2O3	7.11	
			Si	15.33	0.3	11.56	32.8	SiO2	5.44	
			Fe	8.21	0.32	3.11	10.56	FeO	1.46	
			O	44.99	0.43	59.56			28	
			Cation sum	19.01						
17	6	Kotulskite	Pd	38.77	0.6	51.28				
			Te	17.45	0.44	19.25				
			Bi	43.78	0.64	29.48				
25	3	Chlorite	Mg	12.21	0.27	10.64	20.24	MgO	5	
			Al	19.26	0.32	15.12	36.4	Al2O3	7.11	
			Si	15.33	0.3	11.56	32.8	SiO2	5.44	
			Fe	8.21	0.32	3.11	10.56	FeO	1.46	
			O	44.99	0.43	59.56			28	
			Cation sum	19.01						
18	1	Silver (sulfide?)	S	13.64	0.34	31.32				
			Fe	11.71	0.54	15.43				
			Cu	4.88	0.72	5.66				
			Ag	69.77	0.79	47.6				
18	2	Chalcopyrite	S	34.89	0.48	49.61				
			Fe	37.1	0.59	30.29				
			Cu	28.01	0.65	20.1				
19	1	Paolovite	Pd	68.88	0.63	71.17				
			Sn	31.12	0.63	28.83				
19	3	Clinopyroxene	Mg	8.61	0.18	7.88	14.28	MgO	0.79	
			Al	0.97	0.1	0.8	1.83	Al2O3	0.08	
			Si	25.31	0.25	20.05	54.15	SiO2	2	
			Ca	15.03	0.2	8.35	21.04	CaO	0.83	
			Fe	6.77	0.23	2.7	8.71	FeO	0.27	
			O	43.31	0.3	60.23			6	
			Cation sum	3.96						
20	1	Telluropalladinite	Pd	93.12	5.77	84.97				
			Te	39.93	2.89	30.38				
20	2	Chalcopyrite	S	38.47	0.37	53.73				
			Fe	29.99	0.38	24.05				
			Cu	31.54	0.47	22.23				
21	1	Paolovite	Pd	65.36	0.47	67.79				
			Sn	34.64	0.47	32.21				
21	2	Chalcopyrite	S	38.22	0.37	53.5				
			Fe	29.39	0.38	23.62				
			Cu	32.38	0.47	22.87				

PTS #26013-106										
Site #	Spectrum #	Mineral name	Element	Weight%	Weight% sigma	Atomic%	Compound%	Formula	# Ions	An#
22	1	Undetermined PGM	Se	2.21	0.37	4.24				
			Pd	19.18	0.77	27.29				
			Ag	8.31	0.69	11.67				
			Te	11.98	0.58	14.21				
			Pb	58.31	1	42.6				
22	2	Pentlandite	S	37.41	0.39	52.28				
			Fe	27.44	0.38	22.01				
			Ni	22.7	0.42	17.32				
			Cu	11.1	0.41	7.83				
			Ag	1.34	0.3	0.56				
23	1	Paolovite	Pd	65.08	0.49	67.52				
			Sn	34.92	0.49	32.48				
23	2	Pentlandite	S	28.6	0.36	41.53				
			Fe	45.61	0.45	38.02				
			Ni	25.79	0.47	20.45				
24	1	Undetermined PGM	Pd	42	0.68	50.92				
			Te	33.73	0.59	34.1				
			Bi	24.26	0.68	14.98				
24	3	Clinopyroxene	Mg	13.66	0.21	12.4	22.65	MgO	1.23	
			Al	0.59	0.11	0.48	1.11	Al2O3	0.05	
			Si	25.91	0.26	20.35	55.43	SiO2	2.03	
			Ca	0.69	0.08	0.38	0.96	CaO	0.04	
			Fe	15.42	0.29	6.09	19.84	FeO	0.61	
			O	43.73	0.32	60.3				6
			Cation sum		3.95					

PTS #26013-110										
Site #	Spectrum #	Mineral name	Element	Weight%	Weight% sigma	Atomic%	Compound%	Formula	# Ions	An#
1	1	Undetermined PGM	Pd	35.55	1.05	36.92				
			Ag	33.05	1.09	33.85				
			Sn	31.4	0.99	29.23				
1	2	Chalcopyrite	S	36.2	0.37	51.68				
			Fe	23.64	0.36	19.38				
			Cu	40.17	0.47	28.94				
2	1	Undetermined PGM	As	6.44	0.54	9.07				
			Pd	76.14	0.9	75.46				
			Sn	17.42	0.83	15.47				
2	2	Pentlandite	S	43.19	0.39	57.92				
			Fe	12.98	0.29	9.99				
			Co	1.34	0.23	0.98				
			Ni	42.49	0.44	31.11				
3	1	Undetermined PGM	Pd	24.43	1.51	28.41				
			Ag	37.33	1.58	42.82				
			Te	13.47	1.15	13.06				
			Pt	24.76	1.62	15.7				
3	2	Pentlandite	S	40.39	0.41	55.17				
			Fe	14.43	0.31	11.31				
			Co	0.93	0.23	0.69				
			Ni	41.08	0.46	30.64				
			Cu	3.17	0.34	2.19				
4	1	Silver (sulfide?)	S	30.33	0.58	59.43				
			Ag	69.67	0.58	40.57				
4	1		S	33.61	0.57	48.62				
			Fe	28.94	0.58	24.03				
			Cu	37.46	0.72	27.35				
5	1	Undetermined PGM	Pd	52.19	0.64	56.32				
			Sn	9.65	0.52	9.34				
			Te	38.16	0.6	34.34				
5	2	Pentlandite	S	36.04	0.37	50.3				
			Fe	24.62	0.36	19.72				
			Co	1.19	0.25	0.9				
			Ni	38.15	0.45	29.07				
7	1	Paolovite	Pd	70.6	0.63	72.81				
			Sn	29.4	0.63	27.19				
7	3	Plagioclase	Na	1.49	0.14	1.37	2.01	Na2O	0.18	An#
			Al	16.9	0.22	13.27	31.93	Al2O3	1.72	81
			Si	22.79	0.26	17.19	48.75	SiO2	2.23	
			S	0.34	0.08	0.23	0.86	SO3	0.03	
			Ca	11.03	0.19	5.83	15.44	CaO	0.76	
			Fe	0.78	0.13	0.3	1.01	FeO	0.04	
			O	46.66	0.32	61.8			8	
			Cation sum	4.94						
8	1	Undetermined PGM	Pd	64.81	0.98	75.7				
			In	6.62	0.78	7.16				
			Pb	28.57	0.86	17.14				
8	4	Pyrrhotite	S	22.23	0.33	33.97				
			Fe	57.14	0.49	50.12				
			Cu	20.63	0.5	15.91				
9	1	Paolovite	Pd	69.42	0.56	71.69				
			Sn	30.58	0.56	28.31				
9	2	Chalcopyrite	S	38.01	0.38	53.26				
			Fe	29.79	0.38	23.96				
			Cu	32.21	0.48	22.77				
10	1	Undetermined PGM	As	0.67	1.05	1.03				
			Pd	54.38	1.33	58.59				
			Te	44.94	1.29	40.38				
10	2	Chalcopyrite	S	37.45	0.35	52.68				
			Fe	29.83	0.36	24.09				
			Cu	32.73	0.44	23.23				
11	1	Undetermined PGM	Pd	55.59	0.6	61.96				
			Sn	28.21	0.53	28.19				
			Pt	16.2	0.53	9.85				
11	2	Pentlandite	S	44.9	0.38	59.66				
			Fe	9.48	0.26	7.24				
			Ni	45.62	0.41	33.11				

PTS #26013-110										
Site #	Spectrum #	Mineral name	Element	Weight%	Weight% sigma	Atomic%	Compound%	Formula	# Ions	An#
12	1	Undetermined	Pd	44.62	0.66	53.26				
		PGM	Sn	25.5	0.57	27.29				
		(in cp)	Pt	29.87	0.65	19.45				
13	1	Undetermined	Pd	41.23	0.87	51.74				
		PGM	Sn	18.21	0.79	20.49				
			Pt	40.56	0.88	27.77				
13	2	Sericite	Mg	3.82	0.17	3.4	6.34	MgO	1.28	
			Al	8.75	0.21	7.02	16.54	Al2O3	2.65	
			Si	22.1	0.3	17.02	47.28	SiO2	6.43	
			S	4.42	0.19	2.98	11.04	SO3	1.13	
			Cl	5.37	0.2	3.28	0		1.24	
			K	9.85	0.23	5.45	11.87	K2O	2.06	
			Ca	1.12	0.15	0.6	1.57	CaO	0.23	
			O	44.56	0.39	60.25			22.76	
			Cation sum	13.78						
14	1	Undetermined	Pd	62.33	0.63	66.66				
		PGM	Sn	30.27	0.56	29.02				
			Pt	7.4	0.5	4.31				
14	2	Chalcopyrite	S	38.17	0.37	53.43				
			Fe	29.64	0.38	23.82				
			Cu	32.19	0.47	22.74				
15	1	Undetermined	Pd	61.07	0.67	66.32				
		PGM	Sn	27.89	0.58	27.15				
			Pt	11.04	0.57	6.54				
15	2	Chalcopyrite	S	37.51	0.86	52.79				
			Fe	28.88	0.88	23.34				
			Cu	33.62	1.07	23.88				
			Pd	59.51	0.59	65.7				
			Sn	25.58	0.5	25.32				
			Pt	14.92	0.51	8.98				
16	1	Undetermined	Pd	59.51	0.59	65.7				
		PGM	Sn	25.58	0.5	25.32				
			Pt	14.92	0.51	8.98				
16	1	Bornite	S	22.61	1.58	36.06				
			Fe	14.96	1.65	13.7				
			Cu	62.43	2.08	50.24				
17	1	Undetermined	Pd	62.82	0.56	67.4				
		PGM	Sn	28.79	0.5	27.69				
			Pt	8.38	0.45	4.91				
17	2	Pyrrhotite	S	38.34	0.36	53.08				
			Fe	39.96	0.39	31.76				
			Cu	21.7	0.43	15.16				
18	1	Kotulskite	Pd	40.54	0.61	53.53				
			Te	15.14	0.43	16.67				
			Bi	44.32	0.64	29.8				
18	3	Plagioclase	Na	3.66	0.16	3.31	4.93	Na2O	0.43	An#
			Al	14.52	0.2	11.22	27.43	Al2O3	1.45	56
			Si	26.27	0.26	19.5	56.21	SiO2	2.53	
			Ca	8.17	0.17	4.25	11.43	CaO	0.55	
			O	47.38	0.3	61.72			8	
			Cation sum	4.96						
19	1	Undetermined	As	0.74	0.28	1.32				
		PGM	Pd	38.97	0.72	48.54				
			Te	28.79	0.61	29.9				
			Pt	4.23	0.47	2.87				
			Pb	14.04	0.68	8.98				
			Bi	13.22	0.8	8.38				
19	2	Plagioclase	Na	3.29	0.15	2.99	4.44	Na2O	0.39	An#
			Al	14.52	0.19	11.23	27.43	Al2O3	1.45	57
			Si	26.4	0.25	19.62	56.48	SiO2	2.54	
			K	0.23	0.07	0.12	0.27	K2O	0.02	
			Ca	7.75	0.16	4.04	10.85	CaO	0.52	
			Fe	0.41	0.11	0.15	0.52	FeO	0.02	
			O	47.4	0.29	61.84			8	
			Cation sum	4.94						

PTS #26013-110										
Site #	Spectrum #	Mineral name	Element	Weight%	Weight% sigma	Atomic%	Compound%	Formula	# Ions	An#
20	1	Undetermined PGM	As	7.85	0.4	11.48				
			Pd	65.21	0.71	67.16				
			Sn	17.22	0.54	15.9				
			Pt	9.72	0.57	5.46				
20	2	Talnakhite	S	40.2	0.46	55.42				
			Fe	22.85	0.41	18.09				
			Ni	13.61	0.43	10.25				
			Cu	23.33	0.54	16.23				
21	1	Paolovite	Pd	69.73	0.49	71.99				
			Sn	30.27	0.49	28.01				
21	3	Chalcopyrite	S	38.15	0.37	53.42				
			Fe	29.59	0.37	23.78				
			Cu	32.26	0.46	22.8				
22	1	Undetermined PGM	Pd	21.01	0.74	32.11				
			Te	4.67	0.53	5.95				
			Pt	74.32	0.82	61.95				
22	2	Talnakhite	S	37.82	0.38	53.08				
			Fe	27.37	0.38	22.06				
			Ni	3.43	0.26	2.63				
			Cu	31.38	0.47	22.23				
23	1	Sperrylite	As	38.71	0.54	62.19				
			Pt	61.29	0.54	37.81				
23	2	Chalcopyrite	S	39.15	0.36	54.45				
			Fe	29.42	0.36	23.49				
			Cu	31.43	0.45	22.05				

PTS #26015-266										
Site #	Spectrum #	Mineral name	Element	Weight%	Weight% sigma	Atomic%	Compound%	Formula	# Ions	An#
1	1	Undetermined PGM	Cl	1.77	0.18	5.33				
			Pd	67.12	0.74	67.12				
			Sn	16.27	0.6	14.59				
			Sb	14.83	0.63	12.96				
1	2	Talnakhite	S	38.26	0.47	53.41				
			Fe	27.21	0.46	21.8				
			Ni	8.08	0.39	6.16				
			Cu	26.45	0.57	18.63				
2	1	Electrum	Ag	17.77	0.69	28.3				
			Au	82.23	0.69	71.7				
2	2	Pentlandite	S	28.6	0.36	41.53				
			Fe	45.61	0.45	38.02				
			Ni	25.79	0.47	20.45				
3	1	Gold	Ag	0.2	0.3	0.37				
			Au	99.8	0.3	99.63				
3	2	Pyrrhotite	S	37.95	0.35	52.65				
			Fe	40.45	0.39	32.22				
			Cu	21.6	0.43	15.12				
4	1	Electrum	Ag	10.7	0.75	17.95				
			Au	89.3	0.75	82.05				
4	2	Biotite	Mg	10.3	0.21	9.52	17.07	MgO	3.57	
			Al	7.75	0.19	6.46	14.65	Al2O3	2.42	
			Si	18.95	0.26	15.16	40.53	SiO2	5.69	
			K	8.79	0.19	5.05	10.59	K2O	1.9	
			Ti	2.83	0.15	1.33	4.72	TiO2	0.5	
			Fe	9.66	0.28	3.89	12.43	FeO	1.46	
			O	41.72	0.35	58.6				22
		Cation sum	15.55							
5	1	Gold	Ag	0.16	0.59	0.29				
			Au	99.84	0.59	99.71				
5	2	Olivine	Mg	17.01	0.24	16.49	28.2	MgO	1.15	
			Si	17.84	0.23	14.98	38.16	SiO2	1.04	
			Fe	26.15	0.33	11.04	33.64	FeO	0.77	
			O	39.01	0.32	57.49				4
		Cation sum	2.96							
6	1	Gold	Ag	-0.6	0.85	-1.1				
			Au	100.6	0.85	101.1				
6	2	Olivine	Mg	16.81	0.24	16.34	27.87	MgO	1.14	
			Si	17.78	0.23	14.97	38.05	SiO2	1.04	
			Fe	26.49	0.33	11.21	34.08	FeO	0.78	
			O	38.91	0.32	57.48				4
		Cation sum	2.96							
7	1	Undetermined PGM	Ni	26.15	0.52	34.11				
			As	42.08	0.62	43.01				
			Pd	31.77	0.64	22.87				
7	2	Chalcopyrite	S	38.46	0.37	53.74				
			Fe	29.46	0.37	23.64				
			Cu	32.08	0.46	22.62				
8	1	Electrum	Ag	9.03	0.63	15.34				
			Au	90.97	0.63	84.66				
8	2	Olivine	Mg	13.1	0.34	11.94	21.72	MgO	0.79	
			Si	26.42	0.4	20.85	56.52	SiO2	1.38	
			Ca	0.58	0.12	0.32	0.81	CaO	0.02	
			Fe	16.28	0.47	6.46	20.95	FeO	0.43	
			O	43.62	0.49	60.43				4
		Cation sum	2.62							
9	1	Undetermined PGM	As	4.18	0.49	6.41				
			Pd	42.14	0.96	45.58				
			Ag	28.48	0.88	30.39				
			Sn	7.27	0.7	7.05				
9	2	Chalcopyrite	Pt	17.93	0.92	10.58				
			S	40.58	0.37	55.96				
			Fe	28.05	0.36	22.21				
		Cu	31.36	0.45	21.82					

PTS #26015-266										
Site #	Spectrum #	Mineral name	Element	Weight%	Weight% sigma	Atomic%	Compound%	Formula	# Ions	An#
10	1	Sperrylite	As	43.46	0.53	66.69				
			Pt	56.54	0.53	33.31				
10	2	Pyrrhotite	S	40.29	0.35	55.12				
			Fe	38.56	0.37	30.28				
			Cu	21.15	0.41	14.6				
11	1	Paolovite	Pd	64.91	0.64	67.35				
			Sn	35.09	0.64	32.65				
11	2	Pyrrhotite	S	39.89	0.32	53.62				
			Fe	60.11	0.32	46.38				
12	1	Undetermined PGM	Pd	43.08	1.39	45.19				
			Ag	25.58	1.16	26.47				
			Sn	28.33	1.15	26.64				
			Au	3.01	2.08	1.71				
12	1	Chalcopyrite	S	38.14	0.64	53.39				
			Fe	29.88	0.64	24.02				
			Cu	31.98	0.79	22.59				
13	1	Paolovite	Pd	68.78	0.56	71.08				
			Sn	31.22	0.56	28.92				
13	2	Chalcopyrite	S	39.38	0.36	54.66				
			Fe	29.95	0.36	23.87				
			Cu	30.67	0.45	21.48				
14	1	Electrum	Ag	11.66	1.44	19.42				
			Au	88.34	1.44	80.58				
14	2	Biotite	Mg	11.75	0.22	10.63	19.48	MgO	3.97	
			Al	8.01	0.19	6.53	15.13	Al2O3	2.44	
			Si	19.78	0.26	15.5	42.31	SiO2	5.79	
			K	7.82	0.18	4.4	9.42	K2O	1.64	
			Ti	2.69	0.15	1.23	4.48	TiO2	0.46	
			Fe	7.13	0.25	2.81	9.18	FeO	1.05	
			O	42.83	0.35	58.9			22	
			Cation sum	15.35						
15	1	Paolovite	Pd	63.46	0.58	65.95				
			Sn	36.54	0.58	34.05				
15	2	Chalcopyrite	S	41.81	0.73	57.19				
			Fe	27.63	0.67	21.71				
			Cu	30.56	0.86	21.1				
16	1	Electrum	Ag	9.82	0.8	16.58				
			Au	90.18	0.8	83.42				
16	2	Plagioclase	Na	2.63	0.14	2.39	3.54	Na2O	0.31	An#
			Al	16.14	0.21	12.54	30.49	Al2O3	1.63	68
			Si	24.58	0.26	18.35	52.59	SiO2	2.38	
			Ca	9.56	0.18	5	13.38	CaO	0.65	
			O	47.09	0.3	61.71			8	
			Cation sum	4.96						
17	1	Electrum	Ag	20.67	0.74	32.24				
			Au	79.33	0.74	67.76				
17	2	Chalcopyrite	S	37.25	0.65	52.47				
			Fe	29.79	0.67	24.1				
			Cu	32.96	0.82	23.43				
19	1	Electrum	Ag	13.54	1.54	22.23				
			Au	86.46	1.54	77.77				
19	2	Ilmenite	Mg	1.72	0.29	2.09	2.85	MgO	0.1	
			Ti	32.65	0.6	20.2	54.46	TiO2	1.01	
			Fe	33.19	0.7	17.61	42.69	FeO	0.88	
			O	32.45	0.64	60.1			3	
			Cation sum	1.99						
21	1	Sobolevskite	Pd	32.51	1.29	48.62				
			Bi	67.49	1.29	51.38				
21	2	Pentlandite	S	38.28	0.41	53.38				
			Fe	28.25	0.4	22.62				
			Ni	7.64	0.33	5.82				
			Cu	25.84	0.49	18.18				

PTS #26015-266										
Site #	Spectrum #	Mineral name	Element	Weight%	Weight% sigma	Atomic%	Compound%	Formula	# Ions	An#
22	1	Electrum	Ag	13.44	1.14	22.09				
			Au	86.56	1.14	77.91				
22	2	Talnakhite	S	15.64	0.93	25.19				
			Fe	40.01	1.13	37				
			Ni	26.23	1.14	23.07				
			Cu	18.13	1.23	14.74				
23	1	Electrum	Ag	14.5	0.88	23.64				
			Au	85.5	0.88	76.36				
23	2	Biotite	Mg	11.28	0.4	10.27	18.7	MgO	3.85	
			Al	7.99	0.36	6.55	15.09	Al2O3	2.46	
			Si	19.69	0.48	15.52	42.13	SiO2	5.82	
			K	8.56	0.34	4.85	10.32	K2O	1.82	
			Ti	2.2	0.26	1.02	3.67	TiO2	0.38	
			Fe	7.84	0.48	3.11	10.09	FeO	1.17	
			O	42.43	0.65	58.69			22	
			Cation sum	15.48						
24	1	Electrum	Ag	9.83	0.56	16.6				
			Au	90.17	0.56	83.4				
24	2	Olivine	Mg	16.46	0.26	16.08	27.3	MgO	1.12	
			Si	17.62	0.24	14.9	37.7	SiO2	1.04	
			Fe	27.2	0.35	11.57	35	FeO	0.81	
			O	38.71	0.34	57.45			4	
			Cation sum	2.96						
25	1	Paolovite	Pd	62.95	0.56	65.46				
			Sn	37.05	0.56	34.54				
25	2	Orthopyroxene	Mg	13.95	0.23	12.65	23.13	MgO	0.63	
			Si	26.44	0.27	20.75	56.56	SiO2	1.03	
			Fe	15.79	0.31	6.23	20.31	FeO	0.31	
			O	43.82	0.33	60.37			3	
			Cation sum	1.97						
26	1	Stibiopalladinite	Pd	74.21	1.79	76.71				
			Sb	25.79	1.79	23.29				
26	3	Pentlandite	S	37.96	0.4	52.4				
			Fe	27.52	0.39	21.81				
			Ni	30.42	0.46	22.93				
			Cu	4.11	0.35	2.86				
27	1	Sperrylite	As	41.71	0.55	65.07				
			Pt	58.29	0.55	34.93				
27	4	Cubanite	S	38.33	0.37	53.06				
			Fe	40.14	0.41	31.9				
			Cu	21.53	0.45	15.04				
27	2		As	43.06	0.59	53.01				
			Rh	47.39	0.64	42.47				
			Pt	9.56	0.61	4.52				
27	4	Cubanite	S	38.33	0.37	53.06				
			Fe	40.14	0.41	31.9				
			Cu	21.53	0.45	15.04				
28	1	Electrum	Ag	10.6	0.54	17.79				
			Au	89.4	0.54	82.21				
28	2	Clinopyroxene	Mg	14	0.22	12.71	23.21	MgO	1.27	
			Si	26.08	0.27	20.5	55.8	SiO2	2.04	
			Ca	0.72	0.09	0.4	1.01	CaO	0.04	
			Fe	15.53	0.3	6.14	19.98	FeO	0.61	
			O	43.67	0.32	60.25			6	
			Cation sum	3.96						

PTS #26015-266										
Site #	Spectrum #	Mineral name	Element	Weight%	Weight% sigma	Atomic%	Compound%	Formula	# Ions	An#
29	1	Stibiopalladinite	Pd	68.08	0.58	70.94				
			Sb	31.92	0.58	29.06				
29	2	Clinopyroxene	Mg	0.22	11.88	21.58	MgO	1.18		
			Al	0.09	0.36	0.84	Al2O3	0.04		
			Si	0.27	20.45	55.35	SiO2	2.03		
			Ca	0.09	0.55	1.4	CaO	0.05		
			Mn	0.11	0.18	0.57	MnO	0.02		
			Fe	0.3	6.26	20.27	FeO	0.62		
			O	0.33	60.31			6		
			Cation sum	3.95						
30	1	Stibiopalladinite	As	1.26	0.26	1.85				
			Pd	69.07	0.51	71.36				
			Sb	29.67	0.48	26.79				
30	2	Clinopyroxene	Mg	13.65	0.22	12.4	22.63	MgO	1.23	
			Si	26.28	0.27	20.66	56.22	SiO2	2.06	
			Ca	0.86	0.09	0.47	1.2	CaO	0.05	
			Fe	15.51	0.31	6.13	19.96	FeO	0.61	
			O	43.71	0.33	60.33			6	
			Cation sum	3.94						
31	1	Stibiopalladinite	Pd	66.48	0.59	69.42				
			Sb	33.52	0.59	30.58				
31	2	Clinopyroxene	Mg	13.25	0.22	12.07	21.97	MgO	1.2	
			Al	0.43	0.09	0.36	0.82	Al2O3	0.04	
			Si	25.96	0.27	20.48	55.54	SiO2	2.04	
			Ca	0.65	0.08	0.36	0.91	CaO	0.04	
			Mn	0.37	0.11	0.15	0.48	MnO	0.01	
			Fe	15.76	0.3	6.25	20.28	FeO	0.62	
			O	43.57	0.33	60.33			6	
			Cation sum	3.95						
32	1	Electrum	Ag	12.74	0.72	21.04				
			Au	87.26	0.72	78.96				
32	2	Olivine	Mg	16.2	0.25	15.81	26.86	MgO	1.1	
			Si	17.88	0.25	15.11	38.25	SiO2	1.05	
			Fe	27.12	0.35	11.52	34.89	FeO	0.8	
			O	38.8	0.34	57.55			4	
			Cation sum	2.95						
33	1	Electrum	Ag	11.03	0.74	18.46				
			Au	88.97	0.74	81.54				
33	2	Olivine	Mg	16.61	0.26	16.13	27.54	MgO	1.12	
			Si	18.06	0.25	15.18	38.65	SiO2	1.05	
			Fe	26.28	0.35	11.11	33.81	FeO	0.77	
			O	39.04	0.34	57.59			4	
			Cation sum	2.95						
34	1	Electrum	Ag	9.81	0.71	16.57				
			Au	90.19	0.71	83.43				
34	2	Biotite	Mg	12.04	0.47	10.9	19.96	MgO	4.09	
			Al	8.21	0.41	6.69	15.51	Al2O3	2.51	
			Si	19.67	0.54	15.42	42.09	SiO2	5.78	
			K	8.14	0.37	4.58	9.8	K2O	1.72	
			Ti	1.72	0.27	0.79	2.87	TiO2	0.3	
			Fe	7.6	0.53	2.99	9.78	FeO	1.12	
			O	42.63	0.73	58.63			22	
			Cation sum	15.52						
35	1	Gold	Ag	0.12	0.61	0.21				
			Au	99.88	0.61	99.79				
35	2	Clinopyroxene	Mg	13.73	0.22	12.43	22.77	MgO	1.24	
			Al	0.4	0.1	0.33	0.76	Al2O3	0.03	
			Si	26.27	0.27	20.59	56.21	SiO2	2.05	
			Ca	0.54	0.08	0.29	0.75	CaO	0.03	
			Fe	15.17	0.3	5.98	19.51	FeO	0.59	
			O	43.89	0.33	60.38			6	
			Cation sum	3.94						

PTS #26057-96										
Site #	Spectrum #	Mineral name	Element	Weight%	Weight% sigma	Atomic%	Compound%	Formula	# Ions	An#
1	1	Paolovite	Pd	25.22		1.08	27.34			
			Sn	74.78		1.08	72.66			
1	3	Chalcopyrite	S	38.09		1.02	53.4			
			Fe	28.62		1.02	23.04			
			Cu	33.3		1.27	23.56			
2	1	Undetermined PGM	Pd	13.53		0.59	14.86			
			Sn	86.47		0.59	85.14			
2	3	Bornite	S	29.43		0.38	44.68			
			Fe	11.99		0.3	10.45			
			Cu	58.58		0.46	44.88			
2	4	Chalcopyrite	S	38.4		0.61	53.75			
			Fe	28.02		0.61	22.53			
			Cu	33.58		0.76	23.72			
3	1	Paolovite	Pd	65.27		0.45	67.71			
			Sn	34.73		0.45	32.29			
3	2	Chalcopyrite	S	36.99		0.62	52.19			
			Fe	30.11		0.64	24.39			
			Cu	32.9		0.78	23.42			
4	1	Paolovite	Pd	65.49		0.46	67.92			
			Sn	34.51		0.46	32.08			
4	2	Plagioclase	Na	3.75		0.26	3.39	5.05	Na2O	0.44
			Al	14.66		0.33	11.29	27.69	Al2O3	1.46
			Si	26.55		0.43	19.65	56.79	SiO2	2.54
			Ca	7.48		0.27	3.88	10.47	CaO	0.5
			O	47.57		0.49	61.8			8
			Cation sum	4.95						
4	3	Pentlandite	S	38.12		1.21	52.54			
			Fe	22.82		1.16	18.06			
			Ni	39.06		1.45	29.4			
5	1	Paolovite	Pd	63.02		0.49	65.53			
			Sn	36.98		0.49	34.47			
5	2	Chalcopyrite	S	37.82		0.81	53.12			
			Fe	28.67		0.82	23.12			
			Cu	33.51		1.01	23.75			
5	3	Chlorite	Al	10.08		0.24	9.51	19.05	Al2O3	4.48
			Si	15.64		0.27	14.17	33.46	SiO2	6.67
			Ca	0.35		0.1	0.22	0.49	CaO	0.1
			Fe	36.53		0.43	16.64	46.99	FeO	7.84
			O	37.39		0.4	59.46			28
			Cation sum	19.09						
6	1	Paolovite	Pd	60.92		0.51	63.49			
			Sn	39.08		0.51	36.51			
6	2	Chalcopyrite	S	37.26		0.85	52.5			
			Fe	29.62		0.87	23.96			
			Cu	33.12		1.07	23.54			
7	1	Paolovite	Pd	61.88		0.5	64.42			
			Sn	38.12		0.5	35.58			
7	1	Chalcopyrite	S	37.04		1.49	52.34			
			Fe	28.07		1.54	22.77			
			Cu	34.9		1.99	24.89			
8	1	Paolovite	Pd	63.27		0.53	65.77			
			Sn	36.73		0.53	34.23			
8	1	Chalcopyrite	S	38.55		1.01	54.03			
			Fe	25.78		1.01	20.74			
			Cu	35.67		1.29	25.22			
9	1	Paolovite	Pd	64.53		0.46	66.99			
			Sn	35.47		0.46	33.01			
9	6	Biotite	Mg	2.02		0.29	2.51	3.35	MgO	1
			Al	3.2		0.27	3.58	6.04	Al2O3	1.42
			Si	4.06		0.27	4.37	8.69	SiO2	1.73
			S	1.75		0.22	1.65	4.37	SO3	0.65
			Ti	1.18		0.19	0.75	1.97	TiO2	0.3
			V	0.84		0.19	0.5	1.5	V2O5	0.2
			Fe	57.58		0.73	31.16	74.08	FeO	12.36
			O	29.37		0.67	55.48			22
			Cation sum	17.66						

PTS #26057-96										
Site #	Spectrum #	Mineral name	Element	Weight%	Weight% sigma	Atomic%	Compound%	Formula	# Ions	An#
10	1	Electrum	Cu	12.53	0.48	27.87				
			Zn	1.88	0.41	4.06				
			Ag	11.25	0.56	14.74				
			Au	74.34	0.75	53.33				
10	2	Clinopyroxene	Mg	8.19	0.17	7.52	13.57	MgO	0.75	
			Al	1.05	0.1	0.87	1.99	Al2O3	0.09	
			Si	25.06	0.24	19.93	53.62	SiO2	1.98	
			Ca	14.94	0.2	8.33	20.9	CaO	0.83	
			Ti	0.42	0.09	0.2	0.71	TiO2	0.02	
			Fe	7.16	0.22	2.87	9.22	FeO	0.29	
			O	43.17	0.29	60.28			6	
			Cation sum	3.95						
10	3	Plagioclase	Na	3.74	0.14	3.39	5.04	Na2O	0.44	An#
			Al	14.67	0.18	11.33	27.72	Al2O3	1.47	55
			Si	26.16	0.24	19.41	55.96	SiO2	2.52	
			K	0.24	0.07	0.13	0.29	K2O	0.02	
			Ca	7.85	0.15	4.08	10.98	CaO	0.53	
			O	47.34	0.28	61.66			8	
			Cation sum	4.97						
11	1	Paolovite	Pd	60.7	0.54	63.28				
			Sn	39.3	0.54	36.72				
11	2	Pyrrhotite	S	47.96	0.34	61.61				
			Fe	52.04	0.34	38.39				
12	1	Undetermined PGM	Pd	57.17	1.36	59.83				
			Sn	42.83	1.36	40.17				
12	2	Chalcopyrite	S	37.62	0.44	52.84				
			Fe	31.62	0.44	25.5				
			Cu	30.46	0.54	21.59				
13	1	Paolovite	Pd	62.62	0.89	65.14				
			Sn	37.38	0.89	34.86				
13	2	Chalcopyrite	S	36.67	0.35	51.8				
			Fe	31.14	0.37	25.25				
			Cu	32.2	0.45	22.95				
14	1	Paolovite	Pd	59.81	0.8	62.41				
			Sn	40.19	0.8	37.59				
14	1	Chalcopyrite	S	37.34	1.11	52.46				
			Fe	31.97	1.18	25.79				
			Cu	30.69	1.45	21.76				
15	1	Paolovite	Pd	59.93	0.62	62.53				
			Sn	40.07	0.62	37.47				
15	1	Chalcopyrite	S	42.08	0.69	57.4				
			Fe	28.83	0.67	22.58				
			Cu	29.09	0.85	20.03				
17	1	Sperrylite	As	44.18	0.49	67.33				
			Pt	55.82	0.49	32.67				
17	3	Plagioclase	Na	3.49	0.14	3.17	4.7	Na2O	0.41	An#
			Al	15.02	0.19	11.62	28.38	Al2O3	1.51	57
			Si	25.82	0.24	19.18	55.24	SiO2	2.49	
			K	0.22	0.07	0.12	0.26	K2O	0.02	
			Ca	8.16	0.16	4.25	11.42	CaO	0.55	
			O	47.29	0.28	61.67			8	
			Cation sum	4.97						
17	4	Apatite	F	5.22	0.91	6.53	0		1.21	
			P	18.73	0.28	14.36	42.91	P2O5	2.67	
			Cl	1.23	0.09	0.83	0		0.15	
			Ca	35.46	0.43	21.01	49.61	CaO	3.91	
			Ce	0.88	0.21	0.15	1.03	Ce2O3	0.03	
			O	38.49	0.46	57.13			10.63	
			Cation sum	6.61						
18	1	Paolovite	Pd	65.45	0.46	67.88				
			Sn	34.55	0.46	32.12				
18	2	Chalcopyrite	S	36.83	0.87	52.06				
			Fe	29.2	0.9	23.7				
			Cu	33.97	1.1	24.24				

PTS #26057-96										
Site #	Spectrum #	Mineral name	Element	Weight%	Weight% sigma	Atomic%	Compound%	Formula	# Ions	An#
19	1	Paolovite	Pd	64.77	0.45	67.22				
			Sn	35.23	0.45	32.78				
19	2	Chalcopyrite	S	36.9	0.97	52.11				
			Fe	29.72	1	24.1				
			Cu	33.38	1.22	23.79				
20	1	Paolovite	Pd	59.52	0.57	62.12				
			Sn	40.48	0.57	37.88				
20	2	Chalcopyrite	S	38.5	0.36	53.8				
			Fe	29.15	0.36	23.39				
			Cu	32.36	0.44	22.82				
21	1	Paolovite	Pd	61.85	0.48	64.4				
			Sn	38.15	0.48	35.6				
21	2	Chalcopyrite	S	38.04	1.39	53.27				
			Fe	30.35	1.4	24.4				
			Cu	31.6	1.76	22.33				
26	1	Acanthite	S	12.02	0.21	31.49				
			Ag	87.98	0.21	68.51				
26	2	Olivine	Mg	17.65	0.31	17.09	29.27	MgO	1.19	
			Si	17.52	0.29	14.68	37.48	SiO2	1.02	
			Fe	25.85	0.42	10.89	33.25	FeO	0.76	
			O	38.98	0.41	57.34			4	
			Cation sum	2.98						
27	1	Electrum	Ag	11.92	0.55	19.81				
			Au	88.08	0.55	80.19				
27	2	Plagioclase	Na	2.16	0.13	1.97	2.91	Na2O	0.26	An#
			Mg	0.48	0.09	0.42	0.8	MgO	0.05	71
			Al	16.37	0.21	12.76	30.94	Al2O3	1.66	
			Si	23.98	0.25	17.96	51.3	SiO2	2.33	
			Ca	9.58	0.17	5.03	13.4	CaO	0.65	
			Fe	0.5	0.12	0.19	0.65	FeO	0.02	
			O	46.92	0.3	61.67			8	
			Cation sum	4.97						
27	3	Apatite	F	3.97	0.91	4.94	0		0.93	
			P	19.18	0.34	14.65	43.95	P2O5	2.76	
			Cl	0.93	0.11	0.62	0		0.12	
			Ca	36.56	0.48	21.58	51.15	CaO	4.06	
			O	39.36	0.51	58.2			10.95	
			Cation sum	6.82						
28	1	Paolovite	Pd	61.42	0.5	63.97				
			Sn	38.58	0.5	36.03				
28	2	Chalcopyrite	S	38.11	0.9	53.4				
			Fe	29.27	0.9	23.54				
			Cu	32.62	1.12	23.06				
29	1	Undetermined PGM	Pd	53.51	0.61	56.22				
			Sn	46.49	0.61	43.78				
29	2	Apatite	P	18.75	0.62	14.65	42.95	P2O5	2.84	
			Cl	2.89	0.33	1.98	0		0.38	
			Ca	38.7	0.73	23.38	54.16	CaO	4.53	
			O	39.66	0.75	60			11.62	
			Cation sum	7.36						
30	1	Undetermined PGM	Pd	51.75	0.46	27.35	59.53	PdO	5.7	
			Sn	31.88	0.44	15.1	40.47	SnO2	3.15	
			O	16.38	0.34	57.55			12	
			Cation sum	8.85						
30	2	Apatite	P	18.94	0.61	14.82	43.4	P2O5	2.84	
			Cl	4.41	0.45	3.01	0		0.58	
			Ca	37.3	0.74	22.56	52.19	CaO	4.32	
			O	39.35	0.76	59.61			11.42	
			Cation sum	7.16						

PTS #26057-96										
Site #	Spectrum #	Mineral name	Element	Weight%	Weight% sigma	Atomic%	Compound%	Formula	# Ions	An#
31	1	Undetermined PGM	Pd	65.28	0.71	67.83				
			Sn	27.64	0.6	25.74				
			Sb	7.08	0.64	6.43				
31	2	Chalcopyrite	S	38.77	0.91	54.04				
			Fe	29.84	0.91	23.88				
			Cu	31.39	1.13	22.08				
32	1	Undetermined PGM	As	7.97	0.76	12.85				
			Pd	60.99	1.96	69.21				
			Bi	31.04	2.11	17.94				
32	2	Pentlandite	S	40.06	0.96	54.9				
			Fe	26.85	0.92	21.12				
			Ni	19.21	0.96	14.38				
			Cu	13.89	1.04	9.6				
33	1	Sperrylite	As	37.78	0.62	61.26				
			Pt	62.22	0.62	38.74				
33	2	Pentlandite	S	41.99	0.81	56.92				
			Fe	24.71	0.73	19.23				
			Ni	18.99	0.82	14.06				
			Cu	14.31	0.93	9.79				
34	1	Sperrylite	As	36.85	0.71	60.31				
			Pt	63.15	0.71	39.69				
34	1	Pentlandite	S	45.41	0.63	60.01				
			Fe	23.44	0.55	17.79				
			Ni	25.92	0.66	18.71				
			Cu	5.23	0.6	3.49				

PTS #26057-101										
Site #	Spectrum #	Mineral name	Element	Weight%	Weight% sigma	Atomic%	Compound%	Formula	# Ions	An#
1	1	Electrum	Zn	1.38	0.81	3.54				
			Ag	18.16	1.19	28.15				
			Au	80.46	1.35	68.31				
1	2	Plagioclase	Na	2.25	0.21	2.06	3.04	Na2O	0.27	
			Al	16.5	0.32	12.84	31.17	Al2O3	1.66	
			Si	24.28	0.39	18.15	51.93	SiO2	2.35	
			Ca	9.91	0.28	5.19	13.86	CaO	0.67	
			O	47.07	0.46	61.77			8	
			Cation sum	4.95						
2	1	Undetermined PGM	Pd	56.48	0.99	61.36				
			Sn	33.73	0.89	32.84				
			Pt	9.79	0.86	5.8				
2	2	Pentlandite	S	39.59	0.99	54.57				
			Fe	21.8	0.89	17.26				
			Ni	23.12	1.06	17.41				
			Cu	15.48	1.11	10.77				
3	1	Undetermined PGM	As	3.71	0.62	6.33				
			Pd	28.77	1.1	34.52				
			Sn	26.49	1.05	28.5				
			Sb	9.62	1.05	10.09				
			Pt	31.41	1.22	20.56				
3	2	Pentlandite	S	40.87	1.22	55.89				
			Fe	20.43	1.05	16.04				
			Ni	24.18	1.28	18.05				
			Cu	14.52	1.35	10.02				
4	1	Paolovite	Pd	64.35	0.72	66.82				
			Sn	35.65	0.72	33.18				
4	2	Chalcopyrite	S	38.31	1.17	53.64				
			Fe	28.44	1.18	22.87				
			Cu	33.25	1.45	23.5				
5	1	Paolovite	Pd	64.08	0.94	66.56				
			Sn	35.92	0.94	33.44				
5	2	Chalcopyrite	S	38.9	1.31	54.19				
			Fe	29.41	1.32	23.52				
			Cu	31.69	1.64	22.28				
6	1	Undetermined PGM	Pd	62.53	0.82	66.51				
			Sn	31.47	0.75	30.01				
			Pt	6	0.63	3.48				
6	4	Chalcopyrite	S	38.39	1.07	53.76				
			Fe	27.72	1.08	22.29				
			Cu	33.89	1.34	23.95				
6	5	Bornite	S	29.09	0.49	44.33				
			Fe	10.87	0.38	9.51				
			Cu	60.04	0.59	46.16				
7	1	Paolovite	Pd	65.78	0.74	68.19				
			Sn	34.22	0.74	31.81				
7	5	Pentlandite	S	37.23	0.55	51.93				
			Fe	26.16	0.54	20.95				
			Ni	23.34	0.62	17.78				
			Cu	13.28	0.61	9.34				
8	1	Paolovite	Pd	65	0.66	67.45				
			Sn	35	0.66	32.55				
8	2	Pentlandite	S	37.23	0.55	51.93				
			Fe	26.16	0.54	20.95				
			Ni	23.34	0.62	17.78				
			Cu	13.28	0.61	9.34				
9	1	Undetermined PGM	Pd	59.03	1.1	64.1				
			Sn	30.51	0.97	29.7				
			Pt	10.46	0.98	6.2				
9	2	Pentlandite	S	38.35	1.31	53.43				
			Fe	11.89	0.96	9.51				
			Ni	35.8	1.51	27.25				
			Cu	13.96	1.43	9.82				
10	1	Paolovite	Pd	48.21	0.85	50.94				
			Sn	51.79	0.85	49.06				
10	2	Talnakhite	S	20.87	1.07	32.76				
			Fe	12.37	1.05	11.15				
			Ni	49.39	1.66	42.34				
			Cu	17.36	1.68	13.75				

PTS #26057-101										
Site #	Spectrum #	Mineral name	Element	Weight%	Weight% sigma	Atomic%	Compound%	Formula	# Ions	An#
11	1	Undetermined	As	37.27	0.78	55.18				
		PGM	Pd	8.69	0.69	9.06				
			Sn	13.74	0.62	12.84				
			Pt	40.3	0.94	22.92				
11	2	Chalcopyrite	S	37.96	0.52	53.17				
			Fe	30.55	0.53	24.57				
			Cu	31.5	0.65	22.26				
12	1	Sobolevskite	Pd	36.44	1.11	52.96				
			Bi	63.56	1.11	47.04				
12	2	Chalcopyrite	S	38.15	0.53	53.45				
			Fe	28.94	0.54	23.28				
			Cu	32.92	0.65	23.27				
13	1	Paolovite	Pd	60.73	1.16	65.39				
			Sn	31.35	0.92	30.27				
			Bi	7.92	1.28	4.34				
13	2	Chalcopyrite	S	38.78	0.52	54.04				
			Fe	30.05	0.53	24.04				
			Cu	31.17	0.65	21.92				
14	1	Undetermined	Pd	31.19	1.05	33.59				
		PGM	Sn	68.81	1.05	66.41				
14	2	Chalcopyrite	S	38.49	0.52	53.77				
			Fe	29.41	0.52	23.59				
			Cu	32.1	0.64	22.63				
15	1	Froodite	Pd	44.85	2.87	61.5				
			Bi	55.15	2.87	38.5				
15	2	Chalcopyrite	S	38.94	0.99	54.26				
			Fe	29.01	0.98	23.2				
			Cu	32.06	1.22	22.54				
16	1	Undetermined	Pd	61.98	1.16	64.79				
		PGM	Sn	19.64	0.95	18.4				
			Sb	18.39	1.08	16.8				
16	2	Clinopyroxene	Mg	8.69	0.26	7.93	14.41	MgO	0.79	
			Al	0.43	0.12	0.36	0.82	Al2O3	0.04	
			Si	25.65	0.35	20.26	54.87	SiO2	2.02	
			Ca	16.52	0.3	9.14	23.12	CaO	0.91	
			Fe	5.27	0.3	2.1	6.79	FeO	0.21	
			O	43.43	0.42	60.22				6
			Cation sum	3.96						
17	1	Paolovite	Pd	60.43	1.51	63.01				
			Sn	39.57	1.51	36.99				
17	2	Chalcopyrite	S	38.86	0.53	54.21				
			Fe	28.3	0.53	22.67				
			Cu	32.84	0.65	23.12				
18	1	Paolovite	Pd	65.37	0.78	67.8				
			Sn	34.63	0.78	32.2				
18	2	Plagioclase	Na	2.85	0.44	2.58	3.84	Na2O	0.33	An#
			Al	15.45	0.56	11.94	29.19	Al2O3	1.54	63
			Si	25.88	0.72	19.21	55.36	SiO2	2.48	
			Ca	8.3	0.46	4.32	11.61	CaO	0.56	
			O	47.53	0.83	61.95				8
			Cation sum	4.91						
19	1	Undetermined	As	17.65	0.77	27.35				
		PGM	Pd	34.68	1.11	37.84				
			Sn	16.78	0.86	16.42				
			Pt	30.9	1.17	18.39				
19	2	Pentlandite	S	38.47	0.52	53.29				
			Fe	4.12	0.29	3.27				
			Ni	57.41	0.55	43.44				
20	1	Paolovite	Pd	60.71	0.98	64.72				
			Sn	33.24	0.9	31.77				
			Pt	6.05	0.76	3.52				
20	2	Pentlandite	S	36.74	0.54	51.65				
			Fe	16.14	0.44	13.03				
			Ni	32.55	0.63	24.99				
			Cu	14.58	0.62	10.34				

PTS #26057-101										
Site #	Spectrum #	Mineral name	Element	Weight%	Weight% sigma	Atomic%	Compound%	Formula	# Ions	An#
21	1	Paolovite	Pd	51.77	1.11	57.23				
			Sn	35.31	1.03	34.98				
			Pt	12.92	1	7.79				
21	2	Pentlandite	S	39.47	0.52	54.31				
			Fe	4.93	0.29	3.89				
			Ni	55.61	0.55	41.79				
22	2	Paolovite	Pd	70.18	0.65	72.41				
			Sn	29.82	0.65	27.59				
			S	34.75	0.47	49.74				
22	2	Chalcopyrite	Fe	31.48	0.51	25.87				
			Cu	33.77	0.61	24.39				
			Pd	50.36	0.83	53.09				
24	1	Undetermined PGM	Sn	49.64	0.83	46.91				
			S	38.78	1.07	54.07				
24	2	Chalcopyrite	Fe	29.38	1.07	23.52				
			Cu	31.85	1.34	22.41				
			Pd	41.2	0.93	43.87				
25	1	Undetermined PGM	Sn	58.8	0.93	56.13				
			S	34.74	0.44	48.77				
25	2	Pentlandite	Fe	30.65	0.48	24.7				
			Ni	34.61	0.55	26.53				

PTS #26096-717										
Site #	Spectrum #	Mineral name	Element	Weight%	Weight% sigma	Atomic%	Compound%	Formula	# Ions	An#
2	1	Gold	Ag	-0.23	0.41	-0.43				
			Au	100.23	0.41	100.43				
2	2	Clinopyroxene	Mg	10.19	0.21	9.59	16.9	MgO	0.95	
			Al	0.6	0.11	0.51	1.13	Al2O3	0.05	
			Si	25.17	0.28	20.49	53.84	SiO2	2.04	
			Ca	0.76	0.09	0.43	1.06	CaO	0.04	
			Mn	0.56	0.12	0.23	0.73	MnO	0.02	
			Fe	20.48	0.33	8.38	26.34	FeO	0.83	
			O	42.24	0.35	60.37			6	
		Cation sum	3.94							
3	1	Electrum	Zn	0.95	0.42	2.64				
			Ag	7.81	0.6	13.16				
			Au	91.24	0.71	84.2				
3	2	Clinopyroxene	Mg	10.42	0.21	9.8	17.28	MgO	0.97	
			Si	25.39	0.27	20.68	54.32	SiO2	2.06	
			Ca	1.15	0.1	0.66	1.61	CaO	0.07	
			Fe	20.83	0.33	8.53	26.79	FeO	0.85	
			O	42.21	0.34	60.34			6	
		Cation sum	3.94							
4	1	Electrum	Ag	12.45	0.87	20.61				
			Au	87.55	0.87	79.39				
4	2	Clinopyroxene	Mg	10.87	0.21	10.15	18.03	MgO	1.01	
			Si	25.84	0.26	20.88	55.27	SiO2	2.07	
			Ca	0.84	0.08	0.47	1.17	CaO	0.05	
			Mn	0.38	0.11	0.16	0.49	MnO	0.02	
			Fe	19.46	0.31	7.91	25.04	FeO	0.79	
			O	42.61	0.33	60.44			6	
		Cation sum	3.93							
5	1	Undetermined PGM	Pd	51.75	0.71	54.47				
			Sn	48.25	0.71	45.53				
5	2	Apatite	F	4.39	0.79	5.49	0		1.04	
			P	18.31	0.29	14.05	41.95	P2O5	2.65	
			Cl	0.97	0.1	0.65	0		0.12	
			Ca	37.66	0.42	22.34	52.69	CaO	4.21	
			O	38.67	0.43	57.47			10.84	
		Cation sum	6.86							
6	1	Undetermined PGM	Pd	58.01	0.6	60.65				
			Sn	41.99	0.6	39.35				
5	2	Apatite	F	4.39	0.79	5.49	0		1.04	
			P	18.31	0.29	14.05	41.95	P2O5	2.65	
			Cl	0.97	0.1	0.65	0		0.12	
			Ca	37.66	0.42	22.34	52.69	CaO	4.21	
			O	38.67	0.43	57.47			10.84	
		Cation sum	6.86							
7	1	Undetermined PGM	Pd	54.28	0.61	56.98				
			Sn	45.72	0.61	43.02				
5	2	Apatite	F	4.39	0.79	5.49	0		1.04	
			P	18.31	0.29	14.05	41.95	P2O5	2.65	
			Cl	0.97	0.1	0.65	0		0.12	
			Ca	37.66	0.42	22.34	52.69	CaO	4.21	
			O	38.67	0.43	57.47			10.84	
		Cation sum	6.86							
8	1	Paolovite	Pd	61.23	0.58	63.79				
			Sn	38.77	0.58	36.21				
5	2	Apatite	F	4.39	0.79	5.49	0		1.04	
			P	18.31	0.29	14.05	41.95	P2O5	2.65	
			Cl	0.97	0.1	0.65	0		0.12	
			Ca	37.66	0.42	22.34	52.69	CaO	4.21	
			O	38.67	0.43	57.47			10.84	
		Cation sum	6.86							
9	1	Electrum	Ag	19.24	1.15	30.31				
			Au	80.76	1.15	69.69				
9	2	Chalcopyrite	S	38.17	0.38	53.41				
			Fe	30.17	0.39	24.24				
			Cu	31.66	0.47	22.36				

PTS #26096-717										
Site #	Spectrum #	Mineral name	Element	Weight%	Weight% sigma	Atomic%	Compound%	Formula	# Ions	An#
10	1	Gold	Ag	-0.71	1.02	-1.3				
			Au	100.71	1.02	101.3				
10	2	Chalcopyrite	S	37.22	0.38	52.41				
			Fe	30.56	0.39	24.7				
			Cu	32.22	0.48	22.89				
11	1	Electrum	Ag	8.44	0.56	14.41				
			Au	91.56	0.56	85.59				
11	2	Biotite	Mg	5.47	0.18	5.33	9.07	MgO	1.99	
			Al	7.33	0.19	6.43	13.85	Al2O3	2.4	
			Si	18.27	0.25	15.41	39.09	SiO2	5.75	
			Cl	0.64	0.09	0.43	0		0.16	
			K	7.84	0.18	4.75	9.44	K2O	1.77	
			Ti	2.76	0.14	1.37	4.61	TiO2	0.51	
			Fe	18.12	0.33	7.69	23.31	FeO	2.86	
			O	39.57	0.36	58.6			21.84	
			Cation sum	15.27						
12	1	Electrum	Ag	8.29	0.82	14.16				
			Au	91.71	0.82	85.84				
11	2	Biotite	Mg	5.47	0.18	5.33	9.07	MgO	1.99	
			Al	7.33	0.19	6.43	13.85	Al2O3	2.4	
			Si	18.27	0.25	15.41	39.09	SiO2	5.75	
			Cl	0.64	0.09	0.43	0		0.16	
			K	7.84	0.18	4.75	9.44	K2O	1.77	
			Ti	2.76	0.14	1.37	4.61	TiO2	0.51	
			Fe	18.12	0.33	7.69	23.31	FeO	2.86	
			O	39.57	0.36	58.6			21.84	
			Cation sum	15.27						
13	1	Electrum	Ag	9.87	0.61	16.66				
			Au	90.13	0.61	83.34				
13	2	Biotite	Mg	5.08	0.18	5.01	8.43	MgO	1.87	
			Al	7.11	0.19	6.31	13.44	Al2O3	2.36	
			Si	17.74	0.25	15.12	37.94	SiO2	5.64	
			Cl	0.75	0.09	0.51	0		0.19	
			K	7.86	0.17	4.82	9.47	K2O	1.8	
			Ti	2.96	0.15	1.48	4.93	TiO2	0.55	
			Fe	19.46	0.34	8.34	25.04	FeO	3.12	
			O	39.04	0.36	58.42			21.81	
			Cation sum	15.34						
14	1	Gold	Ag	-0.54	0.66	-1				
			Au	100.54	0.66	101				
14	2	Pyrrhotite	S	56.52	0.36	69.36				
			Fe	43.48	0.36	30.64				
15	1	Paolovite	Pd	64.74	0.5	67.19				
			Sn	35.26	0.5	32.81				
15	2	Pyrrhotite	S	55.15	0.38	68.23				
			Fe	43.78	0.37	31.1				
			Cu	1.07	0.22	0.67				
16	1	Paolovite	Pd	61.83	0.54	64.37				
			Sn	38.17	0.54	35.63				
16	2	Chalcopyrite	S	37.3	0.39	52.53				
			Fe	29.9	0.4	24.17				
			Cu	31.68	0.49	22.51				
			Zn	1.13	0.31	0.78				
22	1	Electrum	Ag	16.69	0.84	26.78				
			Au	83.31	0.84	73.22				
22	2	Plagioclase	Na	4.47	0.16	4.02	6.02	Na2O	0.52	An#
			Al	13.97	0.19	10.72	26.39	Al2O3	1.39	46
			Si	27.26	0.25	20.1	58.31	SiO2	2.61	
			Ca	6.63	0.15	3.43	9.28	CaO	0.44	
			O	47.68	0.29	61.73			8	
			Cation sum	4.96						

PTS #26096-717										
Site #	Spectrum #	Mineral name	Element	Weight%	Weight% sigma	Atomic%	Compound%	Formula	# Ions	An#
23	1	Gold	Ag	-0.01	0.55	-0.01				
			Au	100.01	0.55	100.01				
23	2	Clinopyroxene	Mg	9.93	0.21	9.43	16.46	MgO	0.94	
			Si	24.96	0.27	20.52	53.4	SiO2	2.04	
			Ca	0.9	0.09	0.52	1.25	CaO	0.05	
			Mn	0.4	0.12	0.17	0.52	MnO	0.02	
			Fe	22.04	0.33	9.11	28.36	FeO	0.91	
			O	41.76	0.34	60.26			6	
			Cation sum	3.96						
24	1	Paolovite	Pd	50.35	1.85	55.96				
			Sn	23.81	1.56	23.72				
			Sb	12.75	1.62	12.39				
			Pt	13.09	1.55	7.93				
24	2	Chalcopyrite	S	38.53	0.38	53.9				
			Fe	27.9	0.38	22.41				
			Cu	33.57	0.48	23.69				
26	1	Gold	Ag	-1.09	0.68	-2.01				
			Au	101.09	0.68	102.01				
26	2	Biotite	Mg	3.5	0.15	3.48	5.8	MgO	1.29	
			Al	7.18	0.18	6.43	13.57	Al2O3	2.39	
			Si	17.96	0.24	15.45	38.43	SiO2	5.75	
			Cl	0.34	0.09	0.23	0		0.09	
			K	7.73	0.17	4.77	9.31	K2O	1.78	
			Ti	3.36	0.15	1.69	5.6	TiO2	0.63	
			Fe	20.96	0.33	9.07	26.96	FeO	3.38	
			O	38.98	0.35	58.87			21.91	
Cation sum	15.22									
28	1	Electrum	Ag	9.52	0.73	16.11				
			Au	90.48	0.73	83.89				
28	2	Plagioclase	Na	2.37	0.13	2.18	3.2	Na2O	0.28	An#
			Al	16.41	0.2	12.81	31.01	Al2O3	1.66	71
			Si	23.9	0.24	17.92	51.12	SiO2	2.33	
			Ca	10.1	0.17	5.31	14.13	CaO	0.69	
			Fe	0.42	0.11	0.16	0.54	FeO	0.02	
			O	46.8	0.29	61.62			8	
Cation sum	4.98									
29	1	Electrum	Ag	9.42	0.68	15.96				
			Au	90.58	0.68	84.04				
29	3	Biotite	Mg	8.82	0.19	8.27	14.63	MgO	3.09	
			Al	7.81	0.18	6.6	14.75	Al2O3	2.46	
			Si	18.76	0.24	15.22	40.13	SiO2	5.69	
			Cl	0.27	0.08	0.18	0		0.07	
			K	8.04	0.16	4.69	9.69	K2O	1.75	
			Ti	2.93	0.13	1.4	4.89	TiO2	0.52	
			Fe	12.15	0.27	4.96	15.63	FeO	1.85	
O	41.21	0.33	58.7			21.93				
Cation sum	15.37									
30	1	Acanthite	S	30.99	0.46	60.17				
			Ag	69.01	0.46	39.83				
30	3	Chalcopyrite	S	39.77	0.39	55.11				
			Fe	28.69	0.39	22.83				
			Cu	31.54	0.48	22.06				

PTS #26143-320										
Site #	Spectrum #	Mineral name	Element	Weight%	Weight% sigma	Atomic%	Compound%	Formula	# Ions	An#
3	1	Acanthite	S	36.76	0.58	66.17				
			Ag	63.24	0.58	33.83				
3	2	Plagioclase	Na	2.49	0.18	2.27	3.35	Na2O	0.29	An#
			Al	16.14	0.26	12.56	30.49	Al2O3	1.63	70
			Si	24.41	0.31	18.25	52.21	SiO2	2.37	
			Ca	9.97	0.22	5.22	13.95	CaO	0.68	
			O	47	0.37	61.7			8	
			Cation sum	4.97						
3	3	Pentlandite	S	35.16	0.38	49.32				
			Fe	25.57	0.39	20.6				
			Ni	39.27	0.47	30.08				
4	1	Kotulskite	Pd	37.05	0.64	52.44				
			Te	4.77	0.39	5.63				
			Bi	58.18	0.67	41.93				
4	2	Chalcopyrite	S	37.88	0.38	53.13				
			Fe	29.74	0.38	23.95				
			Cu	32.38	0.47	22.92				
6	1	Paolovite	Pd	57.62	0.64	60.27				
			Sn	42.38	0.64	39.73				
6	2	Pentlandite	S	36.45	0.36	50.67				
			Fe	27.71	0.37	22.12				
			Ni	35.85	0.43	27.22				
7	1	Undetermined PGM	S	8.25	0.22	23.08				
			As	9.52	0.35	11.4				
			Ag	74.45	0.56	61.94				
			Pt	7.78	0.5	3.58				
7	3	Pentlandite	S	36.91	0.33	51.16				
			Fe	27.85	0.34	22.17				
			Ni	35.24	0.4	26.68				
8	1	Undetermined PGM	Pd	54.19	2.67	69.91				
			Bi	45.81	2.67	30.09				
8	2	Pentlandite	S	37.71	0.58	52.04				
			Fe	25.81	0.59	20.46				
			Ni	36.48	0.7	27.5				
9	1	Kotulskite	Pd	36.64	0.61	51.69				
			Te	6.11	0.4	7.19				
			Bi	57.25	0.64	41.12				
9	2	Chalcopyrite	S	38.19	0.35	53.43				
			Fe	30.08	0.35	24.16				
			Cu	31.73	0.43	22.4				
10	1	Electrum	Ag	63.49	0.91	76.05				
			Au	36.51	0.91	23.95				
10	2	Apatite	P	18.58	0.29	14.64	42.57	P2O5	2.77	
			Cl	6.87	0.21	4.73	0		0.9	
			Ca	36.14	0.34	22.01	50.56	CaO	4.17	
			O	38.42	0.36	58.62			11.1	
			Cation sum	6.94						
11	1	Electrum	Ag	64.12	0.8	76.55				
			Au	35.88	0.8	23.45				
10	2	Apatite	P	18.58	0.29	14.64	42.57	P2O5	2.77	
			Cl	6.87	0.21	4.73	0		0.9	
			Ca	36.14	0.34	22.01	50.56	CaO	4.17	
			O	38.42	0.36	58.62			11.1	
			Cation sum	6.94						
12	1	Electrum	Ag	58.66	0.6	72.16				
			Au	41.34	0.6	27.84				
10	2	Apatite	P	18.58	0.29	14.64	42.57	P2O5	2.77	
			Cl	6.87	0.21	4.73	0		0.9	
			Ca	36.14	0.34	22.01	50.56	CaO	4.17	
			O	38.42	0.36	58.62			11.1	
			Cation sum	6.94						

PTS #26143-320										
Site #	Spectrum #	Mineral name	Element	Weight%	Weight% sigma	Atomic%	Compound%	Formula	# Ions	An#
13	1	Electrum	Ag	60.36	0.62	73.55				
			Au	39.64	0.62	26.45				
10	2	Apatite	P	18.58	0.29	14.64	42.57	P2O5	2.77	
			Cl	6.87	0.21	4.73	0		0.9	
			Ca	36.14	0.34	22.01	50.56	CaO	4.17	
			O	38.42	0.36	58.62			11.1	
			Cation sum	6.94						
14	1	Electrum	Ag	60.48	0.6	73.64				
			Au	39.52	0.6	26.36				
10	2	Apatite	P	18.58	0.29	14.64	42.57	P2O5	2.77	
			Cl	6.87	0.21	4.73	0		0.9	
			Ca	36.14	0.34	22.01	50.56	CaO	4.17	
			O	38.42	0.36	58.62			11.1	
			Cation sum	6.94						
15	1	Electrum	Ag	57.29	0.55	71				
			Au	42.71	0.55	29				
10	2	Apatite	P	18.58	0.29	14.64	42.57	P2O5	2.77	
			Cl	6.87	0.21	4.73	0		0.9	
			Ca	36.14	0.34	22.01	50.56	CaO	4.17	
			O	38.42	0.36	58.62			11.1	
			Cation sum	6.94						
16	1	Electrum	Ag	58.64	0.62	72.13				
			Au	41.36	0.62	27.87				
10	2	Apatite	P	18.58	0.29	14.64	42.57	P2O5	2.77	
			Cl	6.87	0.21	4.73	0		0.9	
			Ca	36.14	0.34	22.01	50.56	CaO	4.17	
			O	38.42	0.36	58.62			11.1	
			Cation sum	6.94						
17	1	Kotulskite	Pd	37.59	0.74	50.49				
			Te	15.65	0.53	17.53				
			Bi	46.76	0.79	31.98				
17	3	Plagioclase	Na	1.58	0.12	1.45	2.13	Na2O	0.19	An#
			Al	17.1	0.19	13.41	32.31	Al2O3	1.74	80
			Si	23.07	0.23	17.39	49.36	SiO2	2.25	
			Ca	11.13	0.17	5.88	15.57	CaO	0.76	
			Fe	0.49	0.11	0.19	0.63	FeO	0.02	
			O	46.63	0.27	61.68			8	
			Cation sum	4.97						
18	1	Kotulskite	Pd	47.73	1.15	61.59				
			Te	9.74	0.78	10.48				
			Bi	42.53	1.22	27.94				
18	2	Chalcopyrite	S	38.7	0.76	54.02				
			Fe	28.95	0.76	23.2				
			Cu	32.34	0.94	22.78				
19	1	Kotulskite	Pd	38.21	0.6	51.83				
			Te	12.48	0.42	14.12				
			Bi	49.31	0.63	34.05				
19	2	Plagioclase	Na	0.2	0.64	0.59	0.86	Na2O	0.08	An#
			Al	18.11	0.37	14.24	34.22	Al2O3	1.83	91
			Si	22.59	0.43	17.06	48.33	SiO2	2.19	
			Ca	12.48	0.34	6.6	17.46	CaO	0.84	
			O	46.82	0.5	62.09			8	
			Cation sum	4.94						
20	1	Electrum	Ag	67.03	0.57	78.78				
			Au	32.97	0.57	21.22				
20	2	Chalcopyrite	S	38.83	0.85	54.13				
			Fe	29.29	0.85	23.44				
			Cu	31.88	1.06	22.43				
21	1	Electrum	Ag	73.82	0.96	83.73				
			Au	26.18	0.96	16.27				
21	2	Plagioclase	Na	2.99	0.13	2.72	4.03	Na2O	0.35	An#
			Al	15.66	0.18	12.15	29.58	Al2O3	1.58	64
			Si	24.99	0.23	18.63	53.45	SiO2	2.42	
			Ca	9.24	0.16	4.83	12.93	CaO	0.63	
			O	47.12	0.27	61.67			8	
			Cation sum	4.97						

PTS #26143-320										
Site #	Spectrum #	Mineral name	Element	Weight%	Weight% sigma	Atomic%	Compound%	Formula	# Ions	An#
22	1	Kotulskite	Pd	40.28	0.75	56.04				
			Te	3.68	0.51	4.27				
			Bi	56.04	0.78	39.7				
22	2	Apatite	P	18.85	0.28	14.82	43.18	P2O5	2.8	
			Cl	6.92	0.2	4.76	0		0.9	
			Ca	35.66	0.33	21.68	49.9	CaO	4.1	
			O	38.57	0.34	58.74			11.1	
			Cation sum	6.9						
23	1	Electrum	Ag	73.25	0.59	83.33				
			Au	26.75	0.59	16.67				
23	2	Clinopyroxene	Mg	11.53	0.19	10.53	19.12	MgO	1.04	
			Si	27.37	0.25	21.65	58.56	SiO2	2.14	
			Ca	0.73	0.08	0.4	1.01	CaO	0.04	
			Mn	0.43	0.11	0.18	0.56	MnO	0.02	
			Fe	16.13	0.28	6.42	20.75	FeO	0.63	
			O	43.81	0.3	60.82			6	
			Cation sum	3.86						
24	1	Paolovite	Pd	65.25	0.44	67.69				
			Sn	34.75	0.44	32.31				
24	2	Orthopyroxene	Mg	15.8	0.2	13.61	26.2	MgO	0.67	
			Si	30.05	0.25	22.41	64.28	SiO2	1.1	
			Fe	7.4	0.22	2.78	9.53	FeO	0.14	
			O	46.75	0.28	61.2			3	
			Cation sum	1.9						
25	1	Sperrylite	As	44.56	0.51	66.43				
			Rh	3.56	0.42	3.86				
			Pt	51.88	0.54	29.71				
25	2	Chalcopyrite	S	37.9	0.86	53.16				
			Fe	29.47	0.87	23.74				
			Cu	32.63	1.08	23.1				
25	3	Plagioclase	Na	2.13	0.12	1.95	2.87	Na2O	0.25	An#
			Al	16.65	0.19	12.99	31.46	Al2O3	1.68	74
			Si	23.85	0.23	17.87	51.03	SiO2	2.32	
			Ca	10.46	0.17	5.49	14.63	CaO	0.71	
			O	46.9	0.27	61.7			8	
			Cation sum	4.97						
26	1	Stibiopalladinite	Pd	69.59	0.63	72.37				
			Sb	30.41	0.63	27.63				
25	2	Chalcopyrite	S	37.9	0.86	53.16				
			Fe	29.47	0.87	23.74				
			Cu	32.63	1.08	23.1				
27	1	Kotulskite	Pd	37.71	0.63	52.55				
			Te	7.2	0.44	8.36				
			Bi	55.09	0.67	39.09				
25	2	Chalcopyrite	S	37.9	0.86	53.16				
			Fe	29.47	0.87	23.74				
			Cu	32.63	1.08	23.1				
28	1	Sperrylite	As	44.19	0.47	67.34				
			Pt	55.81	0.47	32.66				
28	2	Sericite?	Na	1.22	0.13	1.16	1.65	Na2O	0.42	
			Mg	9.88	0.18	8.83	16.38	MgO	3.24	
			Al	5.12	0.14	4.12	9.67	Al2O3	1.51	
			Si	23.88	0.24	18.49	51.09	SiO2	6.79	
			K	0.35	0.07	0.19	0.42	K2O	0.07	
			Ca	8.23	0.15	4.46	11.51	CaO	1.64	
			Fe	7.22	0.22	2.81	9.29	FeO	1.03	
			O	44.11	0.3	59.94			22	
			Cation sum	14.71						
28	2	hbl?	Na	1.22	0.13	1.16	1.65	Na2O	0.44	
			Mg	9.88	0.18	8.83	16.38	MgO	3.39	
			Al	5.12	0.14	4.12	9.67	Al2O3	1.58	
			Si	23.88	0.24	18.49	51.09	SiO2	7.09	
			K	0.35	0.07	0.19	0.42	K2O	0.07	
			Ca	8.23	0.15	4.46	11.51	CaO	1.71	
			Fe	7.22	0.22	2.81	9.29	FeO	1.08	
			O	44.11	0.3	59.94			23	
			Cation sum	15.37						

PTS #26143-320										
Site #	Spectrum #	Mineral name	Element	Weight%	Weight% sigma	Atomic%	Compound%	Formula	# Ions	An#
29	1	Undetermined	Pd	27.7	0.61	42.94				
		PGM	Bi	72.3	0.61	57.06				
29	2	Chlorite	Mg	9.12	0.21	8.63	15.12	MgO	4.07	
			Al	9.35	0.2	7.97	17.66	Al2O3	3.76	
			Si	18.06	0.25	14.79	38.63	SiO2	6.97	
			Ca	0.64	0.08	0.37	0.89	CaO	0.17	
			Fe	21.53	0.33	8.87	27.7	FeO	4.18	
			O	41.31	0.35	59.39			28	
			Cation sum	19.15						
31	1	Undetermined	Pd	50.82	1.36	64.56				
		PGM	Sn	7.39	1.01	8.41				
			Bi	41.8	1.37	27.03				
31	2	Chalcopyrite	S	38.18	0.43	53.43				
			Fe	29.89	0.44	24.01				
			Cu	31.93	0.54	22.55				
32	1	Paolovite	Pd	61.17	1.42	63.73				
			Sn	38.83	1.42	36.27				
32	2	Chalcopyrite	S	38.47	0.7	53.55				
			Fe	33.37	0.73	26.67				
			Cu	28.16	0.88	19.78				

PTS #26143-1205										
Site #	Spectrum #	Mineral name	Element	Weight%	Weight% sigma	Atomic%	Compound%	Formula	# Ions	An#
1	1	Electrum	Ag	13.49	0.99	22.16				
			Au	86.51	0.99	77.84				
1	2	Olivine	Mg	17.92	0.29	17.25	29.72	MgO	1.2	
			Si	17.85	0.27	14.87	38.19	SiO2	1.04	
			Fe	24.95	0.39	10.45	32.09	FeO	0.73	
			O	39.28	0.38	57.43			4	
			Cation sum	2.96						
2	1	Sperrylite	As	40.71	0.7	62.49				
			Rh	3.59	0.6	4.01				
			Sb	1.86	0.41	1.76				
			Pt	53.84	0.78	31.74				
2	3	Chalcopyrite	S	37.66	0.82	52.88				
			Fe	30.25	0.84	24.38				
			Cu	32.09	1.04	22.74				
2	4	Pentlandite	S	36.39	0.44	50.63				
			Fe	30.5	0.46	24.36				
			Ni	30.62	0.52	23.26				
			Cu	2.48	0.36	1.74				
			Cation sum	4.95						
3	1	Stibiopalladinite	As	3.83	0.39	5.53				
			Pd	69.14	0.69	70.41				
			Sb	27.03	0.65	24.06				
			Na	3.27	0.17	2.97	4.41	Na2O	0.38	An#
			Al	14.69	0.23	11.36	27.76	Al2O3	1.47	59
			Si	26.23	0.29	19.49	56.11	SiO2	2.52	
3	2	Plagioclase	K	0.32	0.09	0.17	0.39	K2O	0.02	
			Ca	8.09	0.19	4.21	11.32	CaO	0.55	
			O	47.39	0.34	61.8			8	
			Cation sum	4.95						
			As	9.04	0.61	12.76				
			Pd	59.9	0.87	59.55				
4	3	Chalcopyrite	Sn	31.06	0.82	27.69				
			S	38.34	0.74	53.61				
			Fe	29.79	0.75	23.91				
			Cu	31.87	0.92	22.48				
5	1	Paolovite	Pd	64.58	0.69	67.04				
			Sn	35.42	0.69	32.96				
5	2	Chlorite	Mg	2.98	0.2	3.12	4.94	MgO	1.48	
			Al	6.41	0.22	6.04	12.1	Al2O3	2.87	
			Si	16.66	0.3	15.1	35.63	SiO2	7.16	
			Ca	0.89	0.11	0.57	1.25	CaO	0.27	
			Fe	34.68	0.47	15.81	44.62	FeO	7.5	
			Pd	1.27	0.3	0.3	1.47	PdO	0.14	
			O	37.12	0.46	59.06			28	
			Cation sum	19.41						
6	1	Paolovite	Pd	56.95	0.83	59.34				
			Ag	4.8	0.8	4.93				
			Sn	38.25	0.75	35.73				
6	2	Cubanite	S	38.4	0.42	53.17				
			Fe	39.35	0.46	31.28				
			Cu	22.25	0.51	15.55				
7	1	Undetermined PGM	Pd	45.41	1.52	59.91				
			Sb	7.1	0.95	8.19				
			Bi	47.49	1.62	31.9				
7	2	Pentlandite	S	37.28	0.54	51.44				
			Fe	33.36	0.59	26.43				
			Ni	29.36	0.65	22.13				
8	1	Undetermined PGM	Pd	25.59	0.82	40.31				
			Bi	74.41	0.82	59.69				
8	2	Chalcopyrite	S	37.84	0.46	53.11				
			Fe	29.32	0.47	23.63				
			Cu	32.85	0.58	23.27				

PTS #26143-1205											
Site #	Spectrum #	Mineral name	Element	Weight%	Weight% sigma	Atomic%	Compound%	Formula	# Ions	An#	
9	1	Undetermined PGM	As	5.6		0.59	10.39				
			Pd	35.3		1.42	46.14				
			Sn	8.9		0.85	10.42				
			Pt	14.19		1.07	10.12				
			Bi	20.42		1.96	13.59				
			Th	15.59		1.43	9.34				
9	2	Pentlandite	S	37.55		0.42	51.74				
			Fe	32.59		0.45	25.78				
			Ni	29.86		0.5	22.47				
10	1	Undetermined PGM	As	31.02		1.35	46.91				
			Pd	14.08		1.58	15				
			Ag	13.24		1.38	13.91				
			Pt	41.65		1.83	24.19				
10	2	Chalcopyrite	S	38.59		0.44	53.92				
			Fe	28.53		0.43	22.89				
			Cu	32.88		0.54	23.19				
12	1	Undetermined PGM	Pd	32.29		1.02	46.73				
			Sn	6.02		0.65	7.81				
			Bi	61.69		1.09	45.46				
12	2	Orthopyroxene	Mg	14.12		0.26	12.75	23.41	MgO	0.63	
			Si	26.73		0.31	20.89	57.19	SiO2	1.04	
			Fe	15.08		0.35	5.92	19.4	FeO	0.29	
			O	44.07		0.37	60.44			3	
			Cation sum	1.96							
13	1	Paolovite	Pd	64.99		0.75	67.43				
			Sn	35.01		0.75	32.57				
12	2	Orthopyroxene	Mg	14.12		0.26	12.75	23.41	MgO	0.63	
			Si	26.73		0.31	20.89	57.19	SiO2	1.04	
			Fe	15.08		0.35	5.92	19.4	FeO	0.29	
			O	44.07		0.37	60.44			3	
			Cation sum	1.96							
14	1	Undetermined PGM	Pd	56.83		0.72	59.49				
			Sn	43.17		0.72	40.51				
14	1	Cubanite	S	39.35		1.03	54.03				
			Fe	41.36		1.14	32.61				
			Cu	19.29		1.35	13.37				
15	1	Undetermined PGM	Pd	54.43		0.68	57.13				
			Sn	45.57		0.68	42.87				
15	3	Cubanite	S	41.39		0.75	57.41				
			Fe	16.36		0.61	13.02				
			Cu	42.25		0.87	29.57				
15	2	Plagioclase	Na	3.33		0.29	3.03	4.49	Na2O	0.39	
			Al	15.37		0.38	11.91	29.04	Al2O3	1.55	
			Si	25.31		0.48	18.83	54.14	SiO2	2.44	
			Ca	8.81		0.32	4.59	12.32	CaO	0.6	
			O	47.18		0.55	61.64			8	
Cation sum	4.98										
16	1	Undetermined PGM	Pd	26.33		1.12	41.25				
			Bi	73.67		1.12	58.75				
16	2	Plagioclase	Na	2.89		0.22	2.63	3.9	Na2O	0.34	
			Al	15.26		0.31	11.83	28.83	Al2O3	1.53	
			Si	25.56		0.39	19.03	54.67	SiO2	2.46	
			Ca	9		0.26	4.7	12.6	CaO	0.61	
			O	47.29		0.45	61.81			8	
Cation sum	4.94										
16	4	Chalcopyrite	S	36.32		1.06	51.48				
			Fe	30.15		1.11	24.54				
			Cu	33.53		1.38	23.98				
17	1	Sperrylite	As	33.12		1.2	49.95				
			Pd	23.42		1.44	24.88				
			Pt	43.46		1.53	25.17				
17	2	Pentlandite	S	36.95		0.55	51.19				
			Fe	28.49		0.57	22.66				
			Ni	34.56		0.66	26.15				
18	1	Paolovite	Pd	58.83		0.87	61.45				
			Sn	41.17		0.87	38.55				
18	2	Cubanite	S	37.8		1.17	52.58				
			Fe	38.81		1.29	31				
			Cu	23.38		1.42	16.42				

PTS #26017-640									
Site #	Spectrum #	Mineral name	Element	Weight%	Weight% sigma	Atomic%	Compound%	Formula	# Ions
1	1	Sperrylite	As	41.73	0.57	64.63			
			Sb	1.99	0.36	1.9			
			Pt	56.27	0.6	33.47			
1	3	Chalcopyrite	S	39.42	0.63	54.79			
			Fe	28.11	0.62	22.43			
			Cu	32.47	0.78	22.77			
2	1	Sperrylite	As	36.69	0.9	60.15			
			Pt	63.31	0.9	39.85			
2	2	Chalcopyrite	S	38	0.4	53.25			
			Fe	29.76	0.4	23.95			
			Cu	32.24	0.5	22.8			
3	1	Undetermined PGM	As	3.72	0.38	7.88			
			Pd	25.85	0.79	38.59			
			Bi	70.43	0.83	53.53			
3	2	Chalcopyrite	S	36.12	0.45	51.13			
			Fe	32.51	0.48	26.42			
			Ni	0.78	0.24	0.6			
			Cu	30.59	0.58	21.85			
4	1	Undetermined PGM	As	19.33	0.77	28.49			
			Pd	42.71	1.04	44.34			
			Sn	15.57	0.86	14.49			
			Pt	22.39	1.01	12.67			
4	2	Chalcopyrite	S	37.85	0.41	53.11			
			Fe	29.03	0.41	23.39			
			Ni	0.84	0.21	0.65			
			Cu	32.27	0.51	22.85			
5	1	Froodite	Pd	22.05	1.12	35.72			
			Bi	77.95	1.12	64.28			
5	2	Cubanite	S	38.42	0.39	53.29			
			Fe	37.35	0.43	29.75			
			Cu	24.23	0.49	16.96			
6	1	Paolovite	Pd	60.64	1.12	63.34			
			Sn	30.52	0.97	28.58			
			Sb	8.84	1.06	8.07			
6	2	Pyrrhotite	S	41.45	0.39	55.22			
			Fe	58.55	0.39	44.78			
7	1	Kotulskite	Pd	33.16	0.67	46.14			
			Sb	6.69	0.48	8.14			
			Te	6.87	0.48	7.97			
			Bi	53.28	0.74	37.75			
7	2	Chalcopyrite	S	38.04	0.4	53.33			
			Fe	28.64	0.4	23.06			
			Ni	0.7	0.2	0.54			
			Cu	32.62	0.5	23.08			
8	1	Sperrylite	As	39.28	0.74	62.75			
			Pt	60.72	0.74	37.25			
8	2	Cubanite	S	38.67	0.41	53.44			
			Fe	39.33	0.45	31.21			
			Cu	22	0.5	15.35			
9	1	Undetermined PGM	Pd	55.24	0.85	57.92			
			Sn	44.76	0.85	42.08			
9	2	Cubanite	S	38.05	0.4	52.81			
			Fe	39.36	0.44	31.36			
			Cu	22.59	0.49	15.82			

PTS #26017-640									
Site #	Spectrum #	Mineral name	Element	Weight%	Weight% sigma	Atomic%	Compound%	Formula	# Ions
10	1	Sperrylite	As	38.94	0.73	62.42			
			Pt	61.06	0.73	37.58			
10	2	Chalcopyrite	S	38.16	0.4	53.44			
			Fe	29.25	0.4	23.52			
			Cu	32.6	0.5	23.04			
11	1	Paolovite	Pd	65.93	0.52	68.34			
			Sn	34.07	0.52	31.66			
11	2	Cubanite	S	38.29	0.39	53.04			
			Fe	39.77	0.43	31.62			
			Cu	21.94	0.48	15.34			
12	1	Sperrylite	As	38.12	0.86	61.6			
			Pt	61.88	0.86	38.4			
12	2	Cubanite	S	37.78	0.46	52.51			
			Fe	39.93	0.51	31.86			
			Cu	22.28	0.56	15.63			
13	1	Electrum	Ag	53.56	0.85	67.8			
			Au	46.44	0.85	32.2			
13	2	Pentlandite	S	39.34	0.38	53.45			
			Fe	40.15	0.42	31.32			
			Ni	20.52	0.43	15.23			
13	5	Cubanite	S	38.7	0.91	53.44			
			Fe	40.11	1	31.8			
			Cu	21.19	1.1	14.76			
14	1	Paolovite	Pd	58.78	0.83	61.4			
			Sn	41.22	0.83	38.6			
14	2	Cubanite	S	37.18	0.39	51.89			
			Fe	39.99	0.43	32.04			
			Cu	22.83	0.48	16.08			
15	1	Paolovite	Pd	23.34	1.13	26.26			
			Sn	67.53	1.35	68.13			
			Pt	9.14	1.15	5.61			
15	2	Chalcopyrite	S	38.49	0.9	53.78			
			Fe	29.24	0.89	23.46			
			Cu	32.27	1.12	22.76			
16	1	Hessite	Ag	56.04	0.86	60.13			
			Te	43.96	0.86	39.87			
16	2	Cubanite	S	37.78	0.57	52.51			
			Fe	39.76	0.63	31.73			
			Cu	22.46	0.69	15.75			

PTS #26045-372										
Site #	Spectrum #	Mineral name	Element	Weight%	Weight% sigma	Atomic%	Compound%	Formula	# Ions	An#
1	1	Hessite	Ag	63.26	0.77	67.07				
			Te	36.74	0.77	32.93				
1	2	Bravoite	S	45.48	0.64	60.29				
			Fe	6.2	0.38	4.72				
			Ni	48.32	0.68	34.99				
2	1	Paolovite	Pd	64.05	0.86	66.53				
			Sn	35.95	0.86	33.47				
2	2	Chalcopyrite	S	37.68	1.14	52.97				
			Fe	28.86	1.15	23.3				
			Cu	33.46	1.41	23.74				
3	1	Paolovite	Pd	59.77	1.23	62.37				
			Sn	40.23	1.23	37.63				
3	2	Chalcopyrite	S	38.06	0.61	53.32				
			Fe	29.79	0.62	23.96				
			Cu	32.15	0.76	22.72				
4	1	Paolovite	Pd	63.94	0.96	66.42				
			Sn	36.06	0.96	33.58				
4	2	Chalcopyrite	S	37.84	0.61	53.09				
			Fe	29.89	0.62	24.07				
			Cu	32.26	0.77	22.84				
6	1	Undetermined PGM	Pd	65.38	1.01	68.11				
			Sn	16.06	0.84	15				
			Sb	18.55	0.86	16.89				
6	4	Chlorite	Mg	11.82	0.37	10.36	19.6	MgO	4.75	
			Al	6.92	0.31	5.46	13.08	Al2O3	2.51	
			Si	25.52	0.46	19.36	54.59	SiO2	8.88	
			Fe	9.9	0.45	3.78	12.74	FeO	1.73	
			O	45.84	0.57	61.04			28	
			Cation sum	17.87						
6	6	Sericite	Na	0.74	0.19	0.68	1	Na2O	0.24	
			Mg	1.61	0.18	1.41	2.68	MgO	0.5	
			Al	9.13	0.28	7.18	17.24	Al2O3	2.56	
			Si	30.33	0.43	22.92	64.89	SiO2	8.18	
			K	10.53	0.3	5.71	12.69	K2O	2.04	
			Fe	1.17	0.24	0.44	1.5	FeO	0.16	
			O	46.49	0.49	61.65			22	
			Cation sum	13.68						
7	1	Electrum	Ag	90.93	3.45	94.82				
			Au	9.07	3.45	5.18				
7	4	Chalcopyrite	S	38.04	1.38	54				
			Fe	26.71	1.33	21.77				
			Cu	31.79	1.67	22.77				
			Ag	3.46	1.11	1.46				
7	6	Plagioclase	Na	1.71	0.2	1.57	2.3	Na2O	0.2	An#
			Al	9.16	0.26	7.17	17.31	Al2O3	0.93	5
			Si	31.35	0.4	23.58	67.08	SiO2	3.06	
			K	10.84	0.29	5.86	13.06	K2O	0.76	
			Ca	0.18	0.14	0.09	0.25	CaO	0.01	
			O	46.75	0.45	61.73			8	
			Cation sum	4.96						

PTS #26045-372										
Site #	Spectrum #	Mineral name	Element	Weight%	Weight% sigma	Atomic%	Compound%	Formula	# Ions	An#
8	1	Stibiopalladinite	Pd	60.24	0.97	63.16				
			Sn	17.01	0.83	15.99				
			Sb	22.76	0.86	20.85				
8	2	Plagioclase (possible alteration material after plag)	Na	7.95	0.3	7.01	10.72	Na2O	0.91	An#
			Al	9.62	0.28	7.22	18.17	Al2O3	0.94	0
			Si	32.6	0.42	23.52	69.75	SiO2	3.05	
			K	1.08	0.14	0.56	1.3	K2O	0.07	
			Ca	0.04	0.11	0.02	0.06	CaO	0	
			O	48.71	0.46	61.67			8	
			Cation sum	4.97						
9	1	Acanthite	S	11.71	0.51	30.85				
			Ag	88.29	0.51	69.15				
9	4	Sericite	Na	1.88	0.22	1.73	2.54	Na2O	0.62	
			Mg	1.01	0.16	0.88	1.67	MgO	0.31	
			Al	9.27	0.27	7.24	17.52	Al2O3	2.58	
			Si	30.77	0.42	23.1	65.83	SiO2	8.24	
			K	9.29	0.27	5.01	11.19	K2O	1.79	
			Fe	0.97	0.21	0.36	1.24	FeO	0.13	
			O	46.8	0.48	61.68			22	
Cation sum	13.67									
10	1	Silver sulfide	S	16.84	0.44	37.57				
			Fe	7.74	0.44	9.91				
			Cu	5.42	0.54	6.1				
			Ag	70	0.72	46.41				
10	2	Plagioclase (possible alteration material after plag)	Na	8.02	0.89	7.04	10.82	Na2O	2.5	An#
			Al	10.42	0.8	7.79	19.69	Al2O3	2.77	0
			Si	32.55	1.23	23.36	69.63	SiO2	8.31	
			K	0.1	0.31	0.05	0.12	K2O	0.02	
			Ca	-0.18	0.29	-0.09	-0.25	CaO	0	
			O	49.09	1.35	61.86			22	
Cation sum	13.57									
11	1	Paolovite	Pd	64.74	0.51	67.19				
			Sn	35.26	0.51	32.81				
11	2	Chalcopyrite	S	38.71	0.39	53.99				
			Fe	29.73	0.39	23.8				
			Cu	31.56	0.49	22.21				
11	3	Chlorite	Mg	13.66	0.27	12.34	22.65	MgO	5.8	
			Al	7.52	0.22	6.12	14.2	Al2O3	2.88	
			Si	20.62	0.3	16.13	44.12	SiO2	7.58	
			Fe	14.79	0.35	5.82	19.03	FeO	2.73	
			O	43.41	0.4	59.59			28	
Cation sum	18.98									
13	1	Paolovite	Pd	62.67	0.71	65.31				
			Sn	29.42	0.62	27.49				
			Sb	7.91	0.64	7.2				
13	2	Biotite	Mg	5.75	0.19	5.58	9.54	MgO	2.07	
			Al	6.95	0.19	6.07	13.14	Al2O3	2.26	
			Si	18.4	0.26	15.43	39.36	SiO2	5.73	
			Cl	0.57	0.1	0.38	0		0.14	
			K	8	0.18	4.82	9.64	K2O	1.79	
			Ti	4.05	0.17	1.99	6.76	TiO2	0.74	
			Fe	16.32	0.34	6.89	21	FeO	2.56	
			O	39.95	0.37	58.84			21.86	
Cation sum	15.15									

PTS #26031-735										
Site #	Spectrum #	Mineral name	Element	Weight%	Weight% sigma	Atomic%	Compound%	Formula	# Ions	An#
1	1	Silver Sulfide	S	7.4	0.36	21.19				
			Ag	92.6	0.36	78.81				
1	2	Chalcopyrite	S	36.36	0.39	51.54				
			Fe	29.94	0.4	24.36				
			Cu	33.7	0.49	24.1				
2	1	Silver Sulfide	S	23.71	0.37	51.11				
			Ag	76.29	0.37	48.89				
2	2	Pentlandite	S	37.95	0.39	52.8				
			Fe	1.56	0.17	1.25				
			Co	1.14	0.22	0.87				
			Ni	59.34	0.42	45.09				
			S	19.97	0.43	45.63				
			Ag	80.03	0.43	54.37				
3	2	Pentlandite	S	37.17	0.39	51.97				
			Fe	1.44	0.16	1.15				
			Co	1.29	0.21	0.98				
			Ni	60.11	0.41	45.9				
			Pd	65.42	0.5	67.85				
			Sn	34.58	0.5	32.15				
4	2	Chalcopyrite	S	38.51	0.39	53.8				
			Fe	29.31	0.39	23.51				
			Cu	32.18	0.48	22.69				
5	1	Silver Sulfide	S	21.85	0.69	48.46				
			Ag	78.15	0.69	51.54				
5	2	Chalcopyrite	S	37.5	0.41	52.77				
			Fe	29.21	0.41	23.59				
			Cu	33.29	0.51	23.64				
6	1	Paolovite	Pd	64.3	0.66	66.77				
			Sn	35.7	0.66	33.23				
6	2	Plagioclase	Na	1.5	0.13	1.39	2.03	Na2O	0.18	An#
			Al	16.8	0.21	13.21	31.75	Al2O3	1.71	82
			Si	23	0.25	17.37	49.21	SiO2	2.25	
			Ca	11.73	0.19	6.21	16.41	CaO	0.81	
			Fe	0.47	0.12	0.18	0.6	FeO	0.02	
			O	46.49	0.3	61.64				8
			Cation sum	4.98						
8	1	Stibiopalladinite	Pd	68.27	0.51	71.12				
			Sb	31.73	0.51	28.88				
8	2	Chalcopyrite	S	36.07	0.39	51.11				
			Fe	32.1	0.41	26.12				
			Cu	31.84	0.5	22.77				
10	1	Naldrettite	Pd	68.14	0.5	70.99				
			Sb	31.86	0.5	29.01				
10	2	Chalcopyrite	S	37.37	0.39	52.61				
			Fe	29.72	0.4	24.02				
			Cu	32.9	0.49	23.37				
10	3	Biotite	Mg	11.35	0.22	10.35	18.82	MgO	3.88	
			Al	8.2	0.2	6.73	15.49	Al2O3	2.53	
			Si	19.2	0.26	15.15	41.07	SiO2	5.68	
			K	8.66	0.18	4.91	10.43	K2O	1.84	
			Ti	2.56	0.15	1.18	4.26	TiO2	0.44	
			Fe	7.71	0.26	3.06	9.92	FeO	1.15	
			O	42.32	0.36	58.62				22
			Cation sum	15.53						

PTS #26031-735										
Site #	Spectrum #	Mineral name	Element	Weight%	Weight% sigma	Atomic%	Compound%	Formula	# Ions	An#
11	1	Silver Sulfide	S	19.36	0.35	44.68				
			Ag	80.64	0.35	55.32				
11	2	Chalcopyrite	S	39.14	0.37	54.45				
			Fe	29.34	0.37	23.43				
			Cu	31.52	0.45	22.12				
12	1	Silver Sulfide	S	18.1	0.35	42.65				
			Ag	81.9	0.35	57.35				
12	2	Chalcopyrite	S	38.25	0.36	53.55				
			Fe	29	0.37	23.31				
			Cu	32.75	0.45	23.14				
13	1	Silver, Lead sulfide	S	27.36	0.54	60.06				
			Se	10.84	0.41	9.67				
			Ag	29.66	0.7	19.35				
			Pb	32.14	0.93	10.92				
13	2	Chalcopyrite	S	38.32	0.5	53.6				
			Fe	29.42	0.51	23.62				
			Cu	32.26	0.62	22.77				

PTS #26021-103										
Site #	Spectrum #	Mineral name	Element	Weight%	Weight% sigma	Atomic%	Compound%	Formula	# Ions	An#
1	1	Sperrylite	As	42.04	0.57	65.39				
			Pt	57.96	0.57	34.61				
1	2	Chalcopyrite	S	36.95	0.37	52.16				
			Fe	29.91	0.38	24.24				
			Cu	33.13	0.47	23.6				
2	1	Sperrylite	As	41.9	0.5	64.61				
			Sb	2.77	0.32	2.63				
			Pt	55.32	0.53	32.76				
2	2	Plagioclase	Na	1.85	0.13	1.7	2.5	Na2O	0.22	An#
			Al	17.23	0.2	13.47	32.56	Al2O3	1.75	77
			Si	23.19	0.24	17.42	49.62	SiO2	2.26	
			Ca	10.95	0.18	5.76	15.33	CaO	0.75	
			O	46.77	0.28	61.65				8
			Cation sum	4.98						
2	5	Chlorite	Mg	1.38	0.14	1.39	2.28	MgO	0.65	
			Al	12.69	0.22	11.57	23.98	Al2O3	5.44	
			Si	15.33	0.24	13.42	32.79	SiO2	6.3	
			Fe	31.83	0.37	14.02	40.95	FeO	6.58	
			O	38.77	0.36	59.6				28
			Cation sum	18.98						
3	1	Paolovite	Pd	66.46	0.61	69.16				
			Sn	14.51	0.5	13.54				
			Sb	19.03	0.52	17.3				
3	2		S	38.68	0.37	54.02				
			Fe	28.31	0.37	22.7				
			Cu	33.02	0.45	23.27				
3	3	Plagioclase	Na	1.22	0.12	1.13	1.65	Na2O	0.15	An#
			Al	17.55	0.2	13.75	33.16	Al2O3	1.78	84
			Si	22.97	0.24	17.29	49.15	SiO2	2.24	
			Ca	11.46	0.18	6.04	16.04	CaO	0.78	
			O	46.79	0.28	61.8				8
			Cation sum	4.95						
4	1	Undetermined PGM	As	49.5	0.81	63.75				
			Rh	25.46	0.81	23.87				
			Pt	25.04	0.86	12.38				
4	2	Chalcopyrite	S	36.39	0.39	51.5				
			Fe	31.17	0.41	25.33				
			Cu	32.44	0.5	23.17				
4	3	Nickeline	Ni	46.22	0.51	52.3				
			As	53.78	0.51	47.7				
5	1	Stibiopalladinite	As	5.91	1.17	8.47				
			Pd	67.02	1.71	67.65				
			Sb	27.07	1.59	23.88				
5	2	Chalcopyrite	S	38.64	0.37	53.95				
			Fe	29.05	0.37	23.29				
			Cu	32.31	0.46	22.76				
6	1	Paolovite	Pd	60.95	0.81	63.52				
			Sn	39.05	0.81	36.48				
6	2	Chalcopyrite	S	37.26	0.39	52.46				
			Fe	25.48	0.37	20.6				
			Ni	7.98	0.32	6.13				
			Cu	29.29	0.48	20.81				
7	1	Paolovite	Pd	62.91	0.97	65.43				
			Sn	37.09	0.97	34.57				
7	2	Pentlandite	S	37.55	0.42	51.64				
			Fe	42.41	0.48	33.49				
			Ni	16.94	0.45	12.72				
			Cu	3.09	0.37	2.14				

PTS #26021-103										
Site #	Spectrum #	Mineral name	Element	Weight%	Weight% sigma	Atomic%	Compound%	Formula	# Ions	An#
9	1	Stibiopalladinite	Pd	69.2	0.52	71.99				
			Sb	30.8	0.52	28.01				
9	2	Chalcopyrite	S	38.08	0.37	53.38				
			Fe	28.98	0.37	23.32				
			Cu	32.94	0.46	23.3				
10	1	Paolovite	Pd	58.57	0.65	61.2				
			Sn	41.43	0.65	38.8				
10	2	Pentlandite	S	38.41	0.43	53.61				
			Fe	20.9	0.38	16.75				
			Ni	17.08	0.44	13.02				
			Cu	23.61	0.52	16.63				
10	4	Plagioclase	Na	1.32	0.12	1.22	1.78	Na2O	0.16	An#
			Al	17.59	0.2	13.79	33.23	Al2O3	1.79	83
			Si	22.74	0.24	17.13	48.65	SiO2	2.22	
			Ca	11.68	0.18	6.16	16.34	CaO	0.8	
			O	46.67	0.28	61.71			8	
			Cation sum	4.96						
11	1	Paolovite	Pd	61.46	1.68	64.02				
			Sn	38.54	1.68	35.98				
11	2	Pentlandite	S	36.93	0.35	51.02				
			Fe	36.3	0.38	28.79				
			Ni	26.77	0.41	20.2				
12	1	Paolovite	Pd	48.29	0.77	57.83				
			Sn	22.25	0.6	23.88				
			Au	8.74	0.61	5.65				
			Bi	20.73	0.76	12.64				
12	4	Clinopyroxene	Mg	9.03	0.18	8.27	14.98	MgO	0.82	
			Al	0.42	0.09	0.35	0.8	Al2O3	0.03	
			Si	25.57	0.24	20.26	54.71	SiO2	2.02	
			Ca	14.54	0.2	8.07	20.34	CaO	0.8	
			Fe	7.13	0.23	2.84	9.17	FeO	0.28	
			O	43.3	0.3	60.22			6	
			Cation sum	3.96						
13	1	Undetermined PGM	As	4.77	0.35	8.42				
			Pd	15.14	0.53	18.83				
			Sb	45.05	0.63	48.97				
			Pt	35.04	0.64	23.77				
13	4	Plagioclase	Na						0.15	An#
			Al	13.76	0.21	11.13	26	Al2O3	1.8	85
			Si	21.92	0.26	17.03	46.9	SiO2	2.2	
			Ca	19.37	0.25	10.54	27.1	CaO	0.82	
			O	44.95	0.31	61.3			8	
			Cation sum	5.05						
14	1	Paolovite	Pd	67.34	0.49	69.7				
			Sn	32.66	0.49	30.3				
14	2	Chalcopyrite	S	38.01	0.36	53.29				
			Fe	29.27	0.37	23.56				
			Cu	32.72	0.45	23.15				
15	1	Undetermined PGM	Pd	51.32	0.96	62.25				
			Sb	17.35	0.86	18.4				
			Bi	31.33	0.93	19.35				
15	3	Nickeline	Ni	38.75	0.45	44.67				
			As	61.25	0.45	55.33				
16	1	Undetermined PGM	S	29.32	0.49	52.07				
			As	44.89	0.61	34.13				
			Pd	25.79	0.74	13.81				
16	2	Chalcopyrite	S	38.47	0.36	53.77				
			Fe	29.28	0.36	23.49				
			Cu	32.25	0.44	22.74				

PTS #26021-103										
Site #	Spectrum #	Mineral name	Element	Weight%	Weight% sigma	Atomic%	Compound%	Formula	# Ions	An#
17	1	Sperrylite	As	43.9	0.5	67.08				
			Pt	56.1	0.5	32.92				
17	2	Chalcopyrite	S	40.08	0.37	55.48				
			Fe	27.82	0.36	22.11				
			Cu	32.09	0.45	22.41				
18	1	Undetermined PGM	S	3.81	0.23	11.77				
			As	42.03	0.56	55.63				
			Rh	11.11	0.55	10.71				
			Pt	43.05	0.63	21.88				
18	4	Chlorite	Mg	4.89	0.18	4.91	8.11	MgO	2.32	
			Al	8.9	0.2	8.04	16.81	Al2O3	3.8	
			Si	16.56	0.25	14.38	35.43	SiO2	6.8	
			Fe	30.82	0.36	13.46	39.65	FeO	6.37	
			O	38.83	0.36	59.2			28	
			Cation sum	19.29						
19	1	Sperrylite	As	44	0.5	67.17				
			Pt	56	0.5	32.83				
19	2	Chalcopyrite	S	39.38	0.36	54.7				
			Fe	28.97	0.36	23.11				
			Cu	31.65	0.45	22.19				
20	1	Stibiopalladinite	S	3.13	0.16	9.43				
			As	12.23	0.41	15.76				
			Pd	66.84	0.58	60.68				
			Sb	17.8	0.51	14.12				
20	2	Pentlandite	S	44.62	0.41	59.05				
			Fe	25.29	0.38	19.22				
			Co	3.63	0.29	2.62				
			Ni	26.45	0.44	19.12				

PTS #26031-729									
Site #	Spectrum #	Mineral name	Element	Weight%	Weight% sigma	Atomic%	Compound%	Formula	# Ions
1	1	Sperrylite	As	37.95	0.56	59.85			
			Pd	5.07	0.51	5.63			
			Pt	56.98	0.63	34.51			
1	2	Chalcopyrite	S	37.98	0.35	53.25			
			Fe	29.5	0.36	23.75			
			Cu	32.51	0.44	23			
2	1	Paolovite	As	1.97	0.3	2.96			
			Pd	60.16	0.63	63.75			
			Sn	30.64	0.55	29.11			
			Pt	7.23	0.48	4.18			
2	2	Pentlandite	S	36.72	0.35	51.44			
			Fe	3.48	0.19	2.8			
			Ni	59.8	0.37	45.76			
3	1	Sperrylite	As	41.2	0.56	64.18			
			Te	2.05	0.34	1.88			
			Pt	56.74	0.59	33.94			
3	2	Chalcopyrite	S	37.92	0.35	53.19			
			Fe	29.45	0.36	23.72			
			Cu	32.62	0.44	23.09			
4	1	Paolovite	As	5.3	0.48	8.11			
			Pd	51.67	0.83	55.69			
			Sn	28.8	0.73	27.83			
			Pt	14.23	0.73	8.37			
4	2	Chalcopyrite	S	38.63	0.36	53.94			
			Fe	29.09	0.36	23.32			
			Cu	32.28	0.45	22.74			
5	1	Paolovite	Pd	54.14	0.8	60.29			
			Sn	30.34	0.72	30.29			
			Pt	15.52	0.71	9.43			
5	2	Bornite	S	28.92	0.34	44.14			
			Fe	10.64	0.26	9.33			
			Cu	60.43	0.4	46.54			
6	1	Acanthite	S	12.47	0.24	32.4			
			Ag	87.53	0.24	67.6			
6	2	Bornite	S	29.09	0.33	44.28			
			Fe	11.69	0.26	10.22			
			Cu	59.22	0.4	45.5			
7	1	Paolovite	As	8.85	0.55	13.11			
			Pd	51.23	0.85	53.41			
			Sn	29.48	0.74	27.55			
			Pt	10.43	0.74	5.93			
7	3	Chalcopyrite	S	37.96	0.36	53.21			
			Fe	29.78	0.36	23.97			
			Cu	32.26	0.45	22.82			
8	1	Paolovite	Pd	62.55	1.01	65.08			
			Sn	37.45	1.01	34.92			
8	2	Chalcopyrite	S	38.53	0.37	53.81			
			Fe	29.29	0.36	23.49			
			Ni	0.54	0.19	0.41			
			Cu	31.64	0.45	22.3			

PTS #26031-729									
Site #	Spectrum #	Mineral name	Element	Weight%	Weight% sigma	Atomic%	Compound%	Formula	# Ions
9	1	Hessite	Ag	60.82	0.99	64.74			
			Te	39.18	0.99	35.26			
9	2	Chalcopyrite	S	38.25	0.36	53.52			
			Fe	29.5	0.36	23.71			
			Cu	32.25	0.44	22.77			
10	1	Undetermined PGM	Pd	46.72	0.9	48.87			
			Ag	12.39	0.9	12.78			
			Sn	40.9	0.87	38.35			
10	2	Pentlandite	S	36.97	0.35	51.27			
			Fe	25.3	0.35	20.15			
			Ni	37.73	0.43	28.58			
11	1	Undetermined PGM	S	59.9	0.86	88.91			
			Ag	6.66	0.72	2.94			
			Pt	33.44	0.82	8.16			
11	2	Chalcopyrite	S	37.98	0.87	53.67			
			Fe	28.67	0.87	23.26			
			Cu	30.91	1.07	22.04			
			Ag	2.44	0.65	1.02			

Appendix B
Precious Metal Minerals in Concentrate C5 Samples
Energy Dispersive Spectrometry Data

PTS# C5 Con 1						
Site #	Spectrum	Mineral name	Element	Weight%	Weight% sigma	Atomic%
2	1	Sperrylite	As	43.23	0.55	66.47
			Pt	56.77	0.55	33.53
2	2	Cubanite	S	39.09	0.55	53.85
			Fe	39.71	0.6	31.41
			Cu	21.2	0.66	14.74
3	1	Stibiopalladinite	Pd	74.9	0.87	77.34
			Sb	25.1	0.87	22.66
3	2	Chalcopyrite	S	39.99	0.59	55.2
			Fe	31.28	0.6	24.79
			Cu	28.73	0.74	20.01
4	1	Undetermined PGM	Pd	65.24	2.15	78.66
			Bi	34.76	2.15	21.34
Liberated						
5	1	Undetermined PGM	As	22.44	0.53	35.51
			Pd	15.53	0.63	17.3
			Sn	24.3	0.61	24.27
			Pt	37.73	0.77	22.93
5	3	Chalcopyrite	S	37.25	0.82	52.65
			Fe	26.36	0.8	21.39
			Cu	36.4	1.02	25.96
6	1	Paolovite	Pd	64.85	0.64	67.3
			Sn	35.15	0.64	32.7
Liberated						
7	1	Sperrylite	As	36.62	1.72	60.07
			Pt	63.38	1.72	39.93
7	4	Chalcopyrite	S	37.22	0.43	52.45
			Fe	29.72	0.44	24.05
			Cu	33.05	0.54	23.5
8	1	Undetermined PGM	Pd	74	1.49	84.82
			Bi	26	1.49	15.18
Liberated						
9	1	Undetermined PGM	S	19.02	0.65	44.63
			Fe	7.07	0.47	9.52
			Cu	1.72	0.47	2.04
			Pd	51.33	1.29	36.3
			Bi	20.87	1.54	7.51
Liberated						
10	1	Silver sulfide	S	29.18	0.44	58.09
			Ag	70.82	0.44	41.91
10	2	Pentlandite	S	38.22	0.37	53.06
			Fe	2.69	0.18	2.14
			Ni	59.09	0.39	44.8

PTS# C5 Con 2						
Site #	Spectrum	Mineral name	Element	Weight%	Weight% sigma	Atomic%
1	1	Undetermined PGM	Pd	84.24	1.84	91.3
			Bi	15.76	1.84	8.7
Liberated						
2	1	Paolovite	Pd	64.09	0.54	66.56
			Sn	35.91	0.54	33.44
2	2	Chalcopyrite	S	38.17	0.38	53.39
			Fe	30.6	0.38	24.57
			Cu	31.23	0.47	22.04
3	1	Stibiopalladinite	Pd	67.97	0.48	70.83
			Sb	32.03	0.48	29.17
Liberated						
4	1	Tellurium	S	13.55	0.27	33.05
			Fe	11.38	0.34	15.93
			Cu	8.11	0.4	9.98
			Te	66.96	0.49	41.04
4	2	Chalcopyrite	S	37.72	0.37	52.95
			Fe	30.01	0.37	24.19
			Cu	32.28	0.46	22.86
5	1	Paolovite	Pd	63.75	0.55	66.24
			Sn	36.25	0.55	33.76
5	2	Chalcopyrite	S	38.14	0.39	53.45
			Fe	28.89	0.39	23.24
			Cu	32.96	0.48	23.31
6	1	Paolovite	Pd	59.6	0.56	62.21
			Sn	40.4	0.56	37.79
6	2	Chalcopyrite	S	36.95	0.38	52.16
			Fe	29.66	0.39	24.05
			Cu	33.39	0.47	23.79
7	1	Sperrylite	As	41.58	0.76	63.34
			Pd	5.1	0.64	5.47
			Pt	53.32	0.83	31.19
7	2	Chalcopyrite	S	38.02	0.39	53.25
			Fe	30.23	0.4	24.31
			Cu	31.75	0.48	22.44

PTS# C5 Con 2						
Site #	Spectrum	Mineral name	Element	Weight%	Weight% sigma	Atomic%
8	1	Undetermined PGM	As	6.87	0.62	10.3
			Pd	69.27	1.27	73.13
			Te	9.27	0.93	8.16
			Pt	14.6	1.06	8.4
8	2	Chalcopyrite	S	32.39	2.15	47.19
			Fe	30.65	2.25	25.64
			Cu	36.96	2.76	27.17
9	1	Undetermined PGM	Pd	77.34	0.67	79.62
			Sb	22.66	0.67	20.38
		Liberated				
10	1	Paolovite	Pd	65.41	0.53	67.84
			Sn	34.59	0.53	32.16
10	2	Chalcopyrite	S	37.17	0.38	52.36
			Fe	30.45	0.39	24.63
			Cu	32.38	0.47	23.02

PTS# C5 Con 3						
Site #	Spectrum	Mineral name	Element	Weight%	Weight% sigma	Atomic%
1	1	Hessite	Ag	58.95	0.65	62.95
			Te	41.05	0.65	37.05
1	2	Cubanite	S	38.2	0.35	52.91
			Fe	40.47	0.39	32.19
			Cu	21.33	0.43	14.91
2	1	Undetermined PGM	S	23.35	0.44	52.65
			Pd	62.49	0.83	42.46
			Bi	14.16	1	4.9
2	2	Pentlandite	S	35.31	0.35	49.44
			Fe	28.58	0.36	22.97
			Co	3.82	0.28	2.91
			Ni	32.29	0.42	24.69
3	1	Sperrylite	As	38.01	0.68	61.49
			Pt	61.99	0.68	38.51
3	2		S	37.87	0.36	53.13
			Fe	29.66	0.36	23.89
			Cu	32.47	0.45	22.98
4	1	Paolovite	As	4.53	0.53	6.53
			Pd	63.12	1.05	64.14
			Sn	25.97	0.86	23.66
			Sb	6.38	0.91	5.67
4	2	Pentlandite	S	33.22	0.41	47.43
			Fe	36.29	0.47	29.75
			Ni	14.3	0.44	11.15
			Cu	16.2	0.5	11.67
5	1	Sperrylite	As	40.98	1.32	64.39
			Pt	59.02	1.32	35.61
5	2	Pyrrhotite	S	19.31	0.42	29.82
			Fe	66.78	0.68	59.2
			Ni	2.34	0.4	1.98
			Cu	11.56	0.61	9.01
6	1	Sperrylite	As	44.25	0.93	67.39
			Pt	55.75	0.93	32.61
		Liberated				
7	1	Undetermined PGM	Pd	85.05	2.46	91.79
			Bi	14.95	2.46	8.21
7	2	Chalcopyrite	S	35.2	0.38	50.17
			Fe	32.67	0.42	26.73
			Cu	32.13	0.5	23.11
8	1	Sperrylite	As	41.42	1.22	62.96
			Pd	5.87	1.01	6.28
			Pt	52.71	1.33	30.76
8	2	Chalcopyrite	S	37.11	0.36	52.32
			Fe	30.06	0.37	24.33
			Cu	32.83	0.45	23.35

PTS# C5 Con 3						
Site #	Spectrum	Mineral name	Element	Weight%	Weight% sigma	Atomic%
9	1	Undetermined PGM	Pd	75.92	0.66	78.3
			Sb	24.08	0.66	21.7
9	2	Chalcopyrite	S	33.79	0.55	48.41
			Fe	37.34	0.63	30.72
			Cu	28.87	0.73	20.87
10	1	Empressite	Ag	52.99	0.98	57.15
			Te	47.01	0.98	42.85
10	2	Chalcopyrite	S	37.09	0.36	52.29
			Fe	30.23	0.37	24.46
			Cu	32.68	0.45	23.25
11	1	Undetermined PGM	Pd	52.08	1.28	56.59
			Te	47.92	1.28	43.41
11	2	Chalcopyrite	S	37.57	0.46	52.74
			Fe	30.98	0.47	24.97
			Cu	31.45	0.58	22.28
12	1	Undetermined PGM	Pd	30.03	0.81	33.98
			Te	69.97	0.81	66.02
12	2	Cubanite	S	38.7	0.47	53.4
			Fe	40.75	0.52	32.29
			Cu	20.55	0.57	14.31
13	1	Undetermined PGM	S	35.81	1.04	73.88
			Pd	19.02	1.12	11.82
			Bi	45.17	1.43	14.3
13	2	Chalcopyrite	S	37.28	0.45	52.5
			Fe	29.85	0.47	24.14
			Cu	32.87	0.57	23.36
14	1	Kotulskite	Pd	40.09	0.84	52.55
			Sb	3.23	0.58	3.7
			Te	13.94	0.61	15.23
			Bi	42.74	0.89	28.52
14	2	Pentlandite	S	36.35	0.44	50.54
			Fe	28.89	0.46	23.06
			Ni	34.76	0.54	26.4
15	1	Undetermined PGM	S	11.42	0.44	26.39
			Fe	36.56	0.72	48.52
			Ni	2.3	0.36	2.9
			Cu	4.21	0.48	4.9
			Pt	45.51	0.87	17.29

PTS# C5 Con 4						
Site #	Spectrum	Mineral name	Element	Weight%	Weight% sigma	Atomic%
1	3	Undetermined PGM	Pd	1.57	0.68	1.84
			Sb	91.24	1.18	93.56
			Pt	7.2	1.01	4.61
1	4	Pentlandite	S	36.5	0.46	50.81
			Fe	23.31	0.45	18.63
			Ni	40.19	0.55	30.56
2	1	Sperrylite	As	43.69	0.65	66.9
			Pt	56.31	0.65	33.1
2	2	Talnahkite	S	36.18	0.47	52.11
			Fe	14.98	0.38	12.39
			Cu	48.84	0.56	35.5
3	1	Insizwaite	Sb	32.84	0.79	44.61
			Pt	39.64	0.89	33.61
			Bi	27.52	1.04	21.78
Liberated						
4	1	Undetermined PGM	S	21.37	0.58	47.59
			Fe	7.61	0.39	9.73
			Cu	1.62	0.39	1.82
			Pd	52.08	1.08	34.95
			Bi	17.31	1.33	5.91
4	4	Chalcopyrite	S	36.86	0.46	52.03
			Fe	30.51	0.48	24.73
			Cu	32.63	0.58	23.24
5	1	Paolovite	Pd	55.3	0.75	61.07
			Sn	30.97	0.68	30.66
			Pt	13.73	0.64	8.27
5	2	Chalcopyrite	S	38.2	0.47	53.46
			Fe	29.69	0.47	23.86
			Cu	32.11	0.58	22.68
6	1	Hessite	Ag	58.36	1.27	62.38
			Te	41.64	1.27	37.62
6	2	Talnahkite	S	37.34	0.45	52.52
			Fe	30.91	0.47	24.96
			Cu	31.74	0.57	22.52
7	1	Paolovite	Pd	62.56	0.9	65.08
			Sn	37.44	0.9	34.92
7	2	Talnahkite	S	37.38	0.45	52.61
			Fe	29.84	0.46	24.11
			Cu	32.79	0.56	23.28

PTS# C5 Con 4						
Site #	Spectrum	Mineral name	Element	Weight%	Weight% sigma	Atomic%
8	1	Undetermined PGM	S	20.2	0.58	46.47
			Fe	7.35	0.4	9.71
			Cu	2	0.4	2.32
			Pd	48.91	1.09	33.9
			Bi	21.54	1.37	7.6
8	2	Chalcopyrite	S	36.92	0.57	52.03
			Fe	31.79	0.6	25.72
			Cu	31.29	0.72	22.25
9	1	Kotulskite	Pd	47.26	0.91	59.1
			Sb	3.91	0.62	4.27
			Te	13.67	0.64	14.26
			Bi	35.16	0.92	22.38
9	2	Pentlandite	S	36.32	0.75	50.57
			Fe	25.78	0.77	20.61
			Ni	37.9	0.91	28.82
10	1	Undetermined PGM	S	22.62	0.6	45.71
			Fe	21.06	0.61	24.43
			Ni	2.09	0.33	2.31
			Cu	7.63	0.52	7.79
			Pd	17.76	0.79	10.82
			Bi	28.84	1.23	8.94
10	2	Cubanite	S	37.65	2.86	52.35
			Fe	40.42	3.13	32.27
			Cu	21.93	3.45	15.38

PTS# C5 Con 5						
Site #	Spectrum	Mineral name	Element	Weight%	Weight% sigma	Atomic%
1	1	Kotulskite	Pd	28.96	0.74	38.43
			Te	31.5	0.69	34.85
			Bi	39.54	0.88	26.71
1	2	Talnahkite	S	37.16	0.39	52.34
			Fe	30.47	0.4	24.64
			Cu	32.37	0.49	23.01
2	1	Acanthite	S	65.6	0.87	86.52
			Ag	34.4	0.87	13.48
2	2	Talnahkite	S	37.22	0.45	52.41
			Fe	30.38	0.47	24.56
			Cu	32.4	0.57	23.02
3	1	Undetermined PGM	Pd	79.2	2.01	88.2
			Bi	20.8	2.01	11.8
3	2	Talnahkite	S	36.79	0.39	51.93
			Fe	31.01	0.4	25.13
			Cu	32.2	0.49	22.94
4	1	Kotulskite	Pd	42.84	0.85	58.31
			Te	4.7	0.52	5.34
			Bi	52.45	0.87	36.35
		Liberated				
5	1	Stibiopalladinite	Pd	72.55	0.71	75.15
			Sb	27.45	0.71	24.85
		Liberated				
6	1	Sperrylite	As	43.59	0.54	66.8
			Pt	56.41	0.54	33.2
		Liberated				
7	1	Paolovite	Pd	56.45	0.63	59.11
			Sn	43.55	0.63	40.89
7	2	Pentlandite	S	35.57	0.41	49.68
			Fe	30.27	0.43	24.27
			Ni	34.16	0.5	26.05
8	1	Sperrylite	As	42.49	0.85	65.8
			Pt	57.51	0.85	34.2
8	2	Talnahkite	S	37.46	0.39	52.66
			Fe	30.41	0.4	24.54
			Cu	32.14	0.49	22.8
9	1	Paolovite	Pd	64.39	0.54	66.86
			Sn	35.61	0.54	33.14
9	2	Pentlandite	S	38.17	0.43	52.57
			Fe	27.53	0.42	21.77
			Ni	31.8	0.5	23.92
			Cu	2.49	0.35	1.73
10	1	Paolovite	Pd	56.83	0.67	59.49
			Sn	43.17	0.67	40.51
10	2	Pentlandite	S	35.72	0.78	49.81
			Fe	32.01	0.85	25.63
			Co	5.35	0.65	4.06
			Ni	26.92	0.93	20.5